Development of a Biodynamic Modules for Forensic Applications

Brent Travis Tuohy

Thesis submitted to the Faculty of the
Virginia Polytechnic Institute and State University
In partial fulfillment of the requirements for the degree of

MASTER OF SCIENCE
In
Engineering Mechanics

D. J. Schneck, Chair
J. R. Foy
L. G. Kraige

November 20, 2000
Blacksburg, Virginia

Key Words: MADYMO, Biodynamic Modeling, Forensics

Development of a Biodynamic Modules for Forensic Applications

Brent T. Tuohy

(ABSTRACT)

Work has been done to develop the computer laboratory portion of a course in biodynamic modeling, with particular emphasis towards applications in forensic engineering. Three course modules have been developed which explore the whiplash injury mechanism, pilot ejection and windblast, and gait analysis. These case studies make use of software entitled MADYMO (MAthematical DYnamic MOdeling). Each case study provides the scene, outcome, details, and instructions for setup of the biodynamic model. An "In-House" User's Manual has also been written so that students without previous MADYMO or UNIX experience can become proficient at using the program. Through the case studies presented within this thesis, students will gain insight into injury mechanisms and learn valuable biomechanical modeling tools.

Acknowledgements

During my pursuit of a Master of Science degree in Engineering Mechanics, I received a lot of support from several individuals, and I would like to express my gratitude towards them.

First of all, I would like to thank my advisor, Dr. Daniel J. Schneck for his effort in creating an interesting research topic and providing the funding and advice to arrive at our goals. Office visits with Dr. Schneck were often very interesting and left me motivated to work on this thesis. American Electric Power (A.E.P.) deserves thanks for partially funding a graduate research assistantship and promoting innovation in engineering education. The ESM department's graduate secretary, Loretta Tickle, is perhaps the nicest person I met in Virginia, and I sincerely appreciated her help. I will miss visiting with her. Tim Tomlin assisted me several times concerning computer difficulties and Rob Marshall, from TNO/MADYMO, was very helpful when I had difficulties with the biodynamic modeling software. I would also like to thank Bob Simunds, who helped me become a teaching assistant for a materials "busting" lab, and let me "roam" his beautiful property in search of elusive whitetails and Christmas trees.

I developed several lasting friendships with people who helped me relax and take my mind off of school work. Marc Schultz, Kevin Moorehouse, and Wayne Herring supported me in different ways, and I had fun with them during my stay at Virginia Tech. Most of all, I would like to thank my fiancé and family for their love and support during difficult times. I cannot imagine a more supportive person than my fiancé, Jenny Campbell, and I plan on returning the support for the rest of our lives. My family provided guidance from afar, and they are the reason I have made it this far in life. I can never give them enough gratitude for what they have done and how they make me feel. Finally, I give thanks to God for helping me achieve my educational goals and giving me the opportunity to have a wonderful life.

Table of Contents

List of Tables

List of Figures

Chapter 1.0 Introduction and Problem Statement

There are several different research areas in biomedical engineering, but one of great interest for current students is biomechanics. Biomechanics applies the principles of mechanics to study and analyze the human system. This research has many applications, among them, forensic engineering, which reconstructs injuries, accidents, and physiologic failure mechanisms. Although several universities offer courses in biomechanics, there are only a few universities that offer courses with direct applications to forensic engineering. A laboratory course in biodynamic modeling has been developed here to acquaint students with techniques for analyzing biodynamic events.

With use of a commercial software package titled MADYMO, students will explore different biomechanical environments and the physiologic response to such environments, which may include injury mechanisms and the proper modeling of the biomechanics of injury. Analysis of a biodynamic model and its results is very important for understanding the injury mechanism and this will also be explored.

To learn a fundamental aspect of forensic engineering (i.e., biodynamic modeling) students will undertake the study of modules derived from real-life case studies. Each student will explore injury mechanisms related to:

1) Whiplash (acceleration/deceleration injuries);
2) Pilot Ejection and Windblast (flail injuries)
3) Human Gait (foot injuries)

These course modules have been developed with the use of MADYMO and several results are presented within this thesis. Each module consists of the accident scene, the outcome, and the details of each system in the accident (i.e., victim and vehicular properties). The modules also have a description of the steps needed to simulate the

accident and provide recommendations for analysis procedures. Each case study includes several questions that ask the student to model the same injury with different parameters and circumstances. Although an injury mechanism, such as whiplash, might be common in today's society, different cases of the same injury usually involve people with different weights, ages, anthropometric builds, and biomechanical characteristics. A solid understanding of the slight changes to an accident scene and the corresponding differences in outcome should become apparent to the student after modeling each case. Also, an analytical solution and a MADYMO solution to a simplified whiplash problem are presented in Chapter 4.0 of this thesis.

The work provided within this thesis has been performed to develop the laboratory portion of a course in biodynamic modeling. Three completely different biomechanical situations have been explored for the sole purpose of enhancing students' knowledge and visualization of biodynamic problems. Animation files for each of the case studies explored can be viewed at http://www.esm.vt.edu/~adanielj/btuohy/. A qualified professor should perform instruction in the fundamentals of dynamics during a lecture period or prior to any biodynamic model development. This will help the student understand the dynamics of the course modules presented within this thesis.

Chapter 2.0 Review of Current Modeling Software & Courses

2.1 Modeling Software

Different biodynamic modeling software was researched, and it became evident that there is an abundance of equipment and software available for experimental biomechanics and less for computer modeling and simulation. Several programs had a broad range of applications including finite-element analysis and rigid-body dynamics for biomechanical and non-biomechanical modeling. Through search engines on the Internet, with keywords such as biomechanics software, biodynamic modeling, etc., several software programs relevant to biomechanics were found. The most relevant software for biodynamic modeling is shown in Table 1.

Table 1: Biodynamic Modeling Software

Software Package	Main Use	Biomechanics	Multi-body	Finite Element
MADYMO	Vehicle Occupant Modeling	Yes	Yes	Yes
DADS	Mechanical System Simulation	Yes	Yes	Yes
ADAMS	Mechanical System Simulation	Yes	Yes	Yes
SIMM	Musculoskeletal Modeling	Yes	Yes	No
HVE/GATB	Accident Reconstruction	Yes	Yes	No
ATB/Dynaman	Multi-body Dynamics	Yes	Yes	No
Autolev	Symbolic Manipulator for Motion Analysis	Yes	Yes	No
AutoSim	Equation Modeling	Yes	Yes	No

MADYMO, SIMM, and ATB are used mainly for biomechanics. Both MADYMO and SIMM provide excellent graphical learning tools and make use of 3-dimensional modeling. An advantage of SIMM over MADYMO is that it provides surgery simulations and other medical related products (1). However, SIMM is more applicable to a course specifically dealing with musculoskeletal modeling and health care and is not as applicable to forensic engineering and injury causation. MADYMO and ATB are efficient in modeling contact between multi-body elements but the latter does not make

use of finite elements or provide users with a database of pre-developed dummies and human models as does MADYMO (2). HVE/GATB is similar to the ATB program; however, it is primarily applied to auto accident reconstruction. A pre-developed multi-body human model is composed of 15 rigid ellipsoids connected by 14 joints (3). It is not possible to increase the number of joints on the model. HVE/GATB does not provide the biodynamic modeler with enough variability in creating multi-body models to represent a human. Websites for both ADAMS and DADS show that the programs are very powerful and can properly model biodynamic situations; however, they do not focus on biomechanics and, therefore, do not contain extensively researched biodynamic models (crash test dummies), as does MADYMO. Autolev and AutoSim are tailored to generating and simulating equations of motion and provide users with an understanding of the dynamics of a system (4). The graphical output and applicability of MADYMO to forensic engineering, however, makes it a more useful tool in a course dealing with injury causation and for this reason, it was chosen as the appropriate biodynamic modeling software.

2.2 Biodynamic Modeling Courses

Biomechanics is a growing area of research for universities across the country. Gait analysis is probably at the "top of the list" as a research topic. Athletic performance research is another field of biomechanics that remains heavily studied and is of interest to many college disciplines. Forensic engineering has not been the focus of many universities, but programs with emphasis on injury biomechanics do exist.

Researchers at several universities, including Virginia Tech, have used the Articulated Total Body (ATB) Model, developed by the Calspan Corporation in 1975, as a means for solving complex dynamic systems (5). The program, however, is declining in popularity because it is not very user-friendly and cannot be easily updated. MADYMO, which is based on the same principles as ATB, has claimed a majority of the biomechanics research in the automotive industry and is gaining favoritism in universities worldwide. From Arizona State University to Ohio State University to Graz, University

of Technology in Austria, MADYMO is being used to simulate biodynamic events. The program is mainly being used for research purposes and has found its way into the classroom at a few universities, such as Wayne State University and Michigan State University. Wayne State University, located in Detroit, Michigan, currently has a mathematical modeling in bioengineering course (BME/ME 7100) that uses MADYMO during at least three weeks of the course schedule (6). In a telephone conversation, Mrs. Sally Duquesnel, an employee with MADYMO, North America, stated that enrollment in Wayne State's Mathematical Modeling in Bioengineering course has grown from 7 students to 40 students in the last couple of years. This can be attributed to the need for engineers trained with MADYMO in the automotive industry and the interest of students to be hired as occupant safety engineers. The University of Virginia uses MADYMO in its Auto Safety Lab, but according to Dr. Walter Pilkey from the Department of Mechanical, Aerospace, and Nuclear Engineering, U.Va. does not have a biodynamic modeling course. Likewise, Graz University of Technology, located in Austria, uses MADYMO for research purposes but does not offer a course using the software.

A question, posted to over 4,000 recipients on the BIOMCH-L list-serve, regarding the current biodynamic modeling courses available yielded few results, but most of the respondents expressed interest in developing a course similar to the one proposed in this thesis.

Chapter 3.0 Modeling Techniques and Simulation

3.1 MADYMO Applications

MADYMO (MAthematical DYnamic MOdeling) was developed by TNO-Automotive primarily for studying occupant behavior during a vehicle collision. However, it has proven effective in simulating occupant behavior in several different forms of transportation such as planes, trains, and motorcycles (7). MADYMO is also effective in simulating injury mechanisms associated with biomechanics of human motion.

The commercially available program is used by many biomechanics consulting and research companies throughout the world and according to MADYMO representatives, it holds 95% of the industry market. The "Big 3" automakers, GM, Ford, and Chrysler, all use MADYMO in their occupant safety departments. It has proven invaluable in analyzing the effectiveness of different seat belt arrangements and air bag placement and control. Costs for expensive mechanical prototypes and time spent constructing them have decreased due to the use of MADYMO to effectively simulate the same occupant behavior as an actual crash-test dummy. Computer simulations are a beneficial alternative to full-scale dummy testing because of the relatively low cost and variability of testing parameters (8). Cessna and NASA also use this powerful program to create a safer environment for their flight occupants. The usefulness of MADYMO and its wide variety of users was a major factor in choosing a biodynamic modeling program suitable for students to learn.

Several accident reconstruction companies use MADYMO to investigate vehicle damage and occupant injury. A study performed by Renfroe Engineering, an accident reconstruction company located in Arkansas, showed excellent conformity between MADYMO simulations and actual test results for a vehicle rollover (9). In this dynamically complicated accident, the occupant behavior was analyzed and injury

parameters were found. Tests of this sort could not be performed in an actual vehicle rollover without subjecting the occupant to an extreme amount of danger and probability for injury. To manufacture a vehicle that could sustain the impact forces generated during a vehicle rollover and protect an occupant would be very expensive, time consuming, and probably produce faulty occupant data. Therefore, MADYMO simulations are invaluable for injury investigations and are becoming increasingly popular with insurance companies and law firms that need an analysis of a victim's injury mechanisms.

Due to the ability of the program to simulate complex dynamic responses without subjecting individuals to injury, MADYMO has a wide range of applications in the biomechanics research industry. There is a close corroboration between crash dummy designers/ testers and TNO computer simulation developers, insuring that the MADYMO output results and applications will be accurate and verifiable. The popularity of the program in industry insures further research with MADYMO to expand its capabilities.

3.2 MADYMO Theory

MADYMO is essentially a differential equation solver. It employs the use of three different integration methods to solve biodynamic equations of motion for multibody and finite element simulations, producing data output and graphics files. The ability to combine rigid multibody segments with finite elements makes the software extremely powerful in analyzing forces, moments, torques, stresses, and strains. MADYMO users must specify the initial conditions of a system by inputing relevant data into a data input file. The data file is divided into 10 major "blocks" as listed below:

1) General Input
2) Inertial Space
3) Null Systems
4) System

5) FEM Model
6) Airbag Chamber
7) Force Models
8) Contact Interactions
9) Control Module
10) Output Control Parameters

Since the course modules developed in this work did not deal explicitly with blocks 5, 6, or 9, they will not be discussed. The theory behind MADYMO's processes and procedures, excluding finite element modeling, will be discussed in the following paragraphs. The program uses S.I. units in all of its equations (see Appendix A "In-House" MADYMO Manual).

Coordinate Systems

Newtonian mechanics postulate the existence of an absolute reference frame referred to as the inertial space. The absolute reference frame is defined by the intersection of three mutually orthogonal planes that establish the axes of a coordinate system whose axes are not rotating, and whose center is not accelerating. However, these axes can be at rest or moving at a constant velocity with respect to an average position of the distant "fixed stars" (10). The planes are used to describe the motion of systems within the inertial space. MADYMO allows the user to define the inertial coordinate system arbitrarily, but it is common to refer to the inertial coordinate system as one being attached to the Earth with its z-axis pointing outward from the center of the Earth. Although this inertial coordinate system is rotating, the effects of the rotation on a smaller system, such as a vehicle, are negligible.

A null system is described with a specified motion relative to the inertial space. The most relevant example of a null system in MADYMO is a vehicle traveling at a specified velocity for each point in time during the simulation. The coordinates of the

center of gravity of the vehicle are given relative to the origin of the inertial coordinate system. Since the motion of a null system is given as a limited number of data points spaced a finite time interval apart, MADYMO performs a cubic spline interpolation to find the intermediate time points. This is done by calculating the rotation axes and the corresponding rotation angles of two successive time points and then interpolating to find the rotation axes and angles that lie between the given data points. Cubic spline functions represent data as relatively smooth curves that do not have rapid oscillations, such as occur frequently with higher order polynomial interpolations. Cubic spline interpolations are also less computationally intensive (11).

Also, there are coordinate systems associated with a body and a joint, as described in the following two sections.

System Geometry

Planes, ellipsoids, cylinders, facet surfaces, and/or finite elements can represent bodies or systems in MADYMO. This variety of modeling techniques allows a wide range of models to be developed. Multibody systems are primarily comprised of ellipsoids and are connected by kinematic joints in a "tree" structure, which is illustrated in Figure 1.

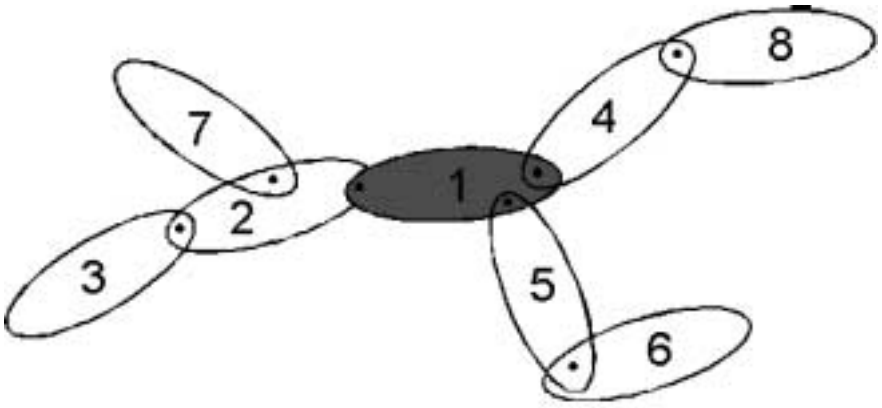

Figure 1: "Tree" structure used to represent bodies (12)

This system, represented by eight ellipsoids, is shown as a tree structure connected by joints, which are represented by dots at the intersection of the ellipsoids. MADYMO requires that the initial configuration of ellipsoids be entered into an input data block by specifying the order of ellipsoids. For example, in Figure 1, ellipsoid 1 is the "parent" for ellipsoids 2 and 4, which would be labeled as the "child" ellipsoids (first generation). Ellipsoid 8 is a child of ellipsoid 4 (second generation of ellipsoid 1), and so on. The bodies are specified in the GEOMETRY block of MADYMO as follows:

$$\begin{bmatrix} 3 & 2 & 1 \\ 6 & 5 & 1 \\ 7 & 2 & 1 \\ 8 & 4 & 1 \end{bmatrix}$$

It should be noted that this is not a matrix; it simply represents the four branches (i.e. branch 1: 3 2 1) of the system. Each branch (row) should end with the main parent body (ellipsoid 1) and be numbered sequentially. The order of branches is not important as long as each branch is in descending order. For this example and most other applications, ellipsoid 1 is connected to the inertial space by a free joint (refer to the Joints section). Each ellipsoid has a local coordinate system associated with the center of gravity of the body, mass, and inertia that can vary depending upon the body modeled and its application. The motion of the body is defined by the time rate of change of the degrees of freedom associated with the local coordinate system of the body. The ellipsoids also have loading characteristics associated with their geometric and physical properties. These characteristics are specified in a FUNCTIONS block and relate force (elastic and damping) to penetration. Friction forces associated with the body can be specified relative to the velocity of the body.

The pre-developed models from the dummy database of MADYMO have the system specifications, such as body mass, inertia, and loading functions, already

specified. The dummy database currently contains 31 dummies and 2 human body models that can be imported directly into a program as a system. Each system also comes with suggestions such as initial joint degrees of freedom and feasible integration time steps.

Joints

MADYMO makes use of 12 types of kinematic joints with differing joint degrees of freedom. For each kinematic joint there is a dynamic joint, with elastic, damping, and friction properties specified by the user. The types of joints used are listed in Table 2.

Table 2: Joints Available and a Brief Description

Joint	Description
Free	Relative motion is not constrained
Bracket	Does not allow relative motion of connected bodies
Revolute	Bodies can rotate about one axis
Translational	Bodies can translate along one axis
Spherical	Rotation about three axes (i.e., ball and socket)
Universal	Bodies can rotate around two axes
Cylindrical	Bodies rotate and/or translate about one axis
Planar	Motion constrained a direction coincident to a plane
Translational/Revolute	Combination of Translational and Revolute joint properties
Revolute/Translational	Combination of Revolute and Translational joint properties
Translational/Universal	Combination of Translational and Universal joint properties
Universal/Translational	Combination of Universal and Translational joint properties

The joints used most often with human body modeling are those listed as 1, 2, 3, and 5 in Table 2. Each joint has a joint coordinate system with characteristic degrees of

freedom that determine its position, velocity, and acceleration. They also determine the appropriate constraint force that needs to be placed on the interconnected bodies. The joints are a common location for forces and torques to be analyzed since several injury mechanisms can occur there. Sometimes it is necessary to lock a joint (i.e. apply a fixation device such as a cast) or apply a sensor to it so that, if the constraint loads of the kinematic joint are exceeded, the joint will break. This feature can be useful when analyzing broken bones and the time frame within which a fracture might have occurred.

Kinematics of Rigid Bodies

Consider a system of two rigid bodies, body *i* and body j, as shown in Figure 2. A user specified kinematic joint connects the bodies.

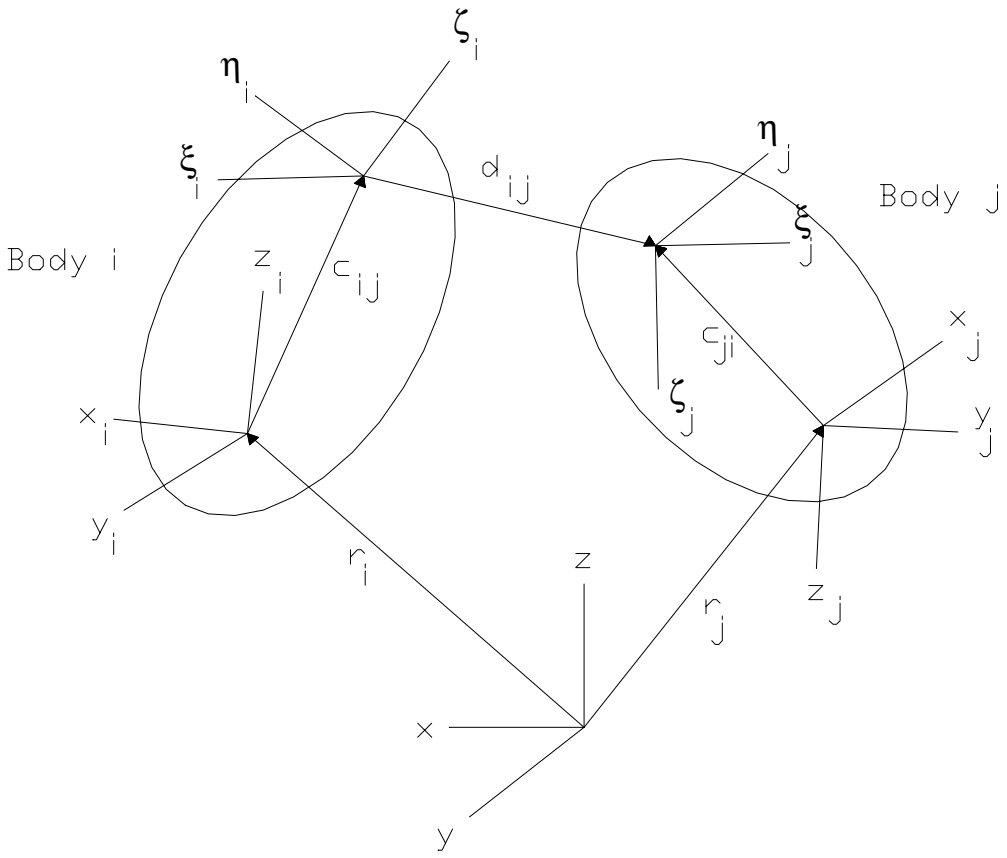

Figure 2: Pair of bodies connected by an arbitrary kinematic joint

The bodies have a joint coordinate system (η, ξ, ζ) and a body local coordinate system (x, y, z). The location of body *i* is located by the position vector $\underline{r}_i$ from the inertial coordinate system. For body *i*, the joint coordinate system is located from its local coordinate system by the vector $\underline{c}_{ij}$, which is a constant value since the body is rigid. Since the joint connecting the two rigid bodies is arbitrary, the vector $\underline{d}_{ij}$ gives the location of the joint coordinate system of body *j* with respect to the joint coordinate system of body *i*. In most cases, $\underline{d}_{ij}$ is equal to zero since a joint rigidly connects the bodies. The rotation matrix D_{ij} gives the rotation between the joint coordinate systems of the two bodies. D_{ij} and $\underline{d}_{ij}$ are given by the type of joint specified in the model and the values of the joint degrees of freedom. Similarly, the rotation matrix C_{ij} defines the rotation of the joint coordinate system relative to the local coordinate system for rigid body *i*. The joint and local coordinate systems for body *j* are defined in the same manner. Rotation matrices, A_i and A_j, provide the orientation of the local coordinate system for body *i* and body *j*, respectively. A_j can be defined in terms of A_i as follows:

$$[A_j] = [A_i][C_{ij}][D_{ij}][C_{ji}{}^T] \tag{3.21}$$

The position of the local coordinate system for body *j*, $\underline{r}_j$, can be written as:

$$\underline{r}_j = \underline{r}_i + \underline{c}_{ij} + \underline{d}_{ij} - \underline{c}_{ji} \tag{3.22}$$

In a system of n bodies, equations (3.21) and (3.22) are applied successively from body 1 to body n, until all positions and orientations are defined relative to the inertial coordinate system. The first time derivative of equation (3.21) and (3.22) yields the following equations for angular velocity and linear velocity, respectively (7).

$$\underline{\omega}_j = \underline{\omega}_i + \underline{\omega}_{ij} \tag{3.23}$$

$$\dot{\underline{r}}_j = \dot{\underline{r}}_i + \underline{\omega}_i \times \underline{c}_{ij} + \dot{\underline{d}}_{ij} - \underline{\omega}_j \times \underline{c}_{ji} \tag{3.24}$$

Similarly, the angular acceleration and linear acceleration are found by taking the time based derivative of equations (3.23) and (3.24).

Equations of Motion

MADYMO uses Newton-Euler equations of motion for rigid bodies as follows:

$$\underline{F}_i = m_i \underline{\ddot{r}}_i \tag{3.25}$$

$$\underline{T}_i = J_i \cdot \underline{\dot{\omega}}_i + \underline{\omega}_i \times J_i \cdot \underline{\omega}_i \tag{3.26}$$

The resultant force vector is $\underline{F}_i$, the mass is m_i, and the linear acceleration of the center of gravity is $\underline{\ddot{r}}$. For equation (3.26), J_i is the inertia tensor with respect to the center of gravity, $\underline{\omega}_i$ is the angular velocity vector, $\underline{\dot{\omega}}_i$ is the angular acceleration vector, and $\underline{T}_i$ is the resultant torque or moment. $\underline{F}_i$ and $\underline{T}_i$ include the joint reaction forces, but these cannot be determined until the acceleration of the system is known. MADYMO uses the principle of virtual work to eliminate the unknown forces and torques (7). This equation is as follows:

$$\sum \delta \underline{r}_i \cdot \{m_i \underline{\ddot{r}}_i - \underline{F}_i\} + \delta \underline{\pi}_i \cdot \{J_i \cdot \underline{\dot{\omega}}_i + \underline{\omega}_i \times J_i \cdot \underline{\omega}_i - \underline{T}_i\} = 0 \tag{3.27}$$

The principle of virtual work makes use of infinitesimal variations in displacement and orientation, $\delta \underline{r}_i$ and $\delta \underline{\pi}_i$. This is performed for each body in the system so that the constraint forces can be found. The second time derivative of the joint degrees of freedom are found and time integration of these values provides the motion and position of the body coordinate systems relative to the inertial coordinate system at a point in time. The initial conditions of the joint must be defined in the MADYMO input file.

Integration Methods

The general input data block is where the start time, end time, time step, and integration method are specified for the simulation. There are three different types of integration methods that MADYMO uses to solve the differential equations of motion: the Euler Method (EULER), Runge-Kutta Method (RUKU4), and Runge-Kutta-Merson Method (RUKU5). Euler's Method is a one step process for approximating the solution of an initial value problem. The equations of motion are derived from the degrees of freedom of each of the coordinate systems as described in the *Coordinate Systems, System Geometry,* and *Joint* sections. The equations of motion can be written as a system of second-order equations:

$$\ddot{\underline{q}} = \underline{h}(\underline{q}, \dot{\underline{q}}, t) \tag{3.28}$$

with initial values q_o and $\dot{q}_o$.

The column matrix $\underline{q}$ represents the generalized coordinates, which in MADYMO are the joint degrees of freedom; $\underline{h}$ defines the equations of motion and t is time. This general acceleration equation (3.28) is integrated using Euler's Method to obtain the velocity variables and then integrated again to find the position variables. The Euler method uses the initial values specified by the user, and calculates the slope of the equation of motion curve at those initial points. It then uses that slope and the next independent variable, determined by the step size, to find the corresponding dependent variable. The slope is then calculated and the process repeats itself until all of the variables are found. These steps can be seen in Figure 3.

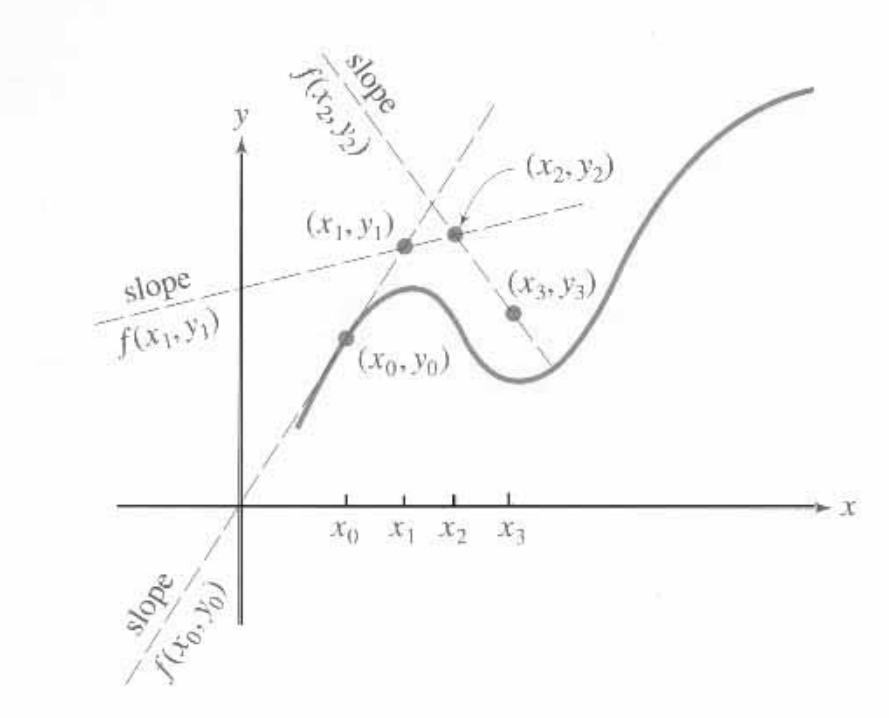

Figure 3: Example of Euler's Method to approximate an analytical solution (13)

The Modified Euler Method is a variation of the method described above; however, the slope is calculated at a point half way between the independent step values. The following equation is an analytic representation of the Modified Euler Method (13):

$$x_{k+1} = x_k + s \cdot f\left(t_k + \frac{s}{2}, x_k + \frac{sf_k}{2}\right) \quad \text{for k = 0, 1, 2, …, n-1; } x(t_o) = x_o \tag{3.29}$$

where: s is equivalent to $t_{k+1} - t_k$, and n is determined by dividing the time step into the total run time for the program. The step value is t, the dependent variable is x, and f represents a slope function.

Runge-Kutta methods are variations of Euler's Method but are based on the modification of a Taylor approximation. RUKU4 has proven to be accurate and also

computationally efficient (13). If a version of the Runge-Kutta method is used, it is helpful to introduce the column matrix $\underline{x}$ as follows:

$$\underline{x} = \begin{bmatrix} \dot{\underline{q}} \\ \underline{q} \end{bmatrix} \tag{3.30}$$

From equation (3.30), the RUKU4 solution can be written as:

$$\underline{x}_{n+1} = \underline{x}_n + \frac{1}{6} \cdot t_s(\underline{k}_1 + 2\underline{k}_2 + 2\underline{k}_3 + \underline{k}_4) \tag{3.31}$$

where:

$$\underline{k}_1 = f(t_n, \underline{x}_n)$$
$$\underline{k}_2 = f(t_n + \frac{1}{2}t_s, \underline{x}_n + \frac{1}{2}t_s\underline{k}_1)$$
$$\underline{k}_3 = f(t_n + \frac{1}{2}t_s, \underline{x}_n + \frac{1}{2}t_s\underline{k}_2)$$
$$\underline{k}_4 = f(t_n + t_s, \underline{x}_n + t_s\underline{k}_3)$$

and t_s is the specified simulation time step. All other variables have been defined above (Eq. 3.29) and k represents values that are functions of the time step. Both EULER and RUKU4 have a fixed time step and are used for both multibody and finite element models. RUKU4 is more accurate than EULER and is less computationally intensive than RUKU5. Therefore, the Runge-Kutta Method (RUKU4) of integration is the preferred method for solving the equations of motion. In order to keep a simulation accurate and stable, an appropriate time step must be specified. If a time step is too large, the error in the solutions to the equations of motion will grow and continue to infinity, in which case the program should be run again using a smaller time step. Without running a program, it is not possible to find the maximum time step because the time step depends on the largest eigenvalue for any given solution. In order to verify that the chosen time

step is valid, another simulation using a different time step should be performed and the results should be compared as in Figure 4.

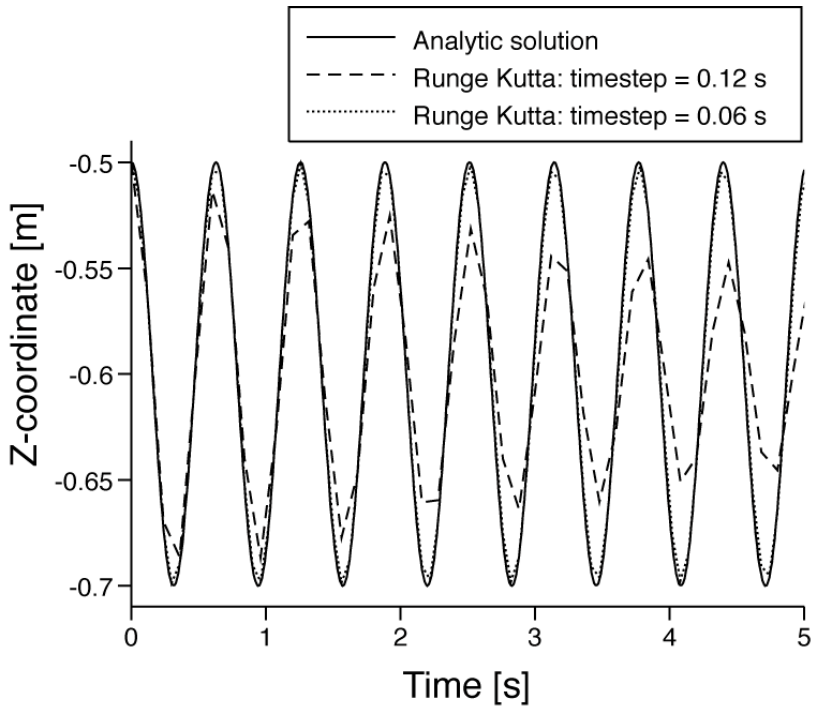

Figure 4: Example of accuracy using different time steps for Runge-Kutta integration (12)

If the results between two different time steps greatly differ as in Figure 4 (0.06s vs. 0.12s), then another simulation with a different time step should be performed and the results should be compared again.

RUKU5 uses a variable time step for improved accuracy but cannot be used with facet surfaces or finite elements. The solution equations derived from equation (3.30) are similar to RUKU4:

$$\underline{x}_{n+1} = \underline{x}_n + \frac{1}{6} \cdot t_s(\underline{k}_1 + 4\underline{k}_4 + \underline{k}_5) \tag{3.32}$$

where:

$$\underline{k}_1 = f(t_n, \underline{x}_n)$$

$$\underline{k}_2 = f(t_n + \frac{1}{3}t_s, \underline{x}_n + \frac{1}{3}t_s\underline{k}_1)$$

$$\underline{k}_3 = f(t_n + \frac{1}{3}t_s, \underline{x}_n + \frac{1}{6}t_s\underline{k}_1 + \frac{1}{6}t_s\underline{k}_2)$$

$$\underline{k}_4 = f(t_n + \frac{1}{2}t_s, \underline{x}_n + \frac{1}{8}t_s\underline{k}_1 + \frac{3}{8}t_s\underline{k}_3)$$

$$\underline{k}_5 = f(t_n + t_s, \underline{x}_n + \frac{1}{2}t_s\underline{k}_1 - \frac{3}{2}t_s\underline{k}_3 + 2t_s\underline{k}_4)$$

Other variables including the error tolerance and the maximum time step must be defined for RUKU5.

Force Modeling

In order to model a crash simulation in MADYMO, an acceleration field, and resulting force field, must be specified by the user. It may also be necessary to input the acceleration of gravity as a 9.81 m/s^2 acceleration in the appropriate direction. Acceleration fields are specified in the FORCE MODELS block of the input file. It should be noted that for simulations involving a vehicle collision, the acceleration field is applied to the occupant rather than the vehicle, thus allowing the user to model the occupant's behavior without modeling the vehicle.

Contact Interactions

No force calculations between interacting bodies will be performed unless a contact interaction constraint is specified in the MADYMO data file. If this is not done, viewing a MAPPK graphics file of a successfully run program will show the body penetrating a surface and continuing to move through the surface in the absence of a resistive force. Contact interactions are essential to any biodynamic model. A contact interaction can be specified between ellipsoids and ellipsoids/planes/cylinders/FE. Likewise, contact can be specified between any of the bodies available in MADYMO.

Contact constraints are used to find the resulting forces imposed on a body due to a collision. The collision can be a bat hitting a ball, a person in an automotive accident, and so on. When viewing a graphic output file, a MADYMO user might observe that bodies not expected to penetrate a surface, are indeed penetrating it. To correct this apparent anomaly and find the forces created from the collision, MADYMO uses the hypothetical depth of penetration, together with the elastic, damping, and friction characteristics (FUNCTIONS block) of the body, to calculate the corresponding resisting elastic, damping, and friction forces that result from contact in order to prevent penetration.

When an ellipsoid contacts a plane, the elastic force is calculated at a point of contact, P that lies in a plane tangent to the ellipsoid at the depth of penetration (7). The point P can be determined from contact characteristics of the ellipsoid, the contact characteristics of the plane, or a combination of both. Contact characteristics are the constitutive properties for each body. If the MADYMO user specifies the combined contact characteristic, P can be found from the penetration into the ellipsoid ($x_{e,el}$) and penetration into the plane ($x_{e,pl}$), i.e.,

$$P = P_{el} + \frac{x_{e,\,el}}{x_{e,\,el} + x_{e,\,pl}} * (P_{pl} - P_{el}) \tag{3.33}$$

where: P_{el} is the contact point on the ellipsoid (i.e., plane assumed to be infinitely stiff) and P_{pl} is the contact point on the plane (i.e., ellipsoid assumed to be infinitely stiff). Figure 5 should help graphically explain equation (3.33).

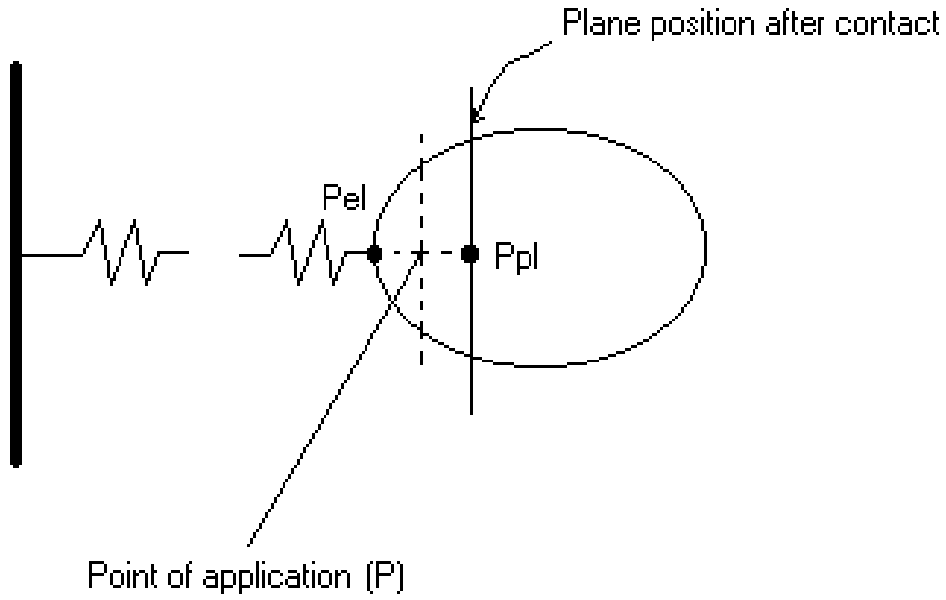

Figure 5: Point of application used for calculating the contact force

The elastic force is then found at *P* using the constitutive equations (force-penetration functions) specified in the data file. To find the damping force, F_d, the relative velocity between the contacting surfaces, v_{norm}, and the elastic force, F_e, is used.

$$F_d = C_d * |v_{norm}| \tag{3.34}$$

$$C_d = C_{1d}(v_{norm}) * C_{2d}(F_e) \tag{3.35}$$

where: C_{1d} is the damping coefficient plus the corresponding value specified in the "damping velocity function" (7). The "damping velocity function" is predefined by MADYMO, if a dummy is used from the dummy database, and relates damping to a corresponding velocity. The value C_{2d} is derived from the "damping elastic force" and the "damping force function," which are also predefined if a dummy is used from the MADYMO database. These values were obtained by experimental testing at TNO Automotive. The MADYMO user must specify the damping coefficient and functions in the input data file if a dummy from the MADYMO database is not used. These quantities

must be found experimentally or through research literature. Likewise, the friction force, F_f, is calculated using a specified friction coefficient, f, i.e.,

$$F_f = C * f(|F_e + F_d|) * |F_e + F_d| \tag{3.36}$$

C is a ramp function that varies between 0 and 1 and is a function of the relative velocity of the body. It is used so that dry friction does not create vibrations on the bodies.

Output Control

In order for output from a biodynamic model to be analyzed, the necessary output from the equation of motion files must be specified in the OUTPUT CONTROL PARAMETERS block in the input data file. Refer to Table 3 for a listing and description of the output commands available.

Table 3: Possible Results Output and the Calculations Performed

Output Command	Output Calculation Performed for Specified Joints/Bodies/Points
LINDIS	Position of a point with respect to the local coordinate system of another body specified
RELDIS	Position of a point with respect to another specified point
LINVEL	Linear velocity usually with respect to the inertial coordinate system
DISVEL	Linear velocity of a point with respect to another point
LINACC	Linear acceleration usually with respect to the inertial coordinate system
ANGVEL	Angular velocity usually with respect to the inertial coordinate system
ANGACC	Angular acceleration usually with respect to the inertial coordinate system
FORCES	Force interactions such as the resultant, elastic, damping, and friction forces; other output (penetration, relative elongation, etc.)
TORQU1	Cardan restraint torques (loads also for spherical and free joints)
TORQU2	Flexion-Torsion restraint torques
JOINT LOADS	Applied joint loads; loads for spherical and free joints can also be written to the TORQU1 and TORQU2 files
TYRES	Tire loads and slip quantities
CONSTRAINT LOADS	Joint constraint forces
JNTPOS	Joint position for a maximum of 7 degrees of freedom
JNTVEL	Joint velocity for up to 6 degrees of freedom
JNTACC	Joint acceleration for a maximum of 6 degrees of freedom
MARKERS	Position tracking similar to JNTPOS
MUSCLES	Forces
ENERGY	Energy quantities; used in FEM only
INJURY PARAMETERS	Injury parameters for different parts of the human body (refer to Table 4); load cell forces calculated

In order for injuries to be analyzed and quantified in a more objective way, injury indices have been developed. These indices provide the basis for the Abbreviated Injury Scale (AIS), which ranks an anatomical injury from 0 to 6. The number 6 represents the maximum injury while 0 represents no injury. This “threat to life” scale is accepted

worldwide (7). These indices allow a "court-qualified expert" to substantiate a victim's injury claim. It also allows the biodynamic modeler to compare results between similar models with differing parameters. Listed in Table 4 are 12 such injury indices that MADYMO makes use of to quantify injuries.

Table 4: Injury Indices Available in MADYMO

Injury Index/Parameter	Description
HIC	Head Injury Criterion used most frequently for head impact tolerance
GSI	Gadd Severity Index quantifies the tolerance of the head to impact
3MS	Linear acceleration quantity (over 3 milliseconds) relating to organ injury in the thorax
TTI	Thoracic Trauma Index predicts injury to the "hard" thorax due to blunt lateral impact
VC	Viscous Injury Response predicts soft tissue injury as a result of high velocity rates and deflections within the body
FNIC	Peak forces and moments in the upper and lower neck
NIJ	Biomechanical neck injury predictor measures injury due to load transferred through the occipital condyles
CTI	Combined Thoracic Index measures injury to the thorax
FFC	Femur Force Criterion measures injury (axial load) to the femur
TI	Tibia Index measure injury (joint constraint load) to the tibia
TCFC	Tibia Compressive Force Criterion predicts injury to the tibia due to a compressive force

Currently, there is no injury criterion that relates flexion-extension bending moment at the lower neck (C7-T1) to whiplash injury. The W.I.S.E index (Whiplash Injury Severity Estimator) has been proposed, but has yet to become a standard for quantifying whiplash injuries (14).

Chapter 4.0 MADYMO Analytical Verification

Before creating complex biodynamic models and performing a simulation, students should be asked to solve analytical problems that arise from simplified models. This will give students a better understanding of what MADYMO is doing to create output in a given situation. Although the program has been validated through extensive research, developing simple analytical solutions from a simplified model will give students more confidence in the MADYMO output. Through the instruction of a professor in dynamics and the use of a multimedia software program, students will attain an enhanced understanding of biodynamic problems.

An example of a simplified whiplash model and the analytical solution is provided. Consider a system of two rigid bodies at rest with a pin joint between each body (Figure 6). The coordinate axes have been labeled to match the coordinate system used by MADYMO (+x to the left, +z up, and +y coming out of the plane). This will provide better clarity between the analytical and MADYMO results. The system is subjected to an acceleration (3.2*g*), due to rear impact, as shown in the free-body-diagram.

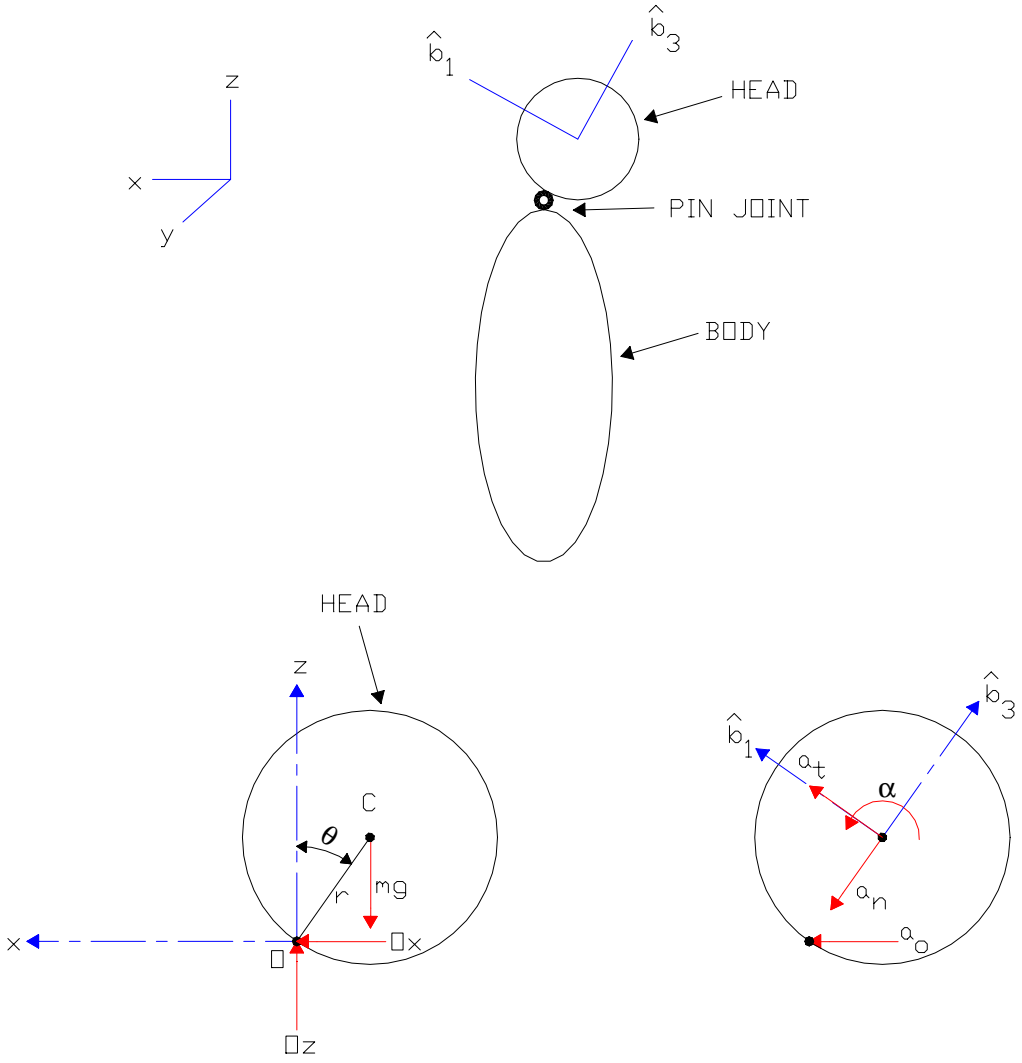

Figure 6: **Free-Body-Diagram of the head subjected to an acceleration (a_o) in the +x-direction**

The "*b*"coordinate system is fixed to the head and rotates with the head. The acceleration of the center of gravity of the head can be represented by a normal acceleration (a_n) and a tangential acceleration (a_t). The center of gravity of the head is located at point *C*, a distance *r* from the pin joint at point *O*. The results needed are the angular acceleration of the head (α) and the reaction forces at the pin joint (O_x and O_z). Let $\hat{i}$, $\hat{j}$, and $\hat{k}$ be unit vectors in the x, y, and z-directions, respectively. From the figure, the following vector quantities can be found:

$$\underline{OC} = r\hat{b}_3 \tag{4.1}$$

$$\underline{a}_o = 3.2g\hat{i} \tag{4.2}$$

The gravitational constant is g. With the axes as shown in Figure 6, the rotating coordinate system, *b*, can be transferred into the fixed reference frame by the following matrices:

$$\begin{bmatrix} \hat{b}_1 \\ \hat{b}_2 \\ \hat{b}_3 \end{bmatrix} = \begin{bmatrix} \cos\theta & 0 & \sin\theta \\ 0 & 1 & 0 \\ -\sin\theta & 0 & \cos\theta \end{bmatrix} \begin{bmatrix} \hat{i} \\ \hat{j} \\ \hat{k} \end{bmatrix} \tag{4.3}$$

The first step is to develop a vector expression for the acceleration of the center of gravity of the head ($\underline{a}_c$). The general acceleration equation for the center of gravity can be written as:

$$\underline{a}_c = \underline{a}_{c/o} + \underline{a}_o = \underline{\alpha} \times \underline{OC} + \underline{\omega} \times (\underline{\omega} \times \underline{OC}) + \underline{a}_o \tag{4.4}$$

From Figure 6 and the previous equations, the acceleration in terms of the inertial reference frame can be written as follows:

$$\underline{a}_c = (\alpha \cdot r\cos\theta + \omega^2 r\sin\theta + 3.2g)\hat{i} + (\alpha \cdot r\sin\theta - \omega^2 r\cos\theta)\hat{k} \tag{4.5}$$

Now that the acceleration of the center of gravity of the head has been found, the next step is to sum the forces in the x-direction.

$$\sum F_x = ma_{cx}$$

$$O_x = m(\alpha \cdot r\cos\theta + \omega^2 r\sin\theta + 3.2g) \tag{4.6}$$

The same method applies in the z-direction.

$$\sum F_z = ma_{cz}$$

$$O_z - mg = m(\alpha \cdot r\sin\theta - \omega^2 r\cos\theta)$$

$$O_z = m(\alpha \cdot r\sin\theta - \omega^2 r\cos\theta + g) \tag{4.7}$$

The next step is to perform a sum of the moments about the center of gravity of the head as follows:

$$\sum M_c = I_c\alpha$$

$$-O_z r\sin\theta - O_x r\cos\theta = I_c\alpha \tag{4.8}$$

The following equation for the angular acceleration of the head can be found by solving for O_x and O_z in equations (4.6) and (4.7) and substituting into equation (4.8).

$$\alpha = -\frac{mgr(\sin\theta + 3.2\cos\theta)}{I_c + mr^2} \tag{4.9}$$

To compare with the results that will be produced in the whiplash case study to follow, let $r = 0.0356$ m, $I_c = 0.0211$ kg-m^2, and $m = 4.4$ kg. These values have been used in the 50th percentile male dummy created by MADYMO and will be used in this analysis to provide similarity in solutions. It should be noted that I_c is a given value and not a function of the shape of the head (i.e., a sphere). This will be discussed in the final paragraph of this section. The model is said to start from rest, so at impact (time = 0 sec), $\omega = 0$ rad/s. To compare the results with a MADYMO simulation, an initial θ of 0 degrees is used. The analytical results produce a clockwise angular acceleration (α) of 184.3 rad/s^2, a reaction force in the x-direction (O_x) equal to 109.2 N, and a reaction force in the z-direction (O_z) equal to 43.2 N.

To compare these analytical results to the output of MADYMO, a model was created with the parameters given above ($r = 0.0356$ m, $I_c = 0.0211$ kg-m^2, etc.). The input data file is located in Appendix D. After performing a simulation, the angular acceleration of the center of gravity of the head was found to be –184.3 rad/s^2. This is exactly the same value found in the analytical calculation. Figure 7 provides the angular acceleration versus θ for both the analytical and MADYMO solution.

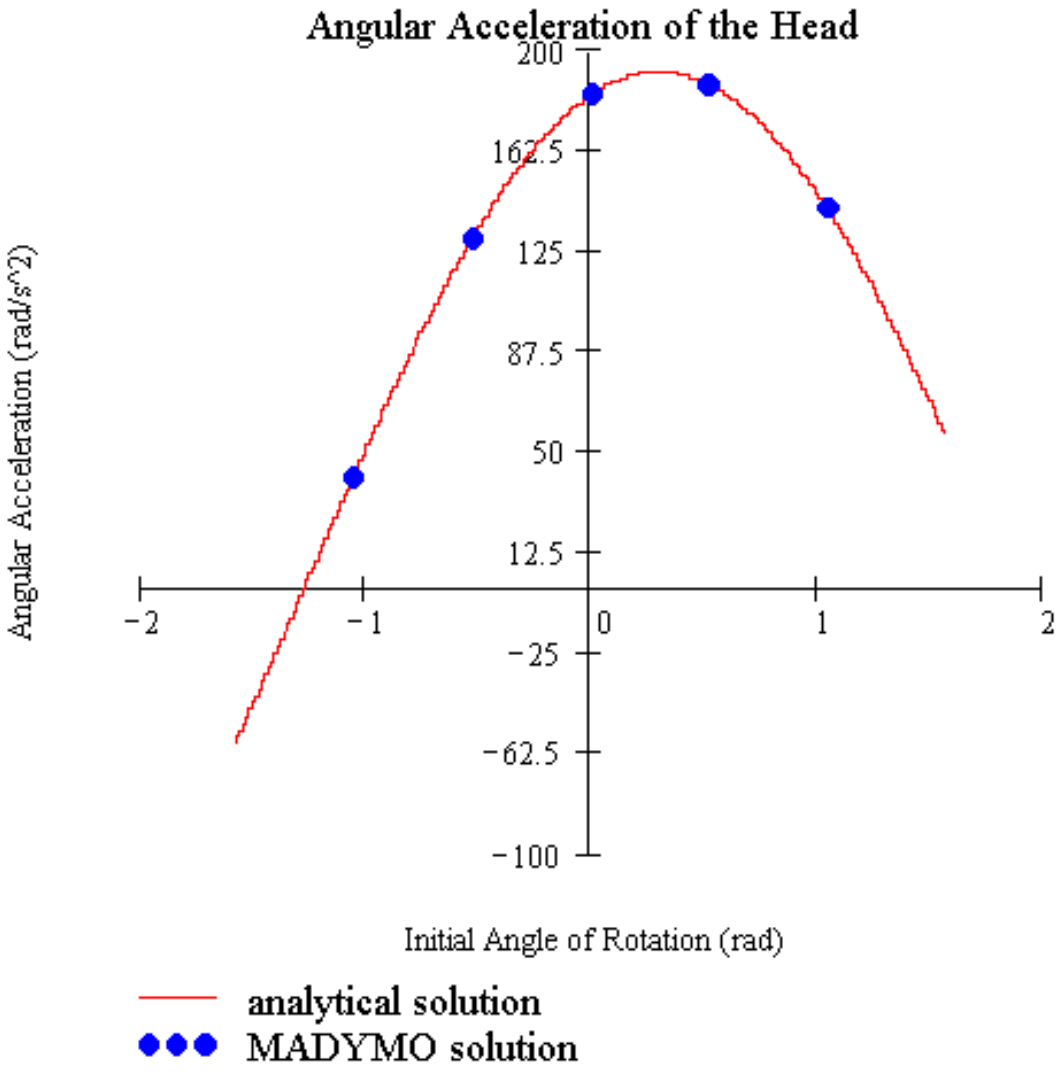

Figure 7: **Analytical and MADYMO results for the angular acceleration of the head versus the angle of head rotation (θ)**

The reaction force in the x-direction (O_x) was found to be 109.2 N. This value is also the same as the analytical result. Likewise, the reaction force in the z-direction (O_z) is the same as the analytical result of 43.2 N. The output files from this MADYMO model are available in Appendix D. The results are identical, so it can be assumed that MADYMO is producing coherent output. As mentioned in section 3.2 of this thesis, MADYMO makes use of Newton-Euler equations of motion for rigid bodies. The velocity of a point on a body is given as equation (3.24). Assume that for the simplified whiplash case, the body is labeled as "*i*" and the head is labeled by "*j*". Since the body is specified as being connected to the inertial space by a "free" joint, then $\underline{r}_i$ is zero and so is $\dot{\underline{r}}_i$. The "free" joint also has its rotation locked, as specified in the MADYMO input file, so $\underline{\omega}_i$ is also equal to zero. Also, since the head is connected to the body by a rigid pin joint, $\dot{\underline{d}}_{ij}$ must also be zero. It should be noted that, for the whiplash case presented, $\underline{c}_{ji}$ is equal to $-\underline{r}$. With these facts in mind and taking the time based derivative of equation (3.24), the following equation results:

$$\ddot{\underline{r}} = \underline{\alpha} \times \underline{r} + \underline{\omega} \times (\underline{\omega} \times \underline{r}) \tag{4.10}$$

The angular acceleration, $\underline{\alpha}$, is the derivative of the angular velocity, $\underline{\omega}$. Since this system is subjected to an additional acceleration, $\underline{a}$, this term must be added into the equation. Equation (4.10) plus the additional acceleration can be placed into equation (3.25) to give the following result.

$$\sum \underline{F} = m(\underline{\alpha} \times \underline{r} + \underline{\omega} \times (\underline{\omega} \times \underline{r}) + \underline{a}) \tag{4.11}$$

This equation is identical to the vector expression of equations (4.6) and (4.7). Similarly, equation (3.26) simplifies to be a sum of the moments about the center of gravity just like equation (4.8). For these reasons, MADYMO calculates the same angular acceleration and reaction forces, as does the analytical solution.

MADYMO uses a head mass of 4.4 kg and the distance from the pin joint to the center of gravity of the head is 0.0356m. If the head is approximated as a sphere with this radius, then the actual mass moment of inertia is drastically different from the given value of 0.0211 kg-m^2. Since $I_{sphere}=(2/5)mr^2$, and r is given as 0.0356 m, the mass moment of inertia of the head would be 0.00223 kg-m^2, which is extremely small and unrealistic. With $I_{sphere}=(2/5)mr^2$ and an initial θ of 0˚, equation (4.9) reduces to the result that $\alpha_{sphere}=(5/7)a/r$, where "a" is the acceleration equal to 3.2g. Solving for α produces an angular acceleration of 630 rad/s^2, which is almost 3½ times greater than the actual value. This suggests that representing the head as a sphere is not a good idea. MADYMO allows the user to specify a center of gravity and mass moment of inertia for an arbitrary shape. The geometrical shape of the head (i.e., a sphere), does not affect the equations of motion because it is only used for graphical purposes and determining when contact with another body is made.

Chapter 5.0 Course Modules Developed

The following course modules were developed to allow the MADYMO user to gain familiarity with the modeling program and learn the different factors influencing the biomechanics of a situation. Three course modules, whiplash, pilot ejection and windblast, and gait simulation, have been developed. In addition, an exercise that will let students become familiar with the conventions of MADYMO was developed by the author and is described in Appendix B. The "In-House" User's Manual (Appendix A) has been developed to give students help in writing MADYMO simulations. The supplemental manual explains the most used commands on a UNIX operating system when operating MADYMO and also how to run the program. Examples of what the computer user should see on the monitor are given and instructions for setting up a biodynamic model input file are also provided. This manual is very important for the students to read. After reading the "In-House" User's Manual and working through the bouncing ball exercise in Appendix B, the MADYMO user will be ready to work on the following course modules.

5.1 Case Study #1 Whiplash

In the United States, the economic cost of whiplash has been estimated at $4.5 billion dollars (15). This is a substantial amount of money for an injury that is classified as non-life-threatening and minor. Despite the research efforts of automotive manufacturers and other research organizations, the diagnosis of a whiplash injury is very subjective, making it difficult for insurance companies or other defending parties to litigate whiplash claims in court. Since whiplash injuries affect over 1,000,000 people in the U.S. every year, understanding this injury mechanism is very important and will be explored in the following case study.

Case Study #1

Whiplash

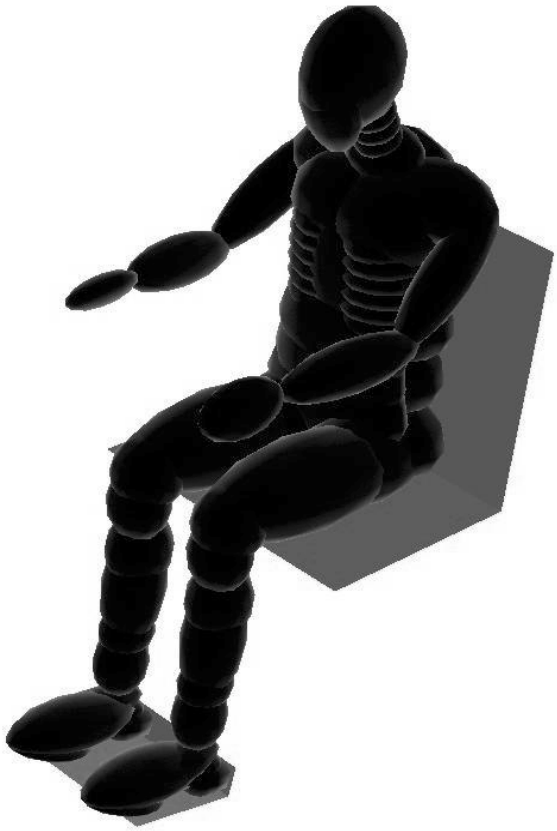

Case Study #1: Whiplash

The Scene:

While traveling from Blacksburg to Charlottesville, VA to watch a Virginia Tech football game, Joe stops at a stop light on Highway 460. The driver in the vehicle behind Joe is busy trying to find a decent radio station when he collides with Joe's 1990 Chevy pickup.

The Outcome:

There is some minor damage to Joe's rear bumper but the other vehicle has substantial front-end damage. After pulling over to the side of 460, Joe notices a lot of pain in his lower neck but received no other injury. The other driver has minor abrasions from his shoulder harness, a headache, and a bruised ego.

The Details:

Vehicle

Joe was wearing a seat belt, which included a shoulder harness and lap belt, but since he was hit from behind, the belt did not play an important role in restraining him except during his rebound from the seat. No airbags are available in the 1990 Chevy pickups. The truck also has an extended cab and a bench seat without headrests. The following seat dimensions have been assumed based upon realistic dimensions. The seat cushion is 42.5 cm. long from front to back and the seat back is only 49.1 cm high. The seat back is oriented so that it makes a 92.2° angle with the seat cushion. The entire seat is then reclined 8.8° about the driver-to-passenger axis that forms the union of the seat cushion and back. Assume the seat padding in Joe's truck is very worn and provides a negligible amount of elastic force or damping.

Victim

Right before the collision, Joe was sitting upright (i.e., not slouching) in his seat and facing forward. Properly positioning the dummy in the seat, due to gravity, will be discussed in the "Instructional Notes." Since he was not expecting the collision, he never anticipated the crash. The collision occurs during a 100-millisecond time frame and the driver causing the accident, the bullet vehicle, is traveling at approximately 7 mph at the time of impact. This corresponds to an acceleration that is 3.2 times the acceleration of gravity. It should be noted that Joe was hit directly from behind. He is 5' 10" tall and weighs 173 pounds.

Questions:

1) Joe claims he suffered whiplash from the accident and wants the other driver's insurance to pay for his medical bills and further chiropractic visits. The seventh cervical vertebrae (C-7) is the part of the neck located furthest from the center of gravity of the head and will, therefore, have the greatest bending moment and possibility for injury. What is the maximum bending moment in the sagittal plane acting on Joe's lower neck (C-7) during the collision?
    a) From your results, what is the likelihood that a clinical whiplash syndrome resulted from this collision?
    b) What criteria did you refer to in order to determine a critical bending moment for whiplash? Include the critical bending moment and cite the reference.

2) Make your MADYMO output produce the Neck Injury Criteria (FNIC) and Neck Injury Predictor (NIJ). What conclusions can be drawn from these injury criteria?

3) How would the results change if the victim's truck were not hit directly from behind, but rather hit from behind in a 15° angle measured clockwise from the direction in which the vehicles were traveling?

4) Assume Joe had a passenger in his truck with the same build as Joe. The passenger, however, is looking at a map and has his head lowered at a 45-degree angle as compared to the driver. What kind of flexion-extension bending moment is his lower neck (C-7) subjected to during the accident? Does this mean it is important to know how the whiplash victim's head is oriented?

5) If Joanne, who is 5' 4" tall and weighs 109 lbs, drove the truck instead of Joe, would she be more likely to get a whiplash injury? Compare the flexion-extension bending moment on the lower neck versus time for Joe and Joanne.

6) Imagine that Joe's older brother, "Big Al", who is 6' 3" tall and weighs 226 lbs, was driving the same Chevy truck. What is the difference in lower neck bending moments in the sagittal plane at C-7 for Joe and Al?

7) The "bullet" vehicle experienced the same g-force but in the opposite direction. The driver was wearing a seat belt composed of a shoulder harness and lap belt. The seat has the same dimensions and properties as those of Joe's truck. Make a comparison between the bending moments on Joe's neck and the other driver's neck.
    a) Who would most likely have the greater chance for injury?

8) Explain how you think neck muscle activation would contribute to the whiplash injury mechanism? A simulation is unnecessary for this question, unless it is performed for extra credit, as stated below.

Extra Credit: Use the CONTROL MODULE in MADYMO to produce a dummy with neck muscle activation and compare to a dummy without a muscular reaction.

Instructional Notes

Basic Model Set Up:

To begin this exercise, make a sketch of the seat. Since the problem states that the elastic and damping forces of the seat padding are negligible, approximate the seat cushion and seat back as planes and choose which directions should be the outward normal to these planes. Choose a dummy from the MADYMO share directory that fits the build of Joe, or use MADYSCALE to scale a 50^{th} percentile male dummy. Become familiar with the dummy's characteristics by reading both the remarks in the dummy data file and also Part 1 of Chapter 1 in the Database Manual.

Create the GENERAL INPUT block and apply the necessary parameters for this case study. Insert a copy of the dummy chosen into the file and make sure to change #1 to 1 throughout the file. This can be done by choosing Search and Replace in the Jot menu system. If #1 is not changed to 1, the file will not run. Because a dummy model has been used, an OUTPUT CONTROL PARAMETERS block will already be inserted into the file. The most common output files requested for the dummy will already be specified, but it is recommended that the unnecessary output parameters be deleted or an asterisk* should be placed before each line. This will cause less output files to be generated when a file is run. Save the file and try to run it with a TE=0.0. When viewed with MAPPK, the dummy should be shown in a seated position. Press the function key corresponding to the coordinate system axes to get a better understanding of the directions needed for modeling parameters.

A seat should be created in the INERTIAL SPACE because the acceleration is going to be applied to the dummy and not the seat in the truck. Use the previously drawn sketch with measurements to create two planes representing the seat cushion and back. It is beneficial to have the intersection of the planes located at (0, 0, 0) in the inertial space. Once the seat planes have been inserted, run the file again with TE=0.0, and view the

model using MAPPK. The center of the dummy's pelvis (H-point) should be in the middle of the intersection of the seat planes. The "H-point" will be used to place the dummy in the seat since it is the center of the parent body (body 1) of the system. It might also be necessary to create a floor plane and heel plane for the feet so that they do not become unstable during the simulation. If the acceleration pulse is strong enough, the feet and legs might swing rearward through the seat cushion and lower body. For this case study, a foot plane and heel plane is optional, since it is possible to LOCK the two knee joints, hip joints, and ankle joints and not affect the whiplash severity to a large degree (approx. 2%). The lower legs will not play an active role in the whiplash injury mechanism. If the joints mentioned above are locked, disregard the "Floor Plane/Heel Plane" contact interactions described in the Dummy Positioning section. However, it is recommended that floor and heel planes be added to the model. Refer to the following section for dummy positioning.

Dummy Positioning:

The dummy is going to be placed above the seat, and the effect of gravity will cause the dummy to be properly situated in the seat. The first step is to place the dummy just barely above the seat planes using the H-point under the JOINT DOF command in the data file. JOINT DOF is located within the SYSTEM block. Change the position (x and z) of the dummy and set TE=0.0. Check the new position using MAPPK and keep changing the joint position until the dummy is located just above the seat. Once the dummy is located just above the seat, apply an acceleration field to represent gravity. This is performed in the FORCE MODELS block. Change the simulation end time (TE) to a value large enough for the motion to be finished at the end time (1 or 2 seconds). Some of the joints should be locked so that they do not move during the dummy positioning. The pelvis, hips, and knees should not be locked, and using JNTPOS in the OUTPUT CONTROL PARAMETERS block, specify these joints to produce output. Lock all other joints that are labeled free by changing FREE to LOCK. Change all joints specified as FREEROTATIONS to LOCKROTATIONS. Note that some joints (all

brackets, sensors, and load cells, as defined by MADYMO) are always locked and they should never be unlocked. The next step is to specify the contact interactions between the dummy and the seat. The following contact interactions must be specified:

Seat Cushion to Lower Torso
Seat Back to Lower Torso
Seat Back to Upper Torso Back
Floor Plane to Left/Right Foot
Floor Plane to Left/Right Heel
Floor Plane to Heel Shoe Sole Left/Right
Floor Plane to Front Shoe Sole Left/Right
Heel Plane to Left/Right Heel

Now run the file and view the simulation with MAPPK. The dummy should have "sunken" into the seat due to gravitational force and should not be moving when the simulation has completed. Refer to the output JNTPOS and write down or copy the end positions of the specified joints. This will be the new starting position (at T0=0.0) for the dummy. Make sure to keep these values in order and change the joint positions in the original data file. Look at the first set of data points for time equal to zero. If this value does not correspond to the initial value, make sure the correct joints are being evaluated or recheck the data file for errors. When all of the pre-simulation final joint positions for joints 1, 23, 24, 27, and 28 have been entered, it is time to apply the crash pulse.

Application of the Crash Pulse:

Once the dummy is properly situated in the seat, acceleration representing the crash must be specified. In the FORCE MODELS block, just below the function for gravity, input another force for the –x direction. This should be applied to system 1 and have a value as stated in the crash details. Change all of the joints that were locked during the pre-simulation back to free or freerotations. Remember to leave the "always

locked" joints locked at all times, and lock the knee joints if a floor/heel plane has not been created. The end time should now be changed to an appropriate value (0.3 s) to analyze the biodynamic model. The output files necessary for the accident investigation should be specified in the OUTPUT CONTROL PARAMETERS block. Save the file and run it using the command specified in the "In-House" User's Manual.

Biodynamic Model Analysis:

Use MAPPK to view the kinematic output, and make note of any unusual ellipsoid movements or interactions. If everything seems to be modeled correctly (i.e., ellipsoids do not pass completely through other objects), view the output files that have been specified in the output block of the data file. The peak file contains the injury parameters and all joint forces and torques. Make note of the moments on the lower neck and compare the values for all of the different cases. Time history plots can be made using MAPPT. Refer to the MAPPT user's guide for an explanation of this program.

Lessons Learned:

This case study should allow the student to get a better understanding of the whiplash injury mechanism and explore the different situations that might be present in a forensic investigation. The user should also become more fluent with MADYMO and learn its capabilities. The dummy positioning process is applicable to any situation involving a person sitting in a seat, and it can also be adapted for other positioning processes such as an individual standing on a surface. MAPPK is a great visual learning tool. The use of MAPPT is helpful in understanding the time frame of injury and analyzing the output. The use of available MADYMO databases is very important and useful to saving time and effort.

5.2 Case Study #2 Pilot Ejection and Windblast

Combat situations often require pilots to abandon an aircraft by ejecting out of it. However, avoiding a life-threatening situation through pilot ejection can subject the ejection seat occupant to large windblast forces. Nearly half of the ejections occurring during combat situations lead to flail injury or death (16). Injury can result from force loads on body tissue or, more commonly with limb dislodgement due to flail, impact with intercepting surfaces, and hyperextension related mechanisms (17). For these reasons, minimizing flail injuries is of major importance to pilots and researchers. The following case study explores pilot ejection and the injuries possible due to windblast.

Case Study #2

Pilot Ejection and Windblast

Case Study #2: Pilot Ejection and Windblast

The Scene:

During combat or even routine exercises, it sometimes becomes necessary for a jet aircraft pilot to eject from the aircraft to avoid a life-threatening situation. However, pilot ejection, in itself, is a dangerous procedure that often results in pilot injury or death. Once the pilot fires the ejection mechanism, he/she is thrust upward, as the canopy is removed, and suddenly is hit by an extreme amount of windblast force (16). The extent of windblast is a function of the speed of the jet and the pilot's ejection angle. During a dogfight in Iraqi air space, jet fighter pilot Bob Doe and co-pilot Maverick Johns (fictitious characters) were hit by artillery fire and forced to eject from the aircraft. Each pilot cleared the jet canopy safely and had a mechanism that triggered the opening of a parachute upon descent. This mechanism was designed for instances in which a pilot was knocked unconscious and could not pull the parachute rip-chord.

The Outcome:

Ground forces rescued both pilots. However, Bob was pronounced dead due to massive head injuries and internal bleeding and Maverick was found unconscious with internal bleeding, broken humerus bones, dislocated shoulders, and torn muscle tissue.

The Details:

Bob and Maverick have the same build, and with their flight suits and gear can be approximated at 222 pounds. They are also comparable in height at 6 feet 2 inches. During the time of ejection, the F-14 Tomcat had slowed considerably and was traveling at 662 mph. This speed corresponds to Mach 0.9 at an elevation of 10,000 feet, with the speed of sound being 735 mph. The jet was traveling at 0 º compared to the horizon (i.e., parallel to the ground) and laminar airflow can be assumed. Maverick braced himself for ejection by leaning his head back by 30˚, as compared to Bob, so that it was closer to the

headrest of his seat. Bob, however, was not leaning his head back. Each pilot also had his arms resting on his thighs. The ejection seat should be represented by planes, and the occupants should wear a shoulder harness and lap belt. The ejection seat uses a hydraulic mechanism to start the ejection process and is followed by the firing of a rocket booster to propel the occupants out of the aircraft, accelerating them from 0 mph relative to the aircraft to approximately 33 mph as they leave the vehicle, in 160 ms (see Instructional Notes). The influence of the aircraft velocity on the pilot is taken into account by the windblast force, which will be discussed in the Instructional Notes.

Questions:

1) Plot a graph of flexion-extension bending moment on the lower neck (C-7) in the sagittal plane vs. time for both pilots during the ejection process. When does the maximum occur? Describe any unforeseen results.

2) Since MADYMO makes use of several injury parameters, find the Gadd Severity Index, Head Injury Criterion (HIC), Viscous Injury Response (VC), 3ms criterion, and Neck Injury Criteria (FNIC).
    a) What does each injury index tell you about the pilots' possibility for injury? Give values for the injury parameters requested and find the critical values.
    b) Would you expect the injuries stated in The Outcome section of this case study?
    c) What is the percent difference between Bob's HIC value and Maverick's HIC value due to their differing anticipation of the ejection and resulting head position? Explain how both pilots HIC values could be lowered.

3) Find the forces and torques in the shoulders and elbows due to windblast.

4) Assume that the jet was traveling at Mach 0.7 during occupant ejection. Simulate pilot ejection at this speed and compare with the results of the Mach 0.9 simulation.
    a) Repeat questions 1 and 2.
    b) What are the percent differences between the injury indices for the different jet speeds?
5) What changes could be made to the occupant's ejection so that the pilot sustains fewer injuries? For example, could you design a safer seat or better restraint system?

Extra Credit:

Create an ejection seat that has armrests and handgrips and using point restraints, connect the pilot's hands to the grips. In experimental studies, a pilot's average grip retention was found to be 600 pounds (17). This means that the pilot has 100% chance of letting go of the armrest grips if his arms are subjected to 600 pounds of dislodging force. Find the difference in results between a simulation using armrests and one without.

Instructional Notes

Basic Model Set Up:

MADYMO has a pilot ejection without windblast already modeled in the applications directory. The purpose of this pre-developed computerized biodynamic model was to find the ejection seat angle that most closely produces the same ejection trajectory as experimental studies. It makes use of MADYMIZER, and although the student can use MADYMIZER for the model setup, it is not needed for this exercise since the purpose of this case study is to find the pilot's chance for injury due to windblast. The following instructions are valid if MADYMIZER is not used.

Since the model has already been created by TNO/MADYMO, the user should change directories to find the ejection data file. This can be done by typing the following on a UNIX system (refer to the "In-House" User's Manual, Appendix A, for the typographical conventions and further instructions):

$ **cd usr/Local/madymo_541/share/appl/madopt**
$ ls
$ jot ejection_inp.opt
$ cd

Copy the file into the user's main directory so that it can be edited. Since MADYMIZER is not going to be used, certain changes to the data file must be made. After the force models block, there should be a sensors command. This needs to be changed to a TRIGGERING CONDITIONS block that has the same reference signals as mentioned in the original SENSORS block (see MADYMO User's Manual). Also, the output parameter HIC must be slightly altered. The "Y{1}" should be removed and an identifier (ID) can be inserted if needed. Change the run time of the program (TE) to 0.0 seconds and run the file. View the graphics file with MAPPK and the user should see a 95th

percentile male dummy seated in an ejection seat. The "Ground-Rail-Structure" also visible, is used to represent the experimental ejection mechanism. Notice the position of the dummy's arms and hands.

The biodynamic modeler should view the ejection control module in the input data file to become familiar with the ejection procedure. After the ejection seat and pilot travel up the rails by translation only, at 160 ms a rocket booster fires at the bottom of the seat and propels the occupant out of the jet at 33 mph relative to the aircraft. The seat is then allowed to rotate because of the joints and control modules specified in the input data file. With this ejection model, the pilot's ejection motion has been validated by experimental studies (18) and this will allow MADYMO users to attain better simulation results. Change the end time of the program to 0.2 ms and view the motion of the ejection seat occupant. Notice that he "slouches down" and needs to be restrained by a lap belt. Create a belt restraint that attaches to the corners of the intersection of the seat back and seat cushion and then connects to the lower torso of the dummy. As an example, view the input data file used for the whiplash case study involving a driver with a lap belt. If the user has not previously created such a model, one can be found in the application directory of MADYMO.

Dummy Contact Interactions:

The current model needs to be modified so that the arms do not go through the dummy's legs or any other body part. Since the dummy's left and right arms may contact each other, the biodynamic modeler should define contact interactions between them. Also, a contact with the legs should be defined. If this is done, however, the lower arm must be reoriented so that it is not initially inside the ellipsoid representing the pilot's thigh. Without the initial position of the lower arms unchanged, they will immediately "bounce" out of the legs when the program begins to run, and this is not correct. Only a minor modification is needed. Contact interaction of the arms with the seat cushion and seat back can also be defined, but since the geometry of the actual ejection seat is

unknown, it is recommended that no contact be specified. Run the program and view the graphical results using MAPPK. Notice any strange contacts or ellipsoids penetrating other surfaces abnormally. Make appropriate modifications until all the necessary contact interactions have been specified.

Application of Windblast Forces:

To this point, the ejection seat occupant is not subjected to forces from windblast. Therefore, this is not an accurate simulation of a pilot ejection during an emergency situation. In addition to the force generated by the ejection mechanism and rocket booster, the pilot is struck by extreme amounts of wind force due to the velocity of the aircraft. In Dr. Schneck's article, "Studies of Limb-Dislodging Forces Acting on an Ejection Seat Occupant," the aerodynamic loading to which a pilot is exposed during high-speed ejections is found as a function of the Mach number (M) and angle of attack (α). The following equation can be used to approximate the forces due to windblast for all body parts (17):

$$F = 1148 \cdot M^2 \cdot \sin^2 \alpha \tag{4.21}$$

The force is given in pounds force and must be converted to Newtons for MADYMO. Students should obtain a copy of the journal article from which this equation is derived and become familiar with the assumptions made. It will be noted that the equation was derived for a pilot's forearm and, therefore, uses specific body dimensions that are not common to every individual or body part. Also, the ejection seat occupant's forearm position changes with respect to time and would, therefore, not be subjected to a constant force. However, for the purpose of this model, this equation can be used for all body parts because the complicated fluid dynamics problem involved with pilot ejection is beyond the scope of this case study.

To find the times at which certain body parts, such as the head, chest, arms, and legs are subjected to windblast, view the kinematics file using MAPPK. Pick a reference point that might be a good approximation of the top of the jet canopy or fluid boundary layer, such as the upper surface of the "Rail-Structure," and find the times that each ellipsoid passes the reference point. These times will be used as the times where a windblast force will strike the specific body part. In the CONTOL MODULE, define the windblast force as a function of time using the FUNCTIONS command. This can be performed using a reference signal and body actuators that supply the specified force to a body at the specified time. Consult the MADYMO User's Manual for the commands needed for setup of the control module. Change the run time to 0.3 ms and view the results.

Biodynamic Model Analysis:

The purpose of this simulation is to find the behavior and chance for injury due to windblast for the ejection seat occupant. The biodynamic modeler must specify the needed force, moment, and injury parameter output in the OUTPUT CONTROL PARAMETERS data block. There are several injury parameters (indices) that should be included in this model since they indicate the chance of injury. It is up to the modeler to specify the correct injury indices and needed results to complete the Questions section of this case study.

Lessons Learned:

Upon firing an ejection seat mechanism to avoid death in a jet aircraft, pilots are then subjected to another dangerous situation, windblast. The motion of an ejection seat occupant can be modeled using MADYMO and some insight into the injuries common with pilot ejection can be formed. The biodynamic modeler should learn that the extent of injury is very dependent upon the wind speed or Mach number of the jet at pilot ejection. To a lesser degree, it is also dependent upon the pilot's angle of attack.

Several injury parameters will be explored and students should learn the critical values for each index so that chance of injury can be determined. The student should also find that the pilot's seating position or preparation for ejection will change the resulting forces and torques placed on the pilot's body. Using MADYMO, different safety precautions can be explored without subjecting experimental subjects to extensive injury. Modeling programs, such as MADYMO, will help researchers and engineers save lives and better prepare pilots for dangerous circumstances.

5.3 Case Study #3 Gait Simulation

Gait analysis is a major topic in biomechanics. Often times, gait analysis is performed to help individuals with walking disorders or abnormal walking traits; it can also be used to enhance athletic performance.

The following case study will explore gait simulation and a clinical syndrome referred to as plantar fasciitis. Contact forces on the bottom of a person's foot will be analyzed and conclusions will be drawn as to the possibility of a plantar fasciitis injury. Plantar fasciitis is a swelling of the protective tissue surrounding muscle fibers. It is a cumulative trauma disorder that is believed to be brought about by obesity or harsh walking environments (19). This case study involves a railroad worker who walks on ballast of varying sizes, and this situation is a current area of interest in the railroad industry.

Case Study #3

Gait Simulation

Case Study #3: Gait Simulation

The Scene:

Kevin is a stationmaster for Jarbidge Railroad and has worked with this company for 17 years. The duties of his job have changed slightly since he was hired, but the amount of time spent working in the rail yard has not. Most of Kevin's work involves inspecting trains and equipment and he spends each workday walking on large sized gravel, referred to as ballast.

The Outcome:

Kevin has gone through several pairs of hard-soled boots in his career and has gradually weakened the muscle tissue in his feet. A doctor from Twin Falls Occupational Health Clinic has diagnosed Kevin with a condition referred to as plantar fasciitis. Plantar fasciitis is a swelling of the protective tissue surrounding the muscle fibers in the bottom of the foot (19). With every step, Kevin experiences dull but irritating pain in his feet. After watching a commercial from Kobayashi & Sons Law Firm, which specializes in personal injury claims, Kevin decides to make an appointment for a free consultation with the law firm. Since Jarbidge Railroad is a large and profitable company, the lawyers talk Kevin into suing the company for his previous medical bills, future rehabilitation, and large amounts of workmen's compensation. It was later noticed by Kobayashi & Sons Law Firm, that over 500 rail workers have made claims of developing plantar fasciitis, a type of cumulative trauma disorder (fatigue failure).

The Details:

Kevin

Kevin has gone through several pairs of hard-soled boots in his 17 years of service with Jarbidge Railroad and often complains about his "aching feet." Kevin

weighs 168 pounds and stands 5'9" tall. His normal walking speed is around 3.6 mph and his step length is about 3 feet.

Ballast

Jarbidge Railroad buys its ballast from a Nevada rock quarry that produces flat surfaced granite stones of varying sizes. This ballast is chosen specifically for its flat surface qualities that provide a better load distribution for the feet. Each piece of ballast has a different geometry, but the following sizes are used for an average representation of the ballast:

Size	Length (cm)	Height (cm)	Width (cm)
Large	8	2.75	5.45
Medium	5	2.75	3.5
Small	3.5	2	2

An ellipsoid is a good approximation of the shape of the rock, with the sizes mentioned as the appropriate axis lengths. Assume that the ballast is extremely hard compared to Kevin's boots or bare feet (i.e., the ballast is infinitely stiff). The "material properties" of Kevin's feet will be found in the MADYMO share directory.

Questions:

1) Kevin claims that he suffers from plantar fasciitis and cannot work effectively. Find the contact forces (elastic force + damping force) acting on the sole of one of Kevin's feet during normal gait for all three sizes of ballast.
    a) What are the contact forces on his foot? Make a plot of the contact force versus time.
    b) At what time, after or during heel-strike, do the maximum forces act on Kevin's foot and where? Explain the major force peaks in the force vs. time plot.
    c) Compare these forces to his body weight. Do they seem reasonable? Explain.

2) Research the conditions necessary for plantar fasciitis to develop. Provide the title, author, and publication date of the article or book referenced.
    a) With this knowledge, is it possible for Kevin to have clinical signs of plantar Fasciitis as a result of his work environment?
    b) What other injuries might occur due to the quality of the walking surface?

3) What is the average walking speed you used for the simulation? Provide a plot of Kevin's walking speed versus time.

4) What were the difficulties encountered in simulating gait and how did you overcome them? How should the model be changed to accurately find the forces and pressure distribution on the bottom of Kevin's feet?

Extra Credit: How do the results change if "Kevin" is a 120 pound female?

Instructional Notes

Basic Model Set Up:

A sketch of the system analyzed should be drawn to attain a better understanding of the difficulties in creating this biodynamic model.

Create the GENERAL INPUT block and apply the necessary parameters for this case study. Insert a copy of the human model into the file and make sure to change #1 to 1 throughout the file. This can be done by choosing Search and Replace in the Jot menu system. If #1 is not changed to 1, the file will not run. Because a human model has been used, an OUTPUT CONTROL PARAMETERS block will already be inserted into the file. The most common output files requested for the dummy will already be specified, but it is recommended that the unnecessary output parameters be deleted or an asterisk* should be placed before each line. This will cause less output files to be generated when a file is run. Save the file and try to run it with a TE=0.0. When viewed with MAPPK, the dummy should be shown in a standing position. Press the function key corresponding to the coordinate system axes to get a better understanding of the directions needed for modeling parameters.

Since a simulation of gait must be performed, the user should define a walking surface. Initially, it is recommended that a plane in the inertial space approximate the walking surface since it will be easier to define contact interactions with the feet. Define contact interactions between the ground and feet using the ellipsoid or facet surfaces on the human model and the plane in the inertial space.

Dummy Positioning:

Run the current file and view the kinematics file using MAPPK. Most likely, the plane representing the ground will be intersecting the human at his pelvis. This is due to the pelvis (H-point as with the dummy models) being located at the coordinates (0,0,0) in

the inertial space. If the plane was created using a z-coordinate other than 0, the plane will not intersect the human at the pelvis. It is recommended that the plane be vertically located at z=0 and the human's position be specified accordingly. This will cause fewer values to be changed when positioning the dummy. With the ground located at z=0, alter the JOINT DOF for the pelvis (joint 1) to place the human just above the ground.

In the FORCE MODELS data block, apply an acceleration field representing gravity. To see if contact has been specified correctly, change the end time of the program (TE) to a value large enough for the dummy to make contact with the ground when gravity is applied. The human model should contact the ground and will, most likely, bend over due to gravity.

Application of Motion:

Once the human model is created and contact has been defined correctly, motion that simulates walking should be specified. This can be performed in a MOTION block that constrains the degrees of freedom (JOINT DOF) for the joint to move with the user specified kinematics. The biodynamic modeler must research different gait analysis reports and technical journals to find data for the joints of the lower extremities. It is an extremely difficult task to find data representing pelvis, hip, knee, and ankle angles associated with gait for both the right and left legs. Graphs that plot the angles mentioned above are available, but actual data points, which are required by MADYMO, are hard to find.

In order to gain insight into human gait and acquire the necessary information needed for motion in MADYMO, the user should download a free software tutorial called SIMM (Software for Interactive Musculoskeletal Modeling). This program has been developed by Musculographics and a free tutorial modeling the motion of a human leg , based on inverse dynamics, can be downloaded onto a PC as follows (1):

1) Go to Musculographics web page at **www.musculographics.com**
2) Click on ***SIMM Download Area.***
3) If using a Windows (95, 98, NT) operating system, choose ***SIMM Tryout (2.9 MB, free Windows version)***.
4) Follow the installation instructions.

Once the program has been properly downloaded, the user should explore the "Demo Leg Model" and acquire data for the joint angles of the pelvis, hip, knee, and ankle. Since only one leg is modeled with the SIMM tutorial, the user must find the appropriate location of the other leg compared to the modeled leg. For example, if a gait cycle is defined as right heel-strike to right heel-strike (0% -- 100%), at what percentage of the gait cycle is the left leg when the right leg is at right heel-strike? When this is found, insert the correct motion for the hip, knee, and ankle into a MOTION block for both legs.

Since this gait simulation is only needed to find the forces on the foot, start the simulation at heel-strike. In other words, the first data point specified in the MOTION block should be for the gait cycle % corresponding to heel-strike. The motion of the pelvis cannot be specified as a prescribed joint motion because it will restrict the pelvis so that it will not react properly during a gait simulation. However, the pelvis should be given an initial rotation about the y-axis and an initial velocity in the x-direction. Specifying the initial values for the pelvis and not restricting its motion will allow the correct interaction to be transmitted from the ground to the pelvis. Once the prescribed joint motions have been defined, perform a "zero-run" (TE=0) to see if the initial position of the human model is correct in relation to the ground. Make sure there is not too much initial penetration between the feet and ground and that the legs are oriented properly with respect to each other. Fix the model accordingly. Once the initial position of the human model looks correct, change the run time to a value large enough for the foot being analyzed to go from heel-strike to toe-off. If the model trips, slips, falls, or does not walk correctly, the prescribed motion for the hip, knee, or ankle might have to be

altered. Before doing this, however, the user should try varying the initial conditions (y-rotation, x-velocity, etc.) of the pelvis.

Helpful Hints:

Simulation of gait is very complicated and involves several different actions by the human body. In order to compensate for the actions of the body that may seem trivial or are not realized, it is useful to specify certain parameters in the MADYMO input file so that gait simulation is possible. Locking different joints of the spine might be needed to simulate walking without the human model bending over so far that he/she falls. Do not over constrain the spine, however, because the model will appear to stop or fall over backwards. The gait simulation also relies heavily on the walking speed and initial angle of lean (pelvis y-rotation), so these parameters should be altered until a walking motion is visualized with MAPPK.

Ballast Modeling:

Once the human model walks successfully across the plane, insert a null system, representing the ballast, into the model. Use the specifications given in the "The Details" and create the ballast out of ellipsoids. The ground, comprised of ballast, can be modeled several different ways, with the ballast being uniform or non-uniform. It is up to the modeler on how the surface is represented. The area covered by ballast is also optional. The area under the foot being analyzed should be covered by ballast and there should also be a surface for the other foot to contact during toe-off and consequent heel-strike.

It is important to specify the correct contact interactions between the foot and ballast. Since the contact is now associated with the ballast and not the plane in the inertial space, delete the contact between the feet and the plane. Insert the appropriate contact interactions between the feet and the newly created null system (ballast).

Biodynamic Model Analysis:

The purpose of this simulation is to find the forces on the feet due to walking on ballast of different sizes. To find the necessary forces, the user must specify that they be output into a corresponding file. This is performed in the OUTPUT CONTROL PARAMETERS data block and is located under the command FORCES. The force associated with contact between the foot and ballast should be specified for output. The data can then be viewed in a ".frc" file. Since two or more ballasts may contact the foot, add the contact forces (elastic force + damping force) due to each contact for each specific time. This force data can then be plotted versus time using Excel or another graphing program. MAPPT is unable to add curves together and is, therefore, unable to process the forces due to more than one contact per body. Always compare the results with published values or figure out if the results are reasonable.

Lessons Learned:

Walking is a very complicated process that some people take for granted since it comes naturally to those not inflicted with a walking disorder. The biodynamic modeler should become familiar with human gait and learn the processes involved in walking. This case study makes use of both SIMM and MADYMO software to allow students to gain insight into one of the everyday activities of the body. Although it may seem trivial to find the forces on the feet during gait, it is a complicated modeling process that would be even more difficult without the use of the human model, recently developed by MADYMO. The human model, only available to academic institutions, is a valuable tool for analyzing biomechanics.

The user should learn the capabilities of MADYMO and also some of its inherent inadequacies. Joint motion may be prescribed in any direction, but this will restrict all joint degrees of freedom for the specified joint. When the motion is known only in one direction, i.e., velocity in the x-direction, MADYMO will not allow a single joint degree of freedom to be fixed during the simulation unless the joint has only one degree of

freedom. This is a problem when performing gait analysis. Students should also have found that for a true analysis of Plantar Fasciitis, a finite element model of the foot should be developed. This, however, is beyond the scope of the current biodynamic modeling course.

Chapter 6.0 Results and Discussion

6.1 Whiplash Results

Whiplash injuries may be caused by forces that occur in everyday activities, and since the precise mechanism of injury is not yet clearly understood (if, indeed, there is one), it is difficult to predict if whiplash will occur. Three different vehicle occupants were analyzed in an automobile collision with the use of MADYMO. Rear impact, frontal impact and oblique impact, all at an acceleration/deceleration 3.2 times gravity, have been explored, as well as an occupant whose head is initially leaning forward 45 degrees in the sagittal plane. Each case involved an occupant who did not anticipate the impact due to a collision and assumptions concerning the vehicle and dummy properties have been made (see section 5.1).

A 50^{th} percentile male, 95^{th} percentile male, and 5^{th} percentile female were found to have a maximum flexion-extension bending moment at the lower neck (C-7) of 62.6 Nm, 82.7 Nm, and 42.4 Nm, respectively. Each occupant experienced rear impact and an acceleration 3.2 times gravity. The 50^{th} percentile male, who was described as a passenger looking down at 45 degrees from the standard seated dummy, is subjected to nearly half of the flexion-extension bending moment of the same dummy in the standard position with a value of 35.3 Nm for the lower neck. It was also found that the passenger's maximum torque on C-7 occurred with the neck in flexion while all of the other dummies produced maximums in extension. Shown in Figure 6 is the flexion-extension bending moment at C-7, for each of the dummies discussed, during the duration of the collision.

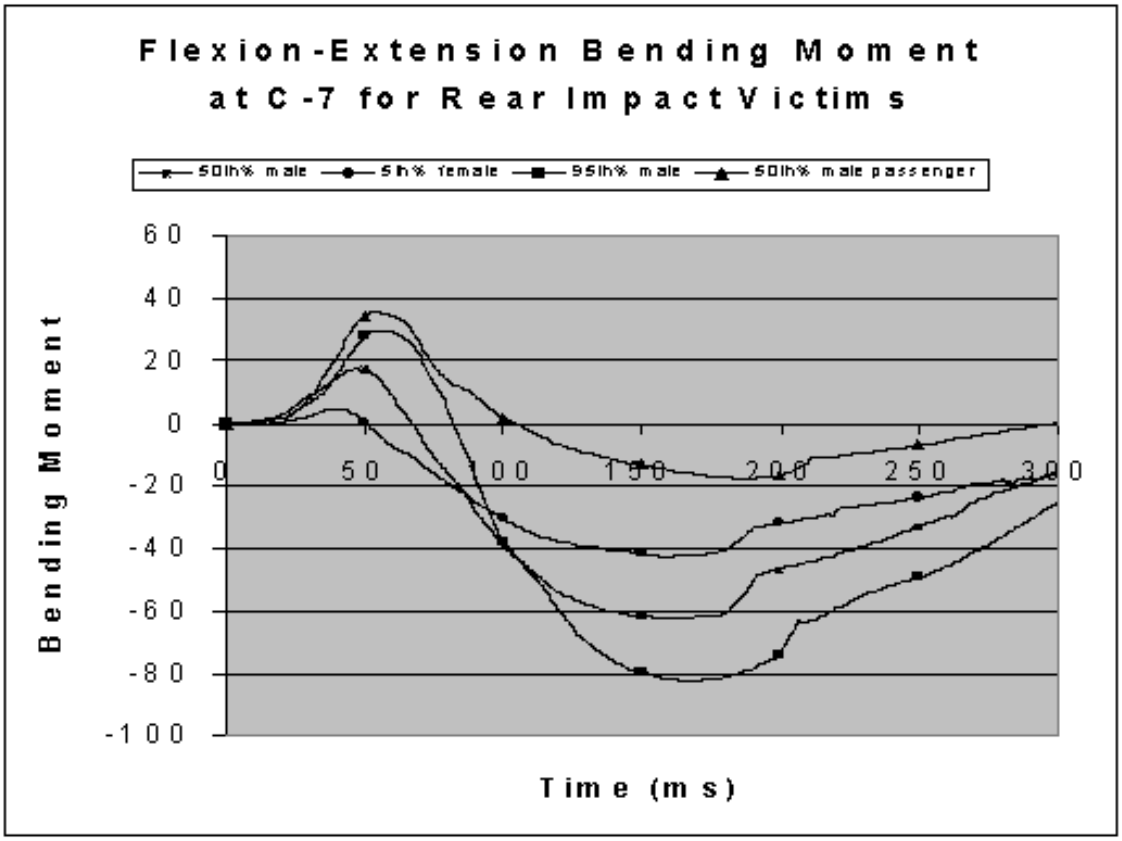

Figure 8: Flexion-extension bending moment on the lower neck for whiplash victims in rear impact

From Figure 8, it is evident that different drivers subjected to the same collision will experience different torques on the neck. Assuming that each individual is in reasonably good health to begin with, the taller person (95^{th} percentile male) is more likely to be affected by whiplash. Shown in Figure 8 is also a large difference in bending moments between the 50^{th} percentile driver and passenger. Therefore, it is very important to know the seating position and posture of the vehicle occupant to accurately determine the whiplash severity. The 50^{th} percentile male driver of the vehicle causing the collision (bullet vehicle), is found to have a 64.2 Nm bending moment about C-7 in the sagittal plane. The 50^{th} percentile male driver experiencing rear impact at a 15º angle from the direction of travel is subjected to a flexion-extension bending moment of 62.4 Nm, which is nearly identical to the torque produced from direct rear impact.

The critical flexion-extension bending moment causing whiplash is not well known. However, a value of 57 Nm is suggested by TNO Automotive (7), based on studies conducted by Mertz and Patrick (20). Using this criterion, only the 50^{th} percentile male driver experiencing frontal, rear, or oblique impact and the 95^{th} percentile male driver will likely develop a whiplash injury.

Comparing injury indices for this case study yields no substantial results, as all of the parameters chosen for output (HIC, 3MS Maximum, FFC, VC, etc.), excluding the Neck Injury Criteria (FNIC), are well below any critical value.

The whiplash cases analyzed make use of dummies developed by TNO/MADYMO. Each dummy has been validated with component tests and tests on the complete dummy. Specifically, component tests on the neck for forward bending, rearward bending, and lateral bending, were performed by TNO Automotive to verify the model behavior (2). Also, the whiplash results found in this thesis are comparable to results found in "Determination of a Whiplash Injury Severity Estimator for Motor Vehicle Occupants Involved in an Automobile Accident," which makes use of the

Articulated Total Body (ATB) model (14). The worst correlation between the two simulations occurred with the 5th percentile female model. The maximum flexion-extension bending moment for the lower neck, found using MADYMO is almost 25% lower than the ATB predicted value for a similar model. However, the flexion-extension bending moment for the 95th percentile male is less than 2% different. It should be noted that the ATB model uses only 1 neck segment while MADYMO uses 5 neck segments, and the orientation of each dummy might have been slightly different. This will affect the results as shown by comparing the 50th percentile male passenger against the 50th percentile male driver seated in an upright position. The passenger's head is rotated 45 degrees forward in the sagittal plane, compared to the upright dummy, and the maximum flexion-extension bending moment on his lower neck is found to be 44% lower. This shows that slight changes in the seating orientation or posture of an occupant will drastically change the resulting bending moments. The results between the two different modeling programs show similarity. To further justify the validity of the MADYMO dummies, they are continually updated through research conducted by TNO Automotive.

6.2 Pilot Ejection Results

Nearly half of the pilots forced to eject from an aircraft will be injured or killed. Case study #2 explores the injuries associated with windblast and allows the student to become familiar with the control module of MADYMO.

A windblast force was placed upon certain parts of a 95th percentile male dummy at certain times with the use of a control module. Since each body part is not subjected to the wind force at the same time, estimates had to be made so that the force was applied at the appropriate time. The estimation was done by viewing a validated pilot ejection model already developed by TNO/MADYMO. The flight trajectory of a pilot in an ejection seat was shown to have good correlation to experimental results and has been validated by TNO/MADYMO (18). A reference point was chosen, with the use of MAPPK, to correspond with the top of the jet canopy or fluid boundary layer. As the dummy was ejected upwards, times at which each critical body part passed the reference point were recorded. The data points served as input to the control module of the input data file and a windblast force was specified. This force has been derived by Schneck (17) and is discussed in section 5.2 of this thesis. A lap belt was added to the pre-developed model so that the dummy did not "slip" off of the ejection seat as it moved upward. This also allowed the file to run for a longer time so that the behavior of the ejection seat occupant could be better analyzed.

The final model shows the dummy translating upward on the ejection seat for 160 ms at which time a rocket booster on the bottom of the seat fires. The dummy's head is subjected to windblast and then the chest, and so on. Of course, the windblast changes the dummy's ejection motion and this leads to different injury parameters. For this reason, the Mach number directly affects the forces placed on the dummy since it is a critical value used to determine the windblast force (17).

A Mach number of 0.9 will cause a flexion-extension bending moment on the lower neck (C-7) of 402 Nm, more than 7 times that considered “safe” from the point of view of whiplash injuries. If the pilot has prepared for ejection by reclining his head towards the seat back, the torque created is less at 317 Nm but still more than 5.5 times “safe” values (7). Illustrated in Figures 7 and 8 are the differences between pilots with different head positions or neck extension/flexion.

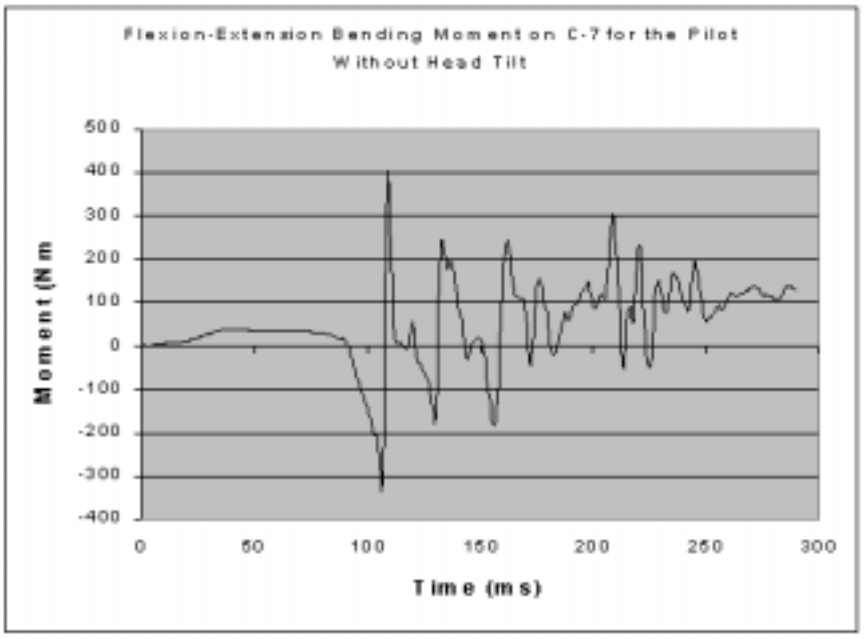

Figure 9: Flexion-extension bending moment on C-7 for the pilot who does not prepare for ejection based upon his head orientation

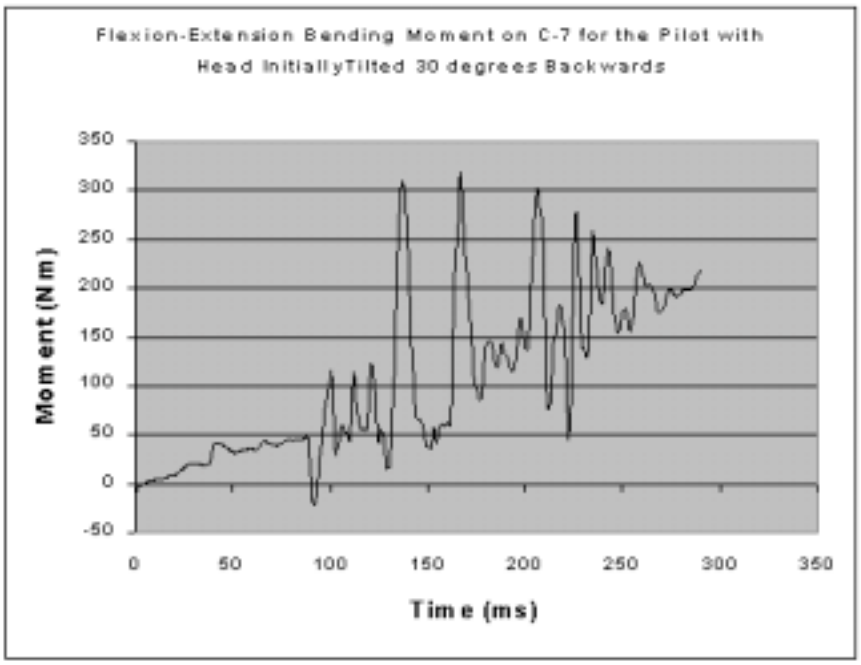

Figure 10: Flexion-extension bending moment for the pilot who prepares for ejection and leans his head 30º backwards

Comparing Figures 9 and 10 illustrates that the pilot leaning his head back has less chance of injury since he has "prepared" for ejection. Likewise, wearing a helmet or a seat with a better head restraint will cause a lower torque to be placed upon the neck.

Since the jet speed, or Mach number, changes the amount of windblast force, simulations using Mach 0.9 and 0.7 have been performed. The bending moment on C-7 in the sagittal plane was found to be 402.4 Nm for Mach 0.9 and 275.2 Nm for Mach 0.7. This is nearly a 32% difference in torques compared to a 22% difference in Mach numbers. The maximum moments also occur at slightly different times of the ejection process, with a bending moment of 400Nm at 110 ms for the pilot traveling Mach 0.9 and 263 Nm at 140 ms for the pilot traveling Mach 0.7. This can be seen in Figures 11 and 12.

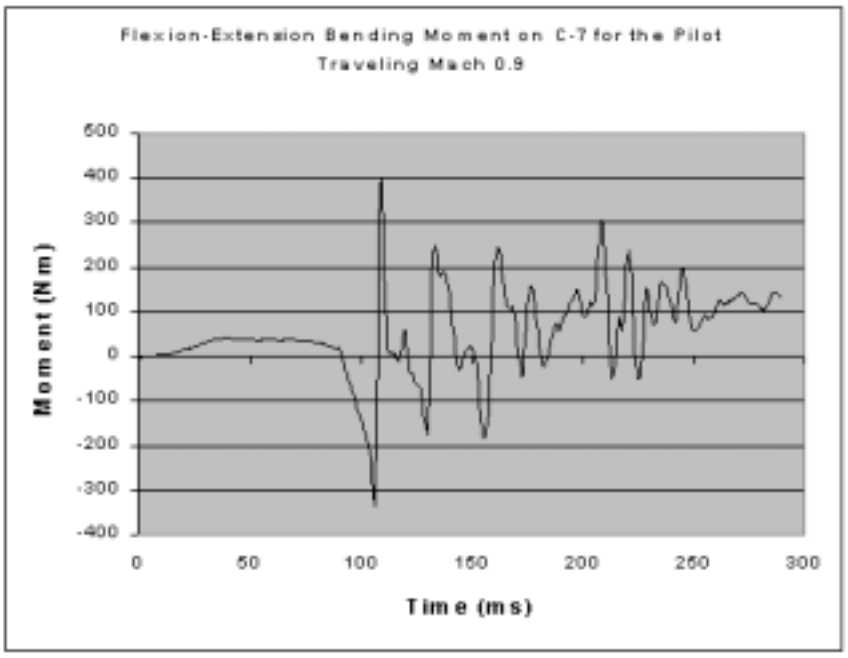

Figure 11: Flexion-extension bending moment on C-7 for the pilot who is traveling at Mach 0.9 at the time of ejection

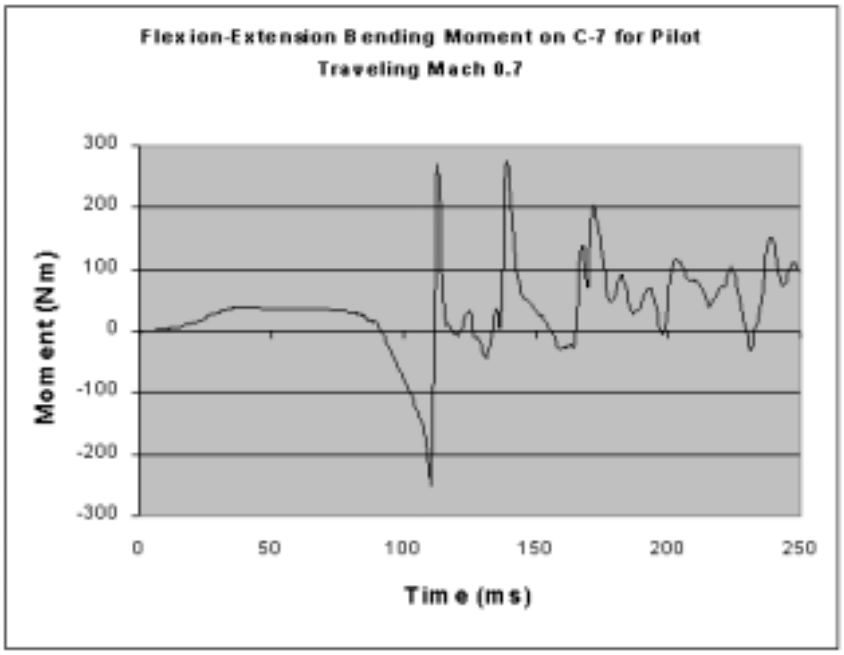

Figure 12: Flexion-extension bending moment on C-7 for the pilot who is traveling at Mach 0.7 at the time of ejection

Notice in Figures 11 and 12, the oscillatory motion of the occupant's head during the ejection process. This motion has been predicted in an analytical study of airflow around articulated limbs (17). Although the windblast force is not input as an oscillating force in MADYMO, a decaying oscillatory head motion results. Limb flailing is also evident when viewing the graphical output of the pilot ejection simulation. Before the rocket booster on the ejection seat is fired, the pilot's shoulders experience a maximum of 20 Nm of torque for both Mach 0.9 and 0.7. After being subjected to windblast, however, the pilot traveling Mach 0.9 is subjecting his shoulders to a maximum of approximately 1125 Nm. This is more than 2.3 times the torque of 480 Nm placed on the pilot traveling Mach 0.7. The pilots' elbows sustain torques of 600 Nm and 400 Nm at application of the windblast for Mach 0.9 and Mach 0.7, respectively.

The injury indices found for the pilot ejection case study yield some valuable results. Pilots for both Mach numbers sustain Head Injury Criterion (HIC) values greater than the critical value of 1000. HIC was developed by the U.S. Government as a quantification of head tolerance to impact (7). Values exceeding 1000 mean that considerable brain damage due to head impact is highly possible for two of the three cases explored. HIC values of 6287 and 346 were found for the pilots traveling Mach 0.9 with two different neck flexions/extensions, respectively, and a HIC value of 3517 for the pilot traveling Mach 0.7 (see Table 5). A somewhat outdated Gadd Severity Index (GSI) was also determined to be above the critical value of 1000 for all three cases explored. The 3MS injury criterion described in Table 4 was also found for each case. The dummy traveling Mach 0.9 with his head in the standard position had a 3MS acceleration of 618 m/s^2, while the dummy traveling Mach 0.7 had a 3MS acceleration of 344 m/s^2. The dummy with its head initially leaned towards the seat back and traveling Mach 0.9 had a 3MS acceleration of 558 m/s^2. Since 60 times the acceleration of gravity (589 m/s^2) is the critical value associated with the 3MS injury criterion, only the pilots traveling Mach 0.9 have a moderately high possibility for severe injury ($AIS \geq 4$) (7). The Abbreviated Injury Scale (AIS) is a ranking of the severity of an injury. It was originally intended for

impacts encountered in motor vehicle accidents but is now applicable to penetrating injuries and burns. The AIS distinguishes several levels of injury with a scale ranging from 0 (no injury) to 6 (maximum injury that cannot be survived). The Viscous Injury Response (VC) relates to soft tissue damage and was found to be approximately 0.8 and 0.3 for the pilots traveling Mach 0.9 and 0.7, respectively. These values are below the critical VC value of 1.0. Therefore, body tissue injury at these speeds is unlikely to occur. Neck injuries can be quantified using the Neck Injury Criteria (FNIC) and the Biomechanical Neck Injury Predictor (Nij). Refer to Table 4 for an explanation of these injury indices. Both criteria surpass the critical values associated with a neck injury. Tables 5, 6, 7, and 8 provide a complete listing of the injury indices found for the pilot ejection case study.

Table 5: Head Injury Criteria for Each Pilot

Mach #	**HIC value**	**Critical Value**	**Possibility For Injury**
0.9	6287.2	1000	High
0.9 w/ head leaned back	346.3	1000	Low
0.7	3517.2	1000	High

Table 6: 3MS Maximum for Each Pilot

Mach #	**3MS Maximum Value (m/s^2)**	**Critical Value (m/s^2)**	**Possibility For Injury**
0.9	618.4	588.6	High
0.9 w/ head leaned back	557.9	588.6	Moderate
0.7	344.2	588.6	Low

Table 7: Viscous Injury Response for Each Pilot

Mach #	VC Value	Critical Value	Possibility For Injury
0.9	0.766	1.0	Low
0.9 w/ head leaned back	0.820	1.0	Low
0.7	0.317	1.0	Low

Table 8: Neck Injury Criteria for Each Pilot

Mach #	FNIC-Bending (Nm)	Critical Value (Nm)	Possibility For Injury
0.9	402.4	57	High
0.9 w/ head leaned back	317.3	57	High
0.7	275.2	57	High

Table 9: Biomechanical Neck Injury Predictor for Each Pilot*

Mach #	NIJ-NTE*	NIJ-NTF	NIJ-NCE	NIJ-NCF	Critical Value	Possibility For Injury
0.9	4.69	1.93	2.82	1.18	1.00	High
0.9 w/ head leaned back	3.79	1.26	2.66	0.73	1.00	High
0.7	3.20	1.30	2.03	0.85	1.00	High

*(NTE) tension-extension, (NTF) tension-flexion, (NCE) compression-extension, (NCF) compression-flexion

The dummies used in this simulation were 95th percentile males that have been validated with component tests and tests on the complete dummy (2). These dummies are part of a "high quality range of recognized crash dummy models, all highly realistic and validated" (5). To find the limb dislodging force due to windblast, equation 4.21 has been used. The Aerospace Medical Association published this equation in the March, 1980 issue of *Aviation, Space, and Environmental Medicine.* As mentioned previously, a validated pilot ejection model, developed by TNO/MADYMO, has been used in this study. The pitch of the pilot's seat upon ejection was optimized to produce results that corresponded highly to experimental testing (18). It is assumed that the tests performed by MADYMO were simulated correctly. The results from TNO/MADYMO can be seen in Figure 13.

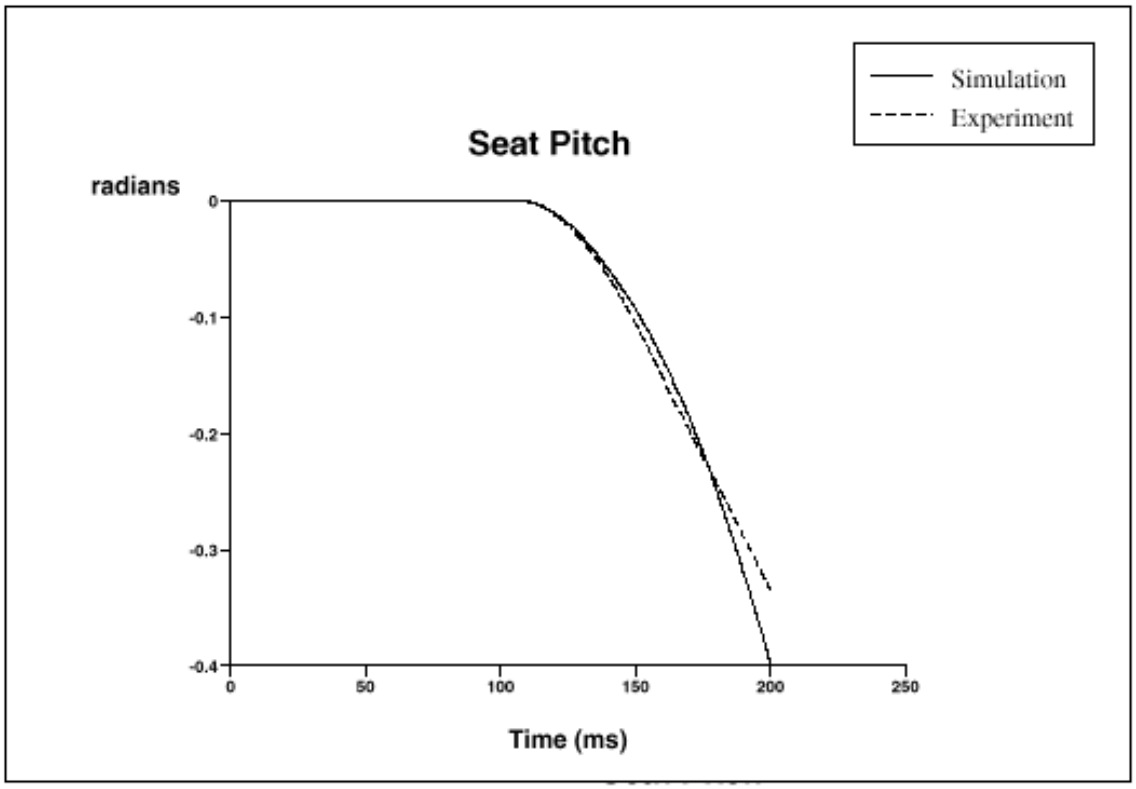

Figure 13: Comparison between optimized ejection seat pitch angle and experimental results, as performed by TNO/MADYMO (18)

6.3 Gait Simulation Results

Gait simulation is a very complicated process that involves three-dimensional motion in several joints of the human body. After analyzing this case study, students should realize the complexity of walking, the limitations of MADYMO to model this process, and the problems associated with trying to simulate cumulative trauma disorders, such as plantar fasciitis and others involving repetitive motions. Computer simulation is an excellent way to model repetitive motion. However, the MADYMO case study developed finds the force on the bottom of one foot for one step and, therefore, one cycle. The model has been greatly simplified and does not directly use finite elements. Assumptions needed for simulating gait with MADYMO are provided in section 5.3. Facet surfaces, which are similar to finite elements, are used on the 50th percentile human model, but they do not allow for pressure distributions to be calculated. This means that the "Gait Simulation" model finds only the contact forces on the bottom of the foot associated with each ballast.

The newly developed human model was used to simulate a walking motion. This motion was found using a demo leg model available from software entitled SIMM™, developed by Musculographics. The leg model (discussed in section 5.3 of this thesis) provides the angles associated with the hip, knee, and ankle during various phases of normal gait. The appropriate angles at each walking phase served as input to a motion block in the input data file. Since only one leg was modeled on SIMM, the motion of the other leg had to use the same angles, but the phases were offset. In other words, as the left heel was at heel-strike, the right foot was at toe-off. Finding the appropriate phase offset is somewhat of a task since the walking motion is very dependent upon the joint angles associated with each leg. Pelvis motion was specified, but it does not allow for the correct walking motion. MADYMO will not let the user specify the motion of a body in one direction without restraining the motion of the body in the other two directions. For example, if a person is said to walk at 1.5 m/s, specifying motion in the x-direction at 1.5 m/s will cause the pelvis to have no displacement in the y or z directions. This, in turn,

makes the human model's feet unrealistically penetrate the ground and doesn't allow for normal gait. To compensate for this problem, specifying an overly high pelvis initial velocity without specifying the motion during the simulation allowed for proper gait to be modeled if certain joints in the spine were locked. Certain vertebrae needed to be locked so that the human model did not bend over too much and fall over due to gravity. Locking the joints is somewhat similar to the muscular reaction of the body to gravity, and is therefore, not a bad specification. Normal gait is simulated using these modeling parameters. The human's pelvis velocity is shown in Figure 14.

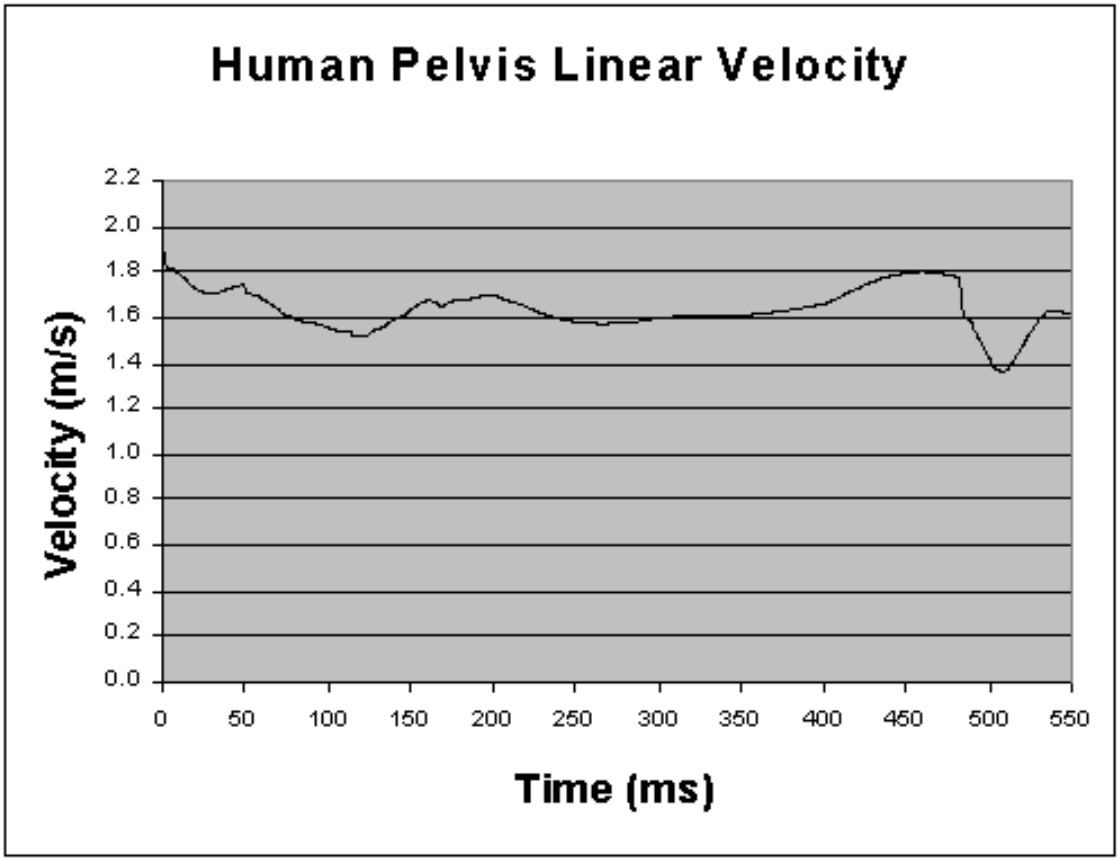

Figure 14: Pelvis velocity during left heel-strike to left toe-off

The average velocity is approximately 1.6 m/s (3.58 mph) and this is an acceptable value for a moderately fast gait (21). However, because of the high initial velocity, the contact force placed upon the foot at heel-strike is unrealistically high at approximately 18 kN for each surface modeled. It is determined that only comparative analyses can be performed with this specific model because of the limitations of MADYMO. An alternative method to modeling gait will be discussed in the following paragraph.

A high initial pelvis velocity and gait simulation yields the motion of the pelvis, which can be chosen as output. This motion is specified in the input data file, in the y and z directions, and the velocity in the x-direction can then be specified as 1.6 m/s. This process also has numerous possibilities for error but is suggested as a more accurate method for finding the forces on the bottom of the foot.

Another simplifying assumption made in the model is that the ballast does not move beneath the person's feet. It is impossible to know the orientation of the ballast and this would be necessary to correctly model ballast moving beneath a person's feet. This is somewhat unrealistic because the rocks are likely to have a random orientation and will settle beneath a person's weight, producing slightly lower contact forces on the feet but more torque on the ankle. It is suggested that spraining an ankle is just as likely to occur as plantar fasciitis because of the properties of the walking surface. Several modifications to this model can be made, but students can analyze the essential features of gait using the model developed herein.

The force results of the gait analysis cannot be validated because they are extremely high. Therefore, the results are only applicable to a comparative analysis in which different parameters can be changed to view differences in gait. For example, what is the change in contact force if a larger initial velocity is specified? The newly developed human body model, however, has been validated extensively by volunteer

tests and post mortem human substitute (PMHS) tests by TNO/MADYMO (22). The geometrical description of the human body model was derived from the software package RAMSIS, which provides anthropometrical data taken from measurements on "various civilian populations" (22). The applications for this model, including gait simulation, will expand in the future and results will become more verifiable.

Chapter 7.0 Conclusions and Future Work

Three biodynamic course modules have been developed to teach students the process of biodynamic modeling and to help them gain insight into forensic engineering topics. MADYMO is a very useful and powerful program used extensively by industry and research organizations to perform vehicle occupant analyses. It is also applicable to forensic investigations and is gaining popularity in this field. A university biomechanics course with application to forensic engineering and biodynamic modeling is needed and the biodynamic modeling tools and course modules have been developed. Biomechanics instruction must accompany these course modules for students to gain a full understanding of the proposed topics.

Using the course module dealing with whiplash, students can explore the injury mechanisms and draw several conclusions. Under the same impact force, different vehicle occupants will experience different torques on the neck and be more likely to develop clinical signs of whiplash. It has been found that occupant size is a major factor determining the magnitude of the flexion-extension bending moment on the lower neck. Increased occupant size yields an increase in bending moment. Surprisingly, the direction of impact, frontal, rear, or oblique, did not produce a seemingly large difference in torques placed upon the neck. However, the seating position and posture of an occupant were found to drastically change the chance for a whiplash injury.

The chance for injury to an ejection seat occupant is directly affected by the jet speed upon ejection (Mach number). Students can model a pilot ejection using MADYMO, and see the difference in results for differing Mach numbers and corresponding windblast. An increase in Mach number causes a proportionally larger increase in the chance for pilot injury or death. Pilots preparing for ejection are less likely to develop a neck or head injury if their head is located closer to the seat back. Limb flailing is of major concern with pilot ejections, and this can be observed by

viewing a graphics output file on postprocessor MAPPK. Extreme amounts of torque are generated in the shoulders, elbows, and knees. Also, the massive acceleration associated with pilot ejection and windblast produces severe injury to the body's organs if the Mach number is above approximately 0.9.

Students can simulate human gait with case study #3 provided within this thesis. They will gain knowledge about the complications involved in walking and learn some of the limitations of modeling gait with MADYMO. Gait simulation is extremely dependent upon the hip, knee, and ankle joint angles and also the phase difference between the left and right legs. Due to the simplicity of the model, different ballast sizes were not shown to affect the magnitude of contact forces placed upon the bottom of the feet. However, a finite element model of the foot and corresponding analysis would likely yield different results.

There is always a need for biodynamic modeling, and the development of more course modules is a never-ending process. It is proposed that course modules dealing with slips/trips/falls, sports related injuries, and workplace accidents be developed to further student knowledge about biomechanics and forensic engineering. Proper training of students requires proper teaching and, therefore, a professor must be adequately skilled in troubleshooting MADYMO. Less professor competency would be needed if a T.A. were assigned to help assist students in troubleshooting MADYMO. In this manner, the professor could focus on teaching the fundamentals of biomechanics, i.e., simple analytical solutions to complex biodynamic problems, while the graduate student would be involved with learning and instructing students on the use of MADYMO. It is proposed that a graduate student interested in biomechanics and MADYMO, take the biodynamic modeling course described within this thesis as an independent study course. The inadequacies of the "In-House" User's Manual (Appendix A) and difficulties with the course modules could be explored before involving several students. The time required for setup of the biodynamic models and analysis of the results could also be

assessed. Successful use of the biodynamic modeling course depends upon this future work.

The development of biodynamic modules for forensic applications has been performed and the material for an interesting computer based laboratory course is now available for students to explore the topics of forensic engineering.

References

(1) http://www.musculographics.com/simm_dm.htm

(2) MADYMO Database Manual, version 5.4; TNO Automotive, May 1999.

(3) H.V.E. Human Vehicle Environment, version 2; Engineering Dynamics Corporation, Beaverton, Oregon, July 1999.

(4) http://www.autolev.com, http://www.trucksim.com/autosim

(5) http://madymo.com

(6) http://ttb.eng.wayne.edu/~king/welcome.html

(7) MADYMO Theory Manual, version 5.4; TNO Automotive, May 1999.

(8) Estep, C. R.; "Modeling of the Human Head/Neck System Using Rigid Body Dynamics." Masters Thesis, Virginia Polytechnic Institute and State University, Blacksburg, Virginia, 1992.

(9) Renfroe, D. A., and Partain, J.; "Modeling of Vehicle Rollover and Evaluation of Occupant Injury Potential Using MADYMO." Renfroe Engineering, Inc., Society of Automotive Engineers, Inc., 1998.

(10) Meirovitch, L.; *Methods of Analytical Dynamics.* Virginia Polytechnic Institute and State University, McGraw-Hill Book Company, 1970.

(11) Atkinson, K.; *Elementary Numerical Analysis, 2nd Edition*. University of Iowa, John Wiley & Sons, Inc., 1993.

(12) Marshall, R.; "WSU.ppt," PowerPoint Presentation, MADYMO, North America, Farmington Hills, Michigan, 1999.

(13) O'Neil, P. V.; *Advanced Engineering Mathematics*. University of Alabama at Birmingham. Brooks/Cole Publishing Company, Pacific Grove, California, 1995.

(14) Moorhouse, K. M.; "Determination of a Whiplash Injury Severity Estimator (WISE Index) for Motor Vehicle Occupants Involved in an Automobile Accident." Masters Thesis, Virginia Polytechnic Institute and State University, Blacksburg, Virginia, 1998

(15) Kleinberger, M., Sun, E., Saunders, J., and Zhou, Z.; "Effects of Head Restraint Position on Neck Injury in Rear Impact." WAD'99 Compendium/Traffic Safety and Auto Engineering, Vancouver, Canada, February 1999.

(16) Schneck, D. J.; "Aerodynamic Forces Exerted on an Articulated Human Body Subjected to Windblast." Aviation, Space, and Environmental Medicine, January 1978.

(17) Schneck, D. J.; "Studies of Limb-Dislodging Forces Acting on an Ejection Seat Occupant." Aviation, Space, and Environmental Medicine, March 1980.

(18) MADYMO Utilities Manual, version 5.4; TNO Automotive, May 1999.

(19) Shapiro, S. L.; "In Depth: Heal Pain Management Starts With Correct Differential Diagnosis." Biomechanics, Miller Freeman, Inc., September 1997.

(20) Mertz, H. J., and Patrick, L. M.; "Strength and Response of the Human Neck." 15th Stapp Car Crash Conference, SAE 710855, 1971.

(21) Craik, R. L., and Oatis, C. A.; *Gait Analysis, Theory and Application*. Mosby-Year Book, Inc., St. Louis, Missouri, 1995.

(22) Morsink, P. J., and Happee, R.; *MADYMO Human Body Models, v5.4*; TNO Automotive, September 1999.

Appendix A "In-House" MADYMO MANUAL

Preface

This manual is intended to help students and faculty in the use of commercial software package, MADYMO. The instructional notes provided below should allow MADYMO users to successfully model different biodynamic cases using similar techniques and procedures. At the time of this writing, there are no preprocessors made by MADYMO for the program. October of 2000 is a planned release date for a MADYMO preprocessor to be developed by Altair Engineering. Unless a preprocessor is used in the future, this introductory manual will only be valid on UNIX machines. It should be noted that MADYMO provides a full set of user's manuals available on any computer that offers the program. The details to follow are simply recommendations or steps that were found useful in modeling biodynamic systems. Because the program can be used in a broad range of applications, all the information needed might not be found in this introductory manual, so please refer to the MADYMO manual set.

I) INTRODUCTION TO MADYMO

MADYMO (MAthematical DYnamic MOdeling) was originally developed by TNO-Automotive for analyzing occupant behavior during automobile crashes. However, the program has a wide range of applicability and is well suited to solve complex biodynamic systems that a forensic engineer might encounter. It will run on UNIX and Windows NT operating systems but a graphical postprocessor is currently not available for Windows NT. If UNIX is used, the package has full operation of the following modules:

1) MADYMO 3D
2) MADYMO FEM + Airbag
3) Dummy Database (contains 31 dummies)
4) Human Body Model
5) Utility BAGGEN/ FOLDER/ MTA
6) Utility GEBOD
7) Utility MADYSCALE
8) Utility MADYMIZER
9) Postprocessor MAPPK
10) Viewmad

MADYMO 3D is the main "engine" of the program and uses ellipses, cylinders, and planes to represent specific 3-dimensional bodies. A set of bodies forms a multi-body system that can be analyzed under dynamic loading conditions. Finite element modeling and airbag modeling is also available and can be incorporated into any rigid multi-body system. There is a dummy database with several validated dummies ranging from infants to adults that can be used in different biomechanical applications (Fig. A-1).

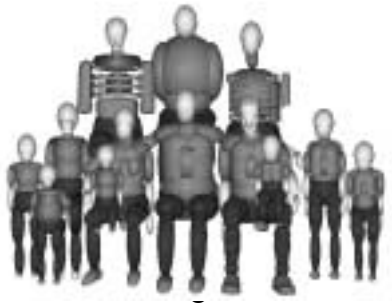

Figure A-1: MADYMO dummy database (7)

A 50th percentile human body model using anthropometric values obtained from RAMSIS and human body properties found from cadaver and human volunteer data is also available. The utilities entitled BAGGEN, FOLDER, and MTA deal with the use of finite element air bags, how they are folded, and tank test analysis for inflators. GEBOD generates inertia and geometric properties for 50th percentile humans with a specified height, weight, and/or age (up to 20 years). MADYSCALE is used to scale different dummies and uses GEBOD routines for different sized people. Utility MADYMIZER is an optimization program that allows the user to define a model parameter and run successive "trial and error" tests with less work. The postprocessor MAPPK allows the MADYMO user to view the system created and is a great visual learning tool. Viewmad or VIEWK is a similar graphical module that has less detail and capabilities. Since the author's work dealt with certain topics that did not use each module, new users should consult the program manuals for a detailed description of each module. MADYMO uses a metric units system as follows:

Quantity	Unit	**Quantity**	Unit
Mass	kg	Velocity	m/s
Length	m	Acceleration	m/s^2
Time	s	Force	N
Temperature	K	Torque	Nm
Angle	radians	Moment of Inertia	kgm^2

II) COMPUTER OPERATION

Typographical Conventions

Throughout this manual, any item of text within square brackets [ ] refers to a key on the keyboard. Any text surrounded by quotation marks " " will be a command on the screen. All commands that need to be typed will be bold faced. It should be noted that UNIX is case sensitive and any command given in these instructions should be typed exactly as shown. Any text that is not within the shell or "winterm" (i.e. Jot editor) will be evident and separated from the paragraph.

Computer Access

Log onto the computer by entering a username and password. Then use the mouse to open a "shell" in the "Toolchest" menu. This is where all commands in UNIX will be typed. Since each computer in the computer lab may not have MADYMO, the user must telnet to a computer with the program in order to run MADYMO files. Ignore the following two commands if MADYMO is available on the computer being used or if running a file is not necessary. Type the following commands to connect to sgi4 (do not type $):

$ **xhost sgi4**
$ **telnet sgi4**

If the user has logged on successfully, he/she will be prompted for a username and password again. Once entered, the user has full function of the previously mentioned program modules.

Useful UNIX Commands

While working with the UNIX operating system, several commands will be useful in running MADYMO. Also, a cut and paste function can be used if the section or word to be copied is highlighted with the mouse. The copied section will be pasted wherever the cursor is located when the middle mouse button is pressed. The following is a short list of the commands found to be of help.

1) **ls**

This will show all of the files under the current directory (i.e. whiplash.dat, whiplash.peak, etc.)

2) **cd**

This changes the current directory to the users main directory when typed alone. If one wants to look in a different directory then **cd** should be followed by the users path and new directory. For example, if an individual wanted to look at the MADYMO share directory, which contains very useful user information such as the MADYMO manual set, he/she would type the following:

cd /usr/Local/madymo_541/share

Typing **ls** here will show the subdirectories available. The MADYMO manual set is found under docs, applications are within appl, and dummies are under dbs. The user should explore these subdirectories by using the **cd …**followed by **ls**. Figure A-2 is an example of what the user would see if looking for files in the users directory then in MADYMO's 3D applications directory.

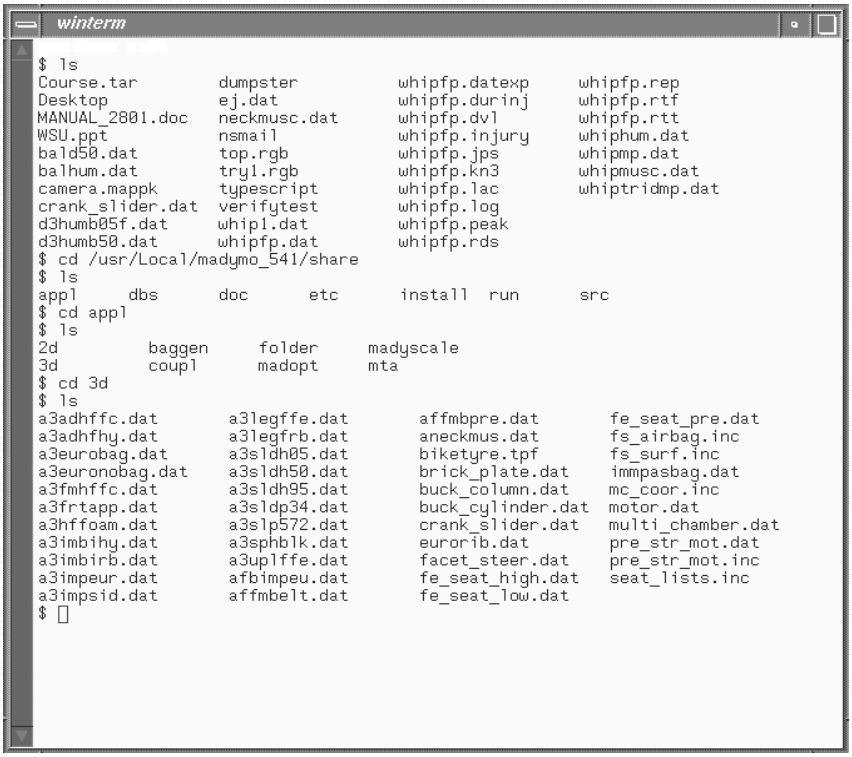

Figure A-2: Commands to change directories

Notice in Figure A-2 that these commands are within the "winterm" which is shown in the upper left corner of the figure. The following is a breakdown of the steps taken to arrive at the previous figure:

$ **ls** [enter]
$ **cd /usr/Local/madymo_541/share** [enter]
$ **ls** [enter]
$ **cd appl** [enter]
$ **ls** [enter]
$ **cd 3d** [enter]
$ **ls** [enter]

Note that [enter] is always pressed after typing a command and it will not be shown in the rest of this manual. Above are the steps to view the files in the MADYMO applications directory. To view files in the other directories, such as dbs, follow the same steps but switch **appl** with **dbs**. Also, the entire command without using **ls** in between steps can be done as follows:

$ **cd usr/Local/madymo_541/share/appl/3d**
$ **ls**

3) **top**

This is a useful command when the user wants to see how long a file has been running or what programs are currently running on the computer. It is a good indicator of why a file might be running slowly or why a graphics processor is not functioning at full speed. If unnecessary programs are running or taking too much computing power, they can be "killed" by typing **k** followed by the PID for the file (i.e. **k 21032**). To quit "top," type **q**. A "$" sign and cursor should appear at the bottom of the screen as in Figure A-3.

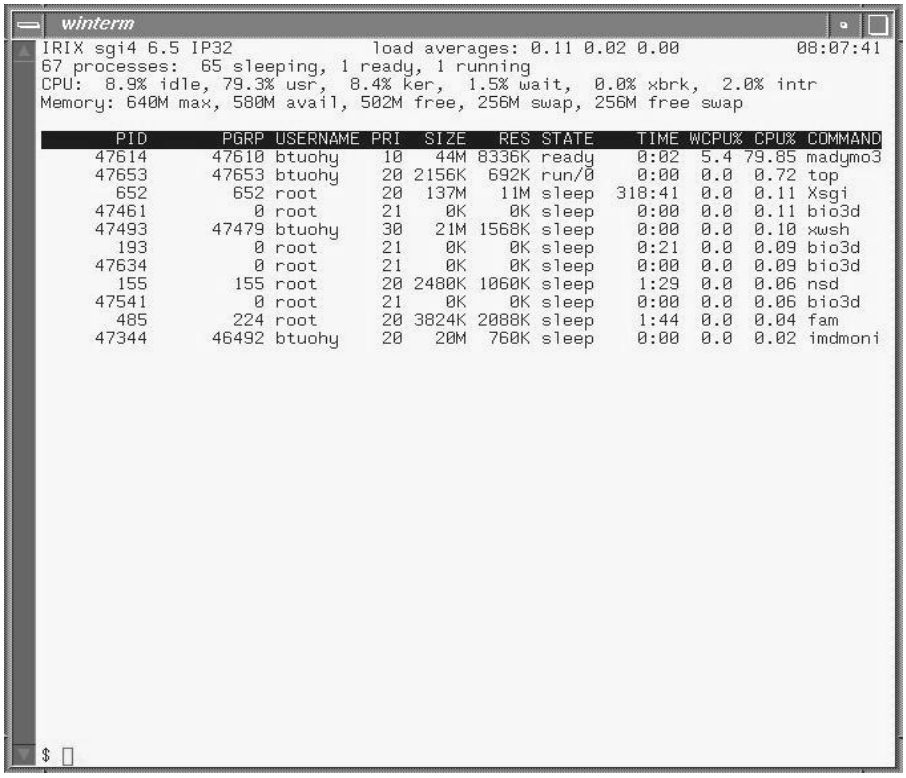

Figure A-3: Computer processes sleeping, running, or ready

Figure A-3 is the result of typing the following:

$ **top**

$ **q**

Notice that the user, “btuohy”, is using 79.3% of the computing power to run a program with a PID of 47614. This program, “madymo3”, has been running for 2 seconds as seen under the column labeled “TIME”. The other commands are processes of the program running or commands that always run when using the system.

4) **mkdir**

This will make a new directory for files to be placed. For example, **mkdir tests** will create a directory titled "tests."

5) **jot**

This opens the Jot editor, which will be used to create the MADYMO files and also to view most of the output. Typing **jot whiplash.dat** will open the MADYMO input file titled whiplash. The .dat stands for data file and is the input file for MADYMO. After running whiplash.dat, some output files such as .rep, .peak, and .injury will be created (see Fig. A-2) and jot can also be used to view these. For a listing of all the output files and their purpose, consult the MADYMO manuals.

6) **madymo541 filename**

Typing this will start the process of running a file called "filename." All output files will be generated and graphics files will be created.

7) **madymo541 –mappt**

This calls the post-processor MAPPT so that time history output data files can be plotted. For complete instructions on how to operate MAPPT, consult the MADYMO User's Manual.

8) **madymo541 –mappk filename.kn3**

This calls the graphics post-processor MAPPK to represent the system solved. It uses the kinematics file titled "filename.kn3". It should be noted that **–viewk** can be used instead of **–mappk** by substituting the command. Viewk is beneficial if the computer has a lot of programs running and the mappk postprocessor is working slowly. The following figure (Fig. A-4) is what mappk might look like for a female whiplash case study.

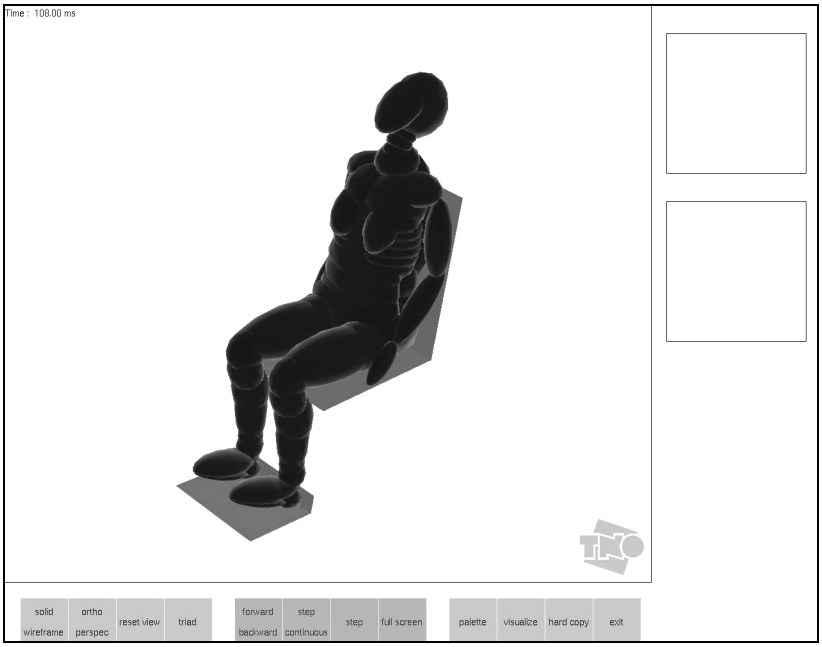

Figure A-4: MAPPK representation of a female dummy subjected to whiplash

The commands at the bottom of the screen (Fig. A-4) represent [F1] through [F12] on a keyboard. Also, the color has been inverted and turned into grayscale only for this manual because it is normally a color screen.

Basic Troubleshooting Techniques

If a file does not have a successful run completion, check the "rep" output file using the jot editor as described above. Error messages should be placed at the bottom of the report with the line number specified. Check the error messages then refer back to the dat file and fix the error. If line numbers are needed to find the error, type **jot filename.datexp** and using the jot commands, choose to show the line numbers with this file. Fix the original dat file then try running the program again. While the file is running, type **top** and see how long the program will run. If it stops after less than 5 seconds, there is probably a simple error or command word (i.e. END ELLIPSOIDS)

missing in the input deck. If the program runs for a fair amount of time but does not complete normally, there might be stability problems or contact between ellipsoids that is not allowed. Try looking at the -mappk representation to find clues as to why the program completed abnormally or did not run the entire time specified. Refer to the MADYMO manuals for further help.

III) PREPARATION FOR BIODYNAMIC MODELING

Before sitting down at a computer, the biodynamic modeler should make a quick sketch of the system represented and how the coordinate systems will be arranged. Any specific data needed for the case study should be written down (i.e. height, weight of subject, etc.) as well as the output required for successful completion of the case study. If a pre-developed dummy or human model is used, make sure its properties fit the application desired. Certain dummy manipulations cannot be performed due to the use of protected MADYMO models within the dummy database, but most dummies and the human models can be adapted (joint locations, angles, etc.) to fit different situations. Users should become familiar with the dummy database and the application files already available so that they do not "re-invent the wheel."

IV) CREATING MADYMO FILES

All input files will have the same format but will differ in the types of commands used. The input file is comprised of several blocks that start with a command name and finish with "END". Below is an example of a file created to represent a ball being dropped onto the ground from a height of 0.5 meter (Fig. A-5). Jot has been used to write the file.

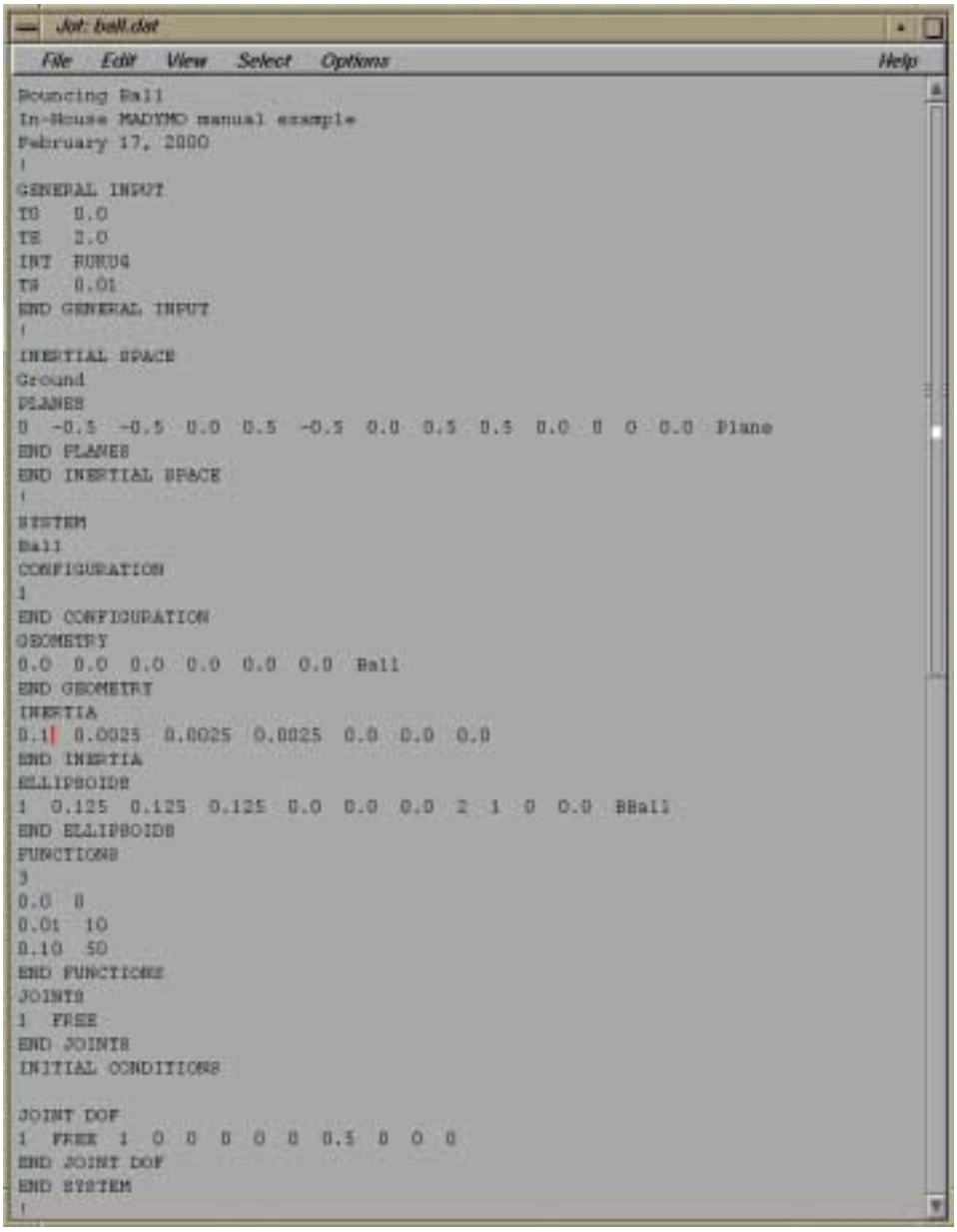

Figure A-5: Example of the Jot Editor

This is not the entire data file. It has been inserted to show the characteristics of the Jot editor. In Figure A-5, notice the different input blocks that are separated by exclamation points! This is done to illustrate the different blocks and is not required in a data file. Both an asterisk* and exclamation point! are not recognized by MADYMO and can be

inserted between commands or used before an explanation. A breakdown of each data block for the entire bouncing ball file will be given in the next few paragraphs. The first three lines of the file are dedicated to describing the file as seen in Figure A-5.

General Input Block

```
GENERAL INPUT
T0   0.0
TE   2.0
INT  RUKU4
TS   0.01
END GENERAL INPUT
```

This block tells MADYMO how the file should be solved. *TO* is the starting time for the simulation and will normally be 0 seconds. TE stands for end time of the simulation and will change the actual "run-time" by increasing or decreasing the value given. When setting up the model, TE should be set to a low number (i.e. 0.001) so that it doesn't require a lot of computing time to graphically view the model. This will produce a picture of the initial position of the model. INT is the integration method chosen for the multibody equations of motion and can be an Euler method (EULER), Runga-Kutta method (RUKU4), or Runga-Kutta-Merson method (RUKU5). EULER and RUKU4 integration methods use a fixed time step and RUKU5 does not. The first two methods will be used most frequently. For a comparison between the three integration methods, please see the MADYMO Theory manual. A time step (TS) of 0.01 seconds has also been chosen. Choosing this value correctly will cause a stable and accurate solution.

Inertial Space Block

```
INERTIAL SPACE
Ground
PLANES
0  -0.5  -0.5  0.0  0.5  -0.5  0.0  0.5  0.5  0.0  0 +
0  0.0  Plane
END PLANES
END INERTIAL SPACE
```

As before, the block begins with the main command. INERTIAL SPACE is followed by an identifier (Ground), which can be any word less than 15 characters. A plane has been chosen for the surface of the ground although ellipses, cylinders, facet surfaces, or a road could have been chosen. This is true for Null Systems and Systems, which are partly discussed in this manual. The numbers on the next line will be discussed in their order of appearance. The first 0 is the number of the body to which the plane is attached and in our case, it is the inertial space. For the inertial space or a null system, any value may be given. The next nine numbers define three points (x_i, y_i, z_i), for i=1, 2, 3, on a plane in the inertial space. The points are at (-0.5, -0.5, 0.0), (0.5, -0.5, 0.0), and (0.5, 0.5, 0.0). The order in which the points are specified defines the outward normal of the plane as shown in Figure A-6.

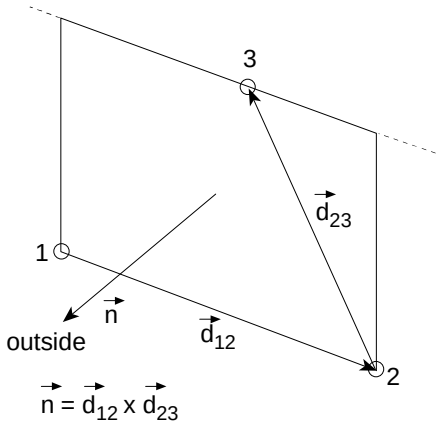

Figure A-6: Defining a plane (7)

After the points defining the plane, the loading function (penetration vs. force applied) is given. For this case, 0 has been specified which means a loading function will not be given. A "+" sign specifies that the next line is a continuation of the preceding line. The following 0 means the unloading function is also not specified . The next 0.0 is the hysteresis applied. It is simply the slope connecting the loading function curve to the unloading function curve. An in-depth explanation is given in the MADYMO Theory manual. The identifier of the PLANE is given as "Plane" but it is not necessary. As

usual, after each command has been specified, the commands are finished with END. If these are omitted, the file will not run successfully.

System Block

```
SYSTEM
Ball
CONFIGURATION
1
END CONFIGURATION
GEOMETRY
0.0  0.0  0.0  0.0  0.0  0.0  Ball
END GEOMETRY
INERTIA
0.1  0.0025  0.0025  0.0025  0.0  0.0  0.0
END INERTIA
ELLIPSOIDS
1  0.125  0.125  0.125  0.0  0.0  0.0  2  1  0  +
0.0  BBall
END ELLIPSOIDS
FUNCTIONS
3
0.0  0
0.01  10
0.10  50
END FUNCTIONS
JOINTS
1  FREE
END JOINTS
INITIAL CONDITIONS

JOINT DOF
1  FREE  1  0  0  0  0  0  0.5  0  0  0
END JOINT DOF
END SYSTEM
```

The system block begins with SYSTEM and has an ID of Ball. Since the ball is only one body, the CONFIGURATION is simply followed by a 1. If the system was three connected bodies, then the values would be "3 2 1" instead of "1". The format is derived from a tree structure as explained in the Theory manual. Body 1 would be the parent body for body 2 and body2 would be the parent for body 3. The first three values

under GEOMETRY refer to the coordinates of the joint connecting body 1 to the parent body. Body one is connected to the inertial space and given coordinates of (0.0, 0.0, 0.0). Next are the coordinates of the center of gravity for the body in the local coordinate system of the body. The center of gravity of the ball is in the center (0.0, 0.0, 0.0) of the ball due to its symmetry. The first value under INERTIA is the mass (.1 kg) of body 1. The following numbers represent Ixx, Iyy, Izz, Ixy, Iyz, and Ixz, respectively. In order for contact between the ground and the ball to be calculated, an ellipsoid for the ball must be defined. The first number (1) is a body number. The following three numbers (0.125, 0.125, 0.125) define the semi-axes of the ellipsoid (a, b, c) as in Figure A-7.

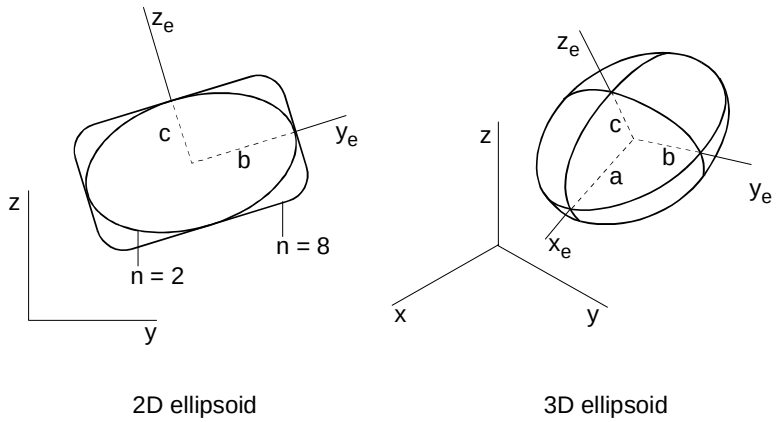

Figure A-7: Ellipsoid geometry (7)

The next three numbers are the coordinates of the ellipsoid center in the local coordinate system of the body.. After that, the degree of the ellipsoid (n) is specified (see Fig. A-7). The next three numbers are the loading, unloading, and hysteresis functions, respectively. Notice for the ball that 1 has been given as the loading function. This means that a function must be specified. Under FUNCTIONS, 3 tells MADYMO that there will be three different data sets given for the loading function of the ellipsoid. A linear interpolation of the data set is performed since the loading function was given a positive number (1). The second data set has a 10 N force if a 0.01 m penetration is found and so on for the third data set. The JOINTS are defined next and since this example uses only one body defined as a ball, the joint is FREE and connected to the inertial space as described above. There are 12 available joints with differing degrees of freedom as

described in the Theory manual. INITIAL CONDITIONS are now specified and a blank line should follow this command. The joint degrees of freedom are given as follows. Joint 1 is a FREE joint with Euler parameters of 1, 0, 0, and 0. The initial position of the ball is at (0, 0, 0.5m) and it has no initial velocities. This means the ball is dropped from 0.5 meters. This is the end of the systems block for this example.

Force Models Block

```
FORCE MODELS
ACCELERATION FIELDS
1  0  0  0  1
END ACCELERATION FIELDS
FUNCTIONS
2
0.0  -9.80665
5.0  -9.80665
END FUNCTIONS
END FORCE MODELS
```

There should be an acceleration field, corresponding to gravity, applied to the ball. After ACCELERATON FIELDS is the system number to which the acceleration field is applied (1). The body number is then specified. If the acceleration field is applied to all bodies in the system, then 0, as in this case, should be the value given. The next three numbers represent the direction (x, y, z) for which the acceleration function (1) is applied. As explained above, a data set for the function is given. The first number given is the time and second number is the acceleration applied. Note that the final time assigned (5.0) should be greater than the simulation end time (TE) by at least one time step (TS).

Contact Interactions Block

```
CONTACT INTERACTIONS
PLANE-ELLIPSOID
INERTIAL SPACE
PLANE  1
SYSTEM  1
ELLIPSOID  1
```

```
CHARACTERISTIC  ELLIPSOID
END PLANE-ELLIPSOID
END CONTACT INTERACTIONS
```

This is a very important block to include since no forces can be calculated if contact between objects is not defined. For example, if contact between the ball and ground is not specified, the ball would drop from 0.5 m and keep falling through the ground. This is not possible so contact must be defined. Since the ball is an ellipsoid and the ground is a plane, PLANE-ELLIPSOID contact is defined. PLANE 1 is located in the INERTIAL SPACE as defined. ELLIPSOID 1 is located within SYSTEM 1 and the CHARACTERISTIC of the ellipsoid was chosen. This means that the elastic force of the ellipsoid, its loading function described in System Block above, is used to calculate the forces and corresponding bounce of the ball.

Output Control Block

```
OUTPUT CONTROL
TSKIN  0.005
KIN3  EXTENDED
TSOUT  0.001
LINACC
1  1  0.0  0.0  0.0  0  0  0  0  BallAccel
END LINACC
END OUTPUT CONTROL
```

The OUTPUT CONTROL is an essential block and can be tailor made to produce only the desired output. This example uses a time interval (TSKIN) for writing data to the KIN3 (graphics/ kinematics) file of 0.005 seconds. This value will change the speed at which the mappk representation is presented. KIN3 EXTENDED tells MADYMO to enter the location and orientation of all bodies into the KIN3 file. A time step for the amount of output written to the time-history files (TSOUT) has been specified as 0.001 seconds. This number could be lowered for this bouncing ball example. The only output file requested for this example is a linear acceleration (LINACC) file. The first and second numbers refer to the system and body requested. The following three values are the coordinates of the point in the body local coordinate system where the acceleration

will be calculated. The next three numbers (0 0 0) correspond to a correction factor for the acceleration in the x, y, or z directions. The next 0 defines how the components of the linear acceleration are expressed with respect to the inertial coordinate system. If this value did not equal 0, then the acceleration is given with respect to an accelerometer coordinate system.

Note: The final line of the data file must be: END INPUT

Virginia Tech Users

Before using the ESM computer lab, users must be registered with the ESM department and have a validated Hokie Passport to enter the lab. Access to the lab is restricted after 4:00pm and only valid I.D.s will open the door. To use the UNIX machines, one must have a username and password. These are obtained through Tim Tomlin (Norris room #301) and can be entered into the system on Friday of each week.

At the time of this writing, MADYMO is available on the three SGI computers nearest the window and the SGI Indigo nearest the lab telephone.

Appendix B MADYMO Exercise (Bouncing Ball)

```
Bouncing Ball
In-House MADYMO Manual Example
February 17, 2000
!
GENERAL INPUT
T0   0.0
TE   2.0
INT  RUKU4
TS   0.01
END GENERAL INPUT
!
INERTIAL SPACE
Ground
PLANES
0 -0.5 -0.5 0.0 0.5 -0.5 0.0 0.5 0.5 0.0 0 0 0.0 Plane
END PLANES
END INERTIAL SPACE
!
SYSTEM
Ball
CONFIGURATION
1
END CONFIGURATION
GEOMETRY
0.0  0.0  0.0  0.0  0.0  0.0  Ball
END GEOMETRY
INERTIA
0.1  0.0025  0.0025  0.0025  0.0  0.0  0.0
END INERTIA
ELLIPSOIDS
1  0.125  0.125  0.125  0.0  0.0  0.0  2  1  0  0.0  BBall
END ELLIPSOIDS
FUNCTIONS
3
0.0  0
0.01  10
0.10  50
END FUNCTIONS
JOINTS
1  FREE
END JOINTS
INITIAL CONDITIONS
```

```
JOINT DOF
1  FREE  1  0  0  0  0  0  0.5  0  0  0
END JOINT DOF
END SYSTEM
!
FORCE MODELS
ACCELERATION FIELDS
1  0  0  0  1
END ACCELRATION FIELDS
FUNCTIONS
2
0.0  -9.80665
5.0  -9.80665
END FUNCTIONS
END FORCE MODELS
!
CONTACT INTERACTIONS
PLANE-ELLIPSOID
INERTIAL SPACE
PLANE  1
SYSTEM  1
ELLIPSOID  1
CHARACTERISTIC  ELLIPSOID
END PLANE-ELLIPSOID
END CONTACT INTERACTIONS
!
OUTPUT CONTROL
TSKIN  0.005
KIN3  EXTENDED
TSOUT  0.001
LINACC
1  1  0.0  0.0  0.0  0  0  0  0  BallAccel
END LINACC
END OUTPUT CONTROL
!
END INPUT
```

Appendix C Computer Code Alterations and Additions

This appendix describes the input data file commands and specifications that were performed to create the three biodynamic models discussed in the body of this thesis. However, the case studies do not have to be modeled with the same parameters presented below and can also be modeled using different commands. The text to follow is simply one method of modeling whiplash, pilot ejection and windblast, and gait. The following input text does not produce a working MADYMO file since certain commands and functions have not been provided. To properly create a MADYMO input file with the commands and functions given below, the "In-House MADYMO Manual" should be explored. To eliminate redundant commands or commands that were not specified by the author, only the commands specific to each case study are included. Since dummies and human body models were used from MADYMO's share directory (see Appendix A), changes and additions to the original system files developed by TNO-MADYMO are presented. Refer to Appendix A for the typographical conventions of MADYMO's input data file. It should be noted that some of the following lines were not altered, but they are shown to provide some clarity to lines preceding and following them. Also, the bold faced text describes the input data file text below it and is not a part of the actual input data file.

Whiplash Text File Changes and Additions

```
Case Study 1
Whiplash 50th% Male Driver (victim)
January 28, 2000
!
```

The GENERAL INPUT, INERTIAL SPACE, and NULL SYSTEM specifications are shown below. An application file located in MADYMO's share directory was used to help create the seat planes and footstop.

```
!
GENERAL INPUT
T0   0.0
TE   0.30
INT  RUKU4
TS   1E-4
```

```
END GENERAL INPUT
!
INERTIAL SPACE
RIGID SEAT
  PLANES
!   1:2
    0  0.000 0.2750 0.000  0.000 -.2750 0.000  0.4200 -.2750 0.0650  +
       0  0  0.0    Seat Cush
    0  -.0940 0.2750 0.4820  -.0940 -.2750 0.4820  0.000 -.2750 0.000  +
       0  0  0.0    Seat Back
    END
END INERTIAL SPACE
!
NULL SYSTEM
    footstop
    PLANES
!   3:4
    0  0.750 0.150 -.1400  0.7500 -.1500 -.1400  0.9100 -.1500 0.0200  +
       0  0  0.0    Floor Plane
    0  0.710 0.150 -.1000  0.7100 -.1500 -.1000  0.7500 -.1500 -.1400  +
       0  0  0.0    Heel Plane
    END PLANES
    MOTION
    POSITION
    0  -.070  0  .0660
    5  -.070  0  .0660
    END POSITION
    ORIENTATIONS
    0  0  1  2  0.45
    5  0  1  2  0.45
    END ORIENTATIONS
END NULL SYSTEM
!
```

As stated section 5.2 of this thesis, the dummy was positioned using gravity and the steps involved are not given below. Refer to the pages mentioned for dummy positioning. The initial position of joints 1, 23, 24, 27, and 28 for the dummy were found, and values were entered into the JOINT DOF block as shown in the following text. Joints 19, 20, 21, and 22 were altered to position the hands on an imaginary steering wheel.

```
!
  JOINT DOF
!   dummy orientation:  x-rotation       y-rotation      z-rotation
    1   FREEROTATIONS   1  -6.515E-4     2  -.17368    3  1.2944E-3    +
!   dummy position:     x-disp           y-disp          z-disp
                        1.083368E-001    1.038930E-003   0.122556
!   left elbow: lateral rotation=yaw left; hyper-extension=pitch down up
    19  FREE   -.50000   -.60000
!   right elbow: medial rotation=yaw left; hyper-extension=pitch down up
    20  FREE   0.50000   -.80000
!   left wrist: lateral axial rotation=yaw left; extension=roll right
    21  FREE  0.00000   0.00000
!   right wrist: medial axial rotation=yaw left; flexion=roll right
```

```
    22  FREE   0.50000   0.00000
!   for protected hip model:
!   left hip: (medial rotation=roll left; extension=pitch down;
!              abduction=yaw left)
    23  FREEROTATIONS   2  -1.05321E-2   1  -1.20554E-3   3  1.112323E-3
!   right hip: (lateral rotation=roll left; extension=pitch down;
!               adduction=yaw left)
    24  FREEROTATIONS   2  -1.04535E-2   1  1.265E-3     3  -1.082128E-3
!   knees: flexion, compression of knee slider
    27  FREE   8.201630E-003  1.199180E-004
    28  FREE   8.742270E-003  1.211963E-004
  END
!
```

An acceleration pulse simulating rear impact was specified as 3.2 times the acceleration due to gravity.

```
!
FORCE MODELS
ACCELERATION FIELDS
1  0  1  0  2
END ACCELERATION FIELDS
FUNCTIONS
4
0.000  -31.3813
0.100  -31.3813
0.101    0.0000
5.000    0.0000
2
0  -9.80665  5  -9.80665
END FUNCTIONS
END FORCE MODELS
!
```

Contact interactions were defined so that the dummy interacted correctly with the seat and foot planes. Some of these interactions and the interaction properties were found in an application file in the MADYMO share directory.

```
!
CONTACT INTERACTIONS
! plane 1 is the seat cushion and plane 2 is the seat back
    PLANE-ELLIPSOID
!     1: Seat Cush to Lower Torso
      INERTIAL SPACE
      PLANE                   1
      SYSTEM                  1
      ELLIPSOID               1
      CHARACTERISTIC          ELLIPSOID
      DAMPING COEFFICIENT     1.0
      DAMPING ELASTIC FORCE   1
      FRICTION COEFFICIENT    0.29
      BOUNDARYWIDTH           0.050
      CORRECTION              OFF
      FUNCTIONS
!   DAMPING ELASTIC FORCE function for lower torso bottom of 50% Hybrid
!   III to rigid plate contact
```

```
!   (apply with DAMPING COEFFICIENT      1.0)
      3
       0.0 0.0
       1190.0 1927.0
       10088.0 10274.0
      END FUNCTIONS
    END PLANE-ELLIPSOID
!
    PLANE-ELLIPSOID
!     2: Seat Cush to Left hips
      INERTIAL SPACE
      PLANE                    1
      SYSTEM                   1
      ELLIPSOID                36
      CHARACTERISTIC           ELLIPSOID
      DAMPING COEFFICIENT      1.0
      DAMPING ELASTIC FORCE    1
      FRICTION COEFFICIENT     0.29
      BOUNDARYWIDTH            0.050
      CORRECTION               ON
      FUNCTIONS
!   DAMPING ELASTIC FORCE function for lower torso bottom of 50% Hybrid
!   III to rigid plate contact
!   (apply with DAMPING COEFFICIENT      1.0)
      3
       0.0 0.0
       1190.0 1927.0
       10088.0 10274.0
      END FUNCTIONS
    END PLANE-ELLIPSOID
!
    PLANE-ELLIPSOID
!     3: Seat Cush to right hip
      INERTIAL SPACE
      PLANE                    1
      SYSTEM                   1
      ELLIPSOID                38
      CHARACTERISTIC           ELLIPSOID
      DAMPING COEFFICIENT      1.0
      DAMPING ELASTIC FORCE    1
      FRICTION COEFFICIENT     0.29
      BOUNDARYWIDTH            0.050
      CORRECTION               ON
      FUNCTIONS
!   DAMPING ELASTIC FORCE function for lower torso bottom of 50% Hybrid
!   III to rigid plate contact
!   (apply with DAMPING COEFFICIENT      1.0)
      3
       0.0 0.0
       1190.0 1927.0
       10088.0 10274.0
      END FUNCTIONS
    END PLANE-ELLIPSOID
!
```

```
    PLANE-ELLIPSOID
!     4: Seat Back to Lower Torso
      INERTIAL SPACE
      PLANE                    2
      SYSTEM                   1
      ELLIPSOID                1
      CHARACTERISTIC           ELLIPSOID
      DAMPING COEFFICIENT      1.0
      DAMPING ELASTIC FORCE    1
      FRICTION COEFFICIENT     0.29
      BOUNDARYWIDTH            INFINITE
      CORRECTION               OFF
      FUNCTIONS
!   DAMPING ELASTIC FORCE function for lower torso bottom of 50% Hybrid
!   III to rigid plate contact
!   (apply with DAMPING COEFFICIENT      1.0)
      3
       0.0 0.0
       1190.0 1927.0
       10088.0 10274.0
      END FUNCTIONS
    END PLANE-ELLIPSOID
!
    PLANE-ELLIPSOID
!     5: Seat Back to Lower Lumbar
      INERTIAL SPACE
      PLANE                    2
      SYSTEM                   1
      ELLIPSOID                5
      CHARACTERISTIC           ELLIPSOID
      DAMPING COEFFICIENT      1.0
      DAMPING ELASTIC FORCE    1
      FRICTION COEFFICIENT     0.29
      BOUNDARYWIDTH            INFINITE
      CORRECTION               ON
      FUNCTIONS
!   DAMPING ELASTIC FORCE function for lower torso bottom of 50% Hybrid
!   III to rigid plate contact
!   (apply with DAMPING COEFFICIENT      1.0)
      3
       0.0 0.0
       1190.0 1927.0
       10088.0 10274.0
      END FUNCTIONS
    END PLANE-ELLIPSOID
!
    PLANE-ELLIPSOID
!     6: Seat Back to Upper Torso
      INERTIAL SPACE
      PLANE                    2
      SYSTEM                   1
      ELLIPSOID                7
      CHARACTERISTIC           ELLIPSOID
      DAMPING COEFFICIENT      3.0
```

```
      FRICTION COEFFICIENT     0.29
      BOUNDARYWIDTH            INFINITE
      CORRECTION               ON
    END PLANE-ELLIPSOID
!
!     7: Floor Plane to Left Foot
!
    PLANE-ELLIPSOID
      NULL SYSTEM              1
      PLANE                    1
      INERTIAL SPACE
      SYSTEM                   1
      ELLIPSOID                43
      CHARACTERISTIC           ELLIPSOID
      DAMPING COEFFICIENT      2.3E2
      FRICTION COEFFICIENT     0.80
      BOUNDARYWIDTH            INFINITE
      CORRECTION               ON
    END PLANE-ELLIPSOID
!
!     8: Floor Plane to Left Heel
!
    PLANE-ELLIPSOID
      NULL SYSTEM              1
      PLANE                    1
      INERTIAL SPACE
      SYSTEM                   1
      ELLIPSOID                44
      CHARACTERISTIC           ELLIPSOID
      DAMPING COEFFICIENT      2.3E2
      FRICTION COEFFICIENT     0.80
      BOUNDARYWIDTH            INFINITE
      CORRECTION               ON
    END PLANE-ELLIPSOID
!
!     9: Floor Plane to Front Shoe Sole Left
!
    PLANE-ELLIPSOID
      NULL SYSTEM              1
      PLANE                    1
      INERTIAL SPACE
      SYSTEM                   1
      ELLIPSOID                45
      CHARACTERISTIC           ELLIPSOID
      DAMPING COEFFICIENT      2.3E2
      FRICTION COEFFICIENT     0.80
      BOUNDARYWIDTH            INFINITE
      CORRECTION               ON
    END PLANE-ELLIPSOID
!
!     10: Floor Plane to Heel Shoe Left
!
    PLANE-ELLIPSOID
      NULL SYSTEM              1
```

```
      PLANE                    1
      INERTIAL SPACE
      SYSTEM                   1
      ELLIPSOID                46
      CHARACTERISTIC           ELLIPSOID
      DAMPING COEFFICIENT      2.3E2
      FRICTION COEFFICIENT     0.80
      BOUNDARYWIDTH            INFINITE
      CORRECTION               ON
    END PLANE-ELLIPSOID
!
!     11: Floor Plane to Right Foot
!
    PLANE-ELLIPSOID
      NULL SYSTEM              1
      PLANE                    1
      INERTIAL SPACE
      SYSTEM                   1
      ELLIPSOID                47
      CHARACTERISTIC           ELLIPSOID
      DAMPING COEFFICIENT      2.3E2
      FRICTION COEFFICIENT     0.80
      BOUNDARYWIDTH            INFINITE
      CORRECTION               ON
    END PLANE-ELLIPSOID
!
!     12: Floor Plane to Right Heel
!
    PLANE-ELLIPSOID
      NULL SYSTEM              1
      PLANE                    1
      INERTIAL SPACE
      SYSTEM                   1
      ELLIPSOID                48
      CHARACTERISTIC           ELLIPSOID
      DAMPING COEFFICIENT      2.3E2
      FRICTION COEFFICIENT     0.80
      BOUNDARYWIDTH            INFINITE
      CORRECTION               ON
    END PLANE-ELLIPSOID
!
!     13: Floor Plane to Front Shoe Sole Right
!
    PLANE-ELLIPSOID
      NULL SYSTEM              1
      PLANE                    1
      INERTIAL SPACE
      SYSTEM                   1
      ELLIPSOID                49
      CHARACTERISTIC           ELLIPSOID
      DAMPING COEFFICIENT      2.3E2
      FRICTION COEFFICIENT     0.80
      BOUNDARYWIDTH            INFINITE
      CORRECTION               ON
```

```
    END PLANE-ELLIPSOID
!
!     14: Floor Plane to Heel Shoe Right
!
    PLANE-ELLIPSOID
      NULL SYSTEM              1
      PLANE                    1
      INERTIAL SPACE
      SYSTEM                   1
      ELLIPSOID                50
      CHARACTERISTIC           ELLIPSOID
      DAMPING COEFFICIENT      2.3E2
      FRICTION COEFFICIENT     0.80
      BOUNDARYWIDTH            INFINITE
      CORRECTION               ON
    END PLANE-ELLIPSOID
!
!     15: Heel Plane to Heel Left Foot
!
    PLANE-ELLIPSOID
      NULL SYSTEM              1
      PLANE                    2
      INERTIAL SPACE
      SYSTEM                   1
      ELLIPSOID                44
      CHARACTERISTIC           ELLIPSOID
      DAMPING COEFFICIENT      2.3E2
      FRICTION COEFFICIENT     0.80
      BOUNDARYWIDTH            INFINITE
      CORRECTION               ON
    END PLANE-ELLIPSOID
!
!     16: Heel Plane to Heel Shoe Left
!
    PLANE-ELLIPSOID
      NULL SYSTEM              1
      PLANE                    2
      INERTIAL SPACE
      SYSTEM                   1
      ELLIPSOID                46
      CHARACTERISTIC           ELLIPSOID
      DAMPING COEFFICIENT      2.3E2
      FRICTION COEFFICIENT     0.80
      BOUNDARYWIDTH            INFINITE
      CORRECTION               ON
    END PLANE-ELLIPSOID
!
!     17: Heel Plane to Right Heel
!
    PLANE-ELLIPSOID
      NULL SYSTEM              1
      PLANE                    2
      INERTIAL SPACE
      SYSTEM                   1
```

```
      ELLIPSOID               48
      CHARACTERISTIC          ELLIPSOID
      DAMPING COEFFICIENT     2.3E2
      FRICTION COEFFICIENT    0.80
      BOUNDARYWIDTH           INFINITE
      CORRECTION              ON
    END PLANE-ELLIPSOID
!
!     18: Heel Plane to Heel Shoe Right
!
    PLANE-ELLIPSOID
      NULL SYSTEM             1
      PLANE                   2
      INERTIAL SPACE
      SYSTEM                  1
      ELLIPSOID               50
      CHARACTERISTIC          ELLIPSOID
      DAMPING COEFFICIENT     2.3E2
      FRICTION COEFFICIENT    0.80
      BOUNDARYWIDTH           INFINITE
      CORRECTION              ON
    END PLANE-ELLIPSOID
!
!     19: Seat back to Left upper arm
!
    PLANE-ELLIPSOID
      INERTIAL SPACE
      PLANE                   2
      SYSTEM                  1
      ELLIPSOID               29
      CHARACTERISTIC          ELLIPSOID
      DAMPING COEFFICIENT     2.3E2
      FRICTION COEFFICIENT    0.8
      BOUNDARYWIDTH           0.050
      CORRECTION              ON
    END PLANE-ELLIPSOID
!
!     20: Seat back to Right upper arm
!
    PLANE-ELLIPSOID
      INERTIAL SPACE
      PLANE                   2
      SYSTEM                  1
      ELLIPSOID               30
      CHARACTERISTIC          ELLIPSOID
      DAMPING COEFFICIENT     2.3E2
      FRICTION COEFFICIENT    0.8
      BOUNDARYWIDTH           0.050
      CORRECTION              ON
    END PLANE-ELLIPSOID
!
!     21: Seat back to Left lower arm
!
    PLANE-ELLIPSOID
```

```
      INERTIAL SPACE
      PLANE                    2
      SYSTEM                   1
      ELLIPSOID                31
      CHARACTERISTIC           ELLIPSOID
      DAMPING COEFFICIENT      2.3E2
      FRICTION COEFFICIENT     0.8
      BOUNDARYWIDTH            0.050
      CORRECTION               ON
    END PLANE-ELLIPSOID
!
!     22: Seat back to Right lower arm
!
    PLANE-ELLIPSOID
      INERTIAL SPACE
      PLANE                    2
      SYSTEM                   1
      ELLIPSOID                32
      CHARACTERISTIC           ELLIPSOID
      DAMPING COEFFICIENT      2.3E2
      FRICTION COEFFICIENT     0.8
      BOUNDARYWIDTH            0.050
      CORRECTION               ON
    END PLANE-ELLIPSOID
!
!     23: Seat Cush to Left hand
!
    PLANE-ELLIPSOID
      INERTIAL SPACE
      PLANE                    1
      SYSTEM                   1
      ELLIPSOID                33
      CHARACTERISTIC           ELLIPSOID
      DAMPING COEFFICIENT      2.3E2
      FRICTION COEFFICIENT     0.8
      BOUNDARYWIDTH            0.050
      CORRECTION               ON
    END PLANE-ELLIPSOID
!
!     24: Seat Cush to Right hand
!
    PLANE-ELLIPSOID
      INERTIAL SPACE
      PLANE                    1
      SYSTEM                   1
      ELLIPSOID                34
      CHARACTERISTIC           ELLIPSOID
      DAMPING COEFFICIENT      2.3E2
      FRICTION COEFFICIENT     0.8
      BOUNDARYWIDTH            0.050
      CORRECTION               ON
    END PLANE-ELLIPSOID
END CONTACT INTERACTIONS
!
```

Since most of the output desired for this case study is already specified in the 50th percentile male dummy model, only a few of the OUTPUT PARAMETERS needed to be changed or made active, and they are presented below.

```
!
  JNTPOS
! left and right knee, DOF1=extension, DOF2=knee slider displacement
   1   1
   1  23
   1  24
   1  27
   1  28
  END
  INJURY PARAMETERS
    FNIC
!     Neck Injury Criteria
!     SEQNR  TYPE     FILTER   ID
      3      TENSION  CFC1000  d3hyb350
      3      SHEAR    CFC1000  d3hyb350
      3      BENDING  CFC600   d3hyb350
    END
    NIJ
!     Neck Injury Predictor
!     SEQNR  TYPE  MYC  FZC   ECC     MFILTER  FFILTER  ID
!     Tension-extension
      3      NTE   125  3600  0.0178  CFC600   CFC1000  d3hyb350
!     Tension-flexion
      3      NTF   410  3600  0.0178  CFC600   CFC1000  d3hyb350
!     Compression-extension
      3      NCE   125  3600  0.0178  CFC600   CFC1000  d3hyb350
!     Compression-flexion
      3      NCF   410  3600  0.0178  CFC600   CFC1000  d3hyb350
    END
    LOAD CELL
!     Load cell signals for in the *.injury file
!     Not standard load cell output is swiched off
!     SEQNR  TYPE    DIR       FILTER   ID
!     Lower neck load cell (forces & torques)
     3      FORCE   JOINT2.R  CFC1000  Fres lwr neck d3hyb350
     3      FORCE   JOINT2.X  CFC1000  Fx shear lwr neck d3hyb350
     3      FORCE   JOINT2.Y  CFC1000  Fy shear lwr neck d3hyb350
     3      FORCE   JOINT2.Z  CFC1000  Fz axial lwr neck d3hyb350
     3      TORQUE  JOINT2.R  CFC600   Mres lwr neck d3hyb350
     3      TORQUE  JOINT2.X  CFC600   Mx lwr neck (roll) d3hyb350
     3      TORQUE  JOINT2.Y  CFC600   My lwr neck (pitch) d3hyb350
     3      TORQUE  JOINT2.Z  CFC600   Mz lwr neck (yaw) d3hyb350
!     Upper neck load cell (forces & torques)
     4      FORCE   JOINT2.R  CFC1000  Fres upp neck d3hyb350
     4      FORCE   JOINT2.X  CFC1000  Fx shear upp neck d3hyb350
     4      FORCE   JOINT2.Y  CFC1000  Fy shear upp neck d3hyb350
     4      FORCE   JOINT2.Z  CFC1000  Fz axial upp neck d3hyb350
     4      TORQUE  JOINT2.R  CFC600   Mres upp neck d3hyb350
     4      TORQUE  JOINT2.X  CFC600   Mx upp neck (roll) d3hyb350
     4      TORQUE  JOINT2.Y  CFC600   My upp neck (pitch) d3hyb350
```

```
     4      TORQUE  JOINT2.Z  CFC600   Mz upp neck (yaw) d3hyb350
    END
  END INJURY PARAMETERS
!
```

These were the text lines altered or added to the d3hyb350.dat dummy file, developed by TNO-MADYMO N.A. and located in the dummy database of the share directory. The other occupant simulations were completed in a similar fashion with the appropriate commands and values.

Pilot Ejection and Windblast Text File Changes and Additions

```
PILOT EJECTION AND WINDBLAST
95% male, M=.9, alpha=90 degrees, a/L=1/8 (Schnecks Eq.)
April 2, 2000
!
```

The following contact interactions were defined within system 1 of the ejection.opt file found in the MADYMO share directory:

```
!
  CONTACT INTERACTIONS
    ELLIPSOID-ELLIPSOID
!     3: Left Hand to Left Thigh
         SYSTEM        1
         ELLIPSOID     33
         SYSTEM        1
         ELLIPSOID     35
         CHARACTERISTIC   COMBINED
    END ELLIPSOID-ELLIPSOID
    ELLIPSOID-ELLIPSOID
!     4: Right Hand to Right Thigh
         SYSTEM        1
         ELLIPSOID     34
         SYSTEM        1
         ELLIPSOID     37
         CHARACTERISTIC   COMBINED
    END ELLIPSOID-ELLIPSOID
    ELLIPSOID-ELLIPSOID
!     5: Left Lower Arm to Left Thigh
         SYSTEM        1
         ELLIPSOID     31
         SYSTEM        1
         ELLIPSOID     35
         CHARACTERISTIC   COMBINED
    END ELLIPSOID-ELLIPSOID
    ELLIPSOID-ELLIPSOID
!     6: Right Lower Arm to Right Thigh
         SYSTEM        1
         ELLIPSOID     32
         SYSTEM        1
         ELLIPSOID     37
         CHARACTERISTIC   COMBINED
    END ELLIPSOID-ELLIPSOID
    ELLIPSOID-ELLIPSOID
!     7: Left Hand to Right Hand
         SYSTEM        1
         ELLIPSOID     33
         SYSTEM        1
         ELLIPSOID     34
         CHARACTERISTIC   COMBINED
    END ELLIPSOID-ELLIPSOID
    ELLIPSOID-ELLIPSOID
!     8: Left Hand to Right Lower Arm
         SYSTEM        1
```

```
          ELLIPSOID     33
          SYSTEM        1
          ELLIPSOID     32
          CHARACTERISTIC   COMBINED
     END ELLIPSOID-ELLIPSOID
     ELLIPSOID-ELLIPSOID
!      9: Left Hand to Right Upper Arm
          SYSTEM        1
          ELLIPSOID     33
          SYSTEM        1
          ELLIPSOID     30
          CHARACTERISTIC   COMBINED
     END ELLIPSOID-ELLIPSOID
     ELLIPSOID-ELLIPSOID
!     10: Right Hand to Left Lower Arm
          SYSTEM        1
          ELLIPSOID     34
          SYSTEM        1
          ELLIPSOID     31
          CHARACTERISTIC   COMBINED
     END ELLIPSOID-ELLIPSOID
     ELLIPSOID-ELLIPSOID
!     11: Right Hand to Left Upper Arm
          SYSTEM        1
          ELLIPSOID     34
          SYSTEM        1
          ELLIPSOID     29
          CHARACTERISTIC   COMBINED
     END ELLIPSOID-ELLIPSOID
     ELLIPSOID-ELLIPSOID
!     12: Left Lower Arm to Right Lower Arm
          SYSTEM        1
          ELLIPSOID     31
          SYSTEM        1
          ELLIPSOID     32
          CHARACTERISTIC   COMBINED
     END ELLIPSOID-ELLIPSOID
     ELLIPSOID-ELLIPSOID
!     13: Left Lower Arm to Right Upper Arm
          SYSTEM        1
          ELLIPSOID     31
          SYSTEM        1
          ELLIPSOID     30
          CHARACTERISTIC   COMBINED
     END ELLIPSOID-ELLIPSOID
     ELLIPSOID-ELLIPSOID
!     14: Left Upper Arm to Right Upper Arm
          SYSTEM        1
          ELLIPSOID     29
          SYSTEM        1
          ELLIPSOID     30
          CHARACTERISTIC   COMBINED
     END ELLIPSOID-ELLIPSOID
   END CONTACT INTERACTIONS
```

```
!
```
In the JOINT DOF block, only the arms were repositioned so that they were not initially penetrating the legs as in the original ejection.opt file. The following lines were changed:
```
!
  JOINT DOF
!   left elbow: lateral rotation=yaw left; hyper-extension=pitch down up
    16  FREE  -0.812291  -1.31
!   right elbow: medial rotation=yaw left; hyper-extension=pitch down up
    17  FREE   0.812291  -1.31
  END JOINT DOF
!
```
The following commands were taken from a3sldh50.dat (located in MADYMO's share directory) but changed slightly so that the belt connected to the intersection of the seat back and cushion and the dummy's hips.
```
!
  BELTS
!   1: Seat Corner to Lower Torso/Abdomen
   2  2  0.00  0.229  0.00  1  2   -.0362  -.1630  -.0546  +
     1  2   6.0E5   0.01   0.05  0.00  0.00  1.0  Rt. Lap Belt
!   2: Lower Torso/Abdomen to Seat Corner
   1  2   -.0362  0.1630  -.0546  2  2   0.00  -0.229  0.00  +
     1  2   6.0E5   0.01   0.05  0.00  0.00  1.0  Lt. Lap Belt
  END BELT SEGEMENT
  FUNCTIONS
!   1: Belt loading (10% web extension)
    13
    0.0 0.0  0.011 1000.0 0.02 2950.0 0.03 4000.0 0.04 4700.0 0.05  +
    5320.0 0.06 6000.0
    0.07 6600.0 0.08 7250.0 0.09 8000.0 0.10 8680.0 0.11 9500.0 0.116  +
    10000.0
!   2: Belt unloading (10% web extension)
    2
    0.0 0.0  0.1 1000.0
  END
!
```
Since the ejection.opt file dealt with MADYMIZER, certain commands needed to be changed. The SENSORS command and corresponding CONTROL MODULE was replaced by:
```
!
!TRIGGERING CONDITIONS
  NUMBER       1
  SIGNALTYPE   REFERENCE SIGNAL
  SEQNUM       1
  NUMBER       2
  SIGNALTYPE   REFERENCE SIGNAL
  SEQNUM       2
END TRIGGERING CONDITIONS
CONTROL MODULE
  REFERENCE SIGNALS
!
    1  FUNC    1
```

```
    2  FUNC    2
    3  FUNC    3
    4  FUNC    4
    5  FUNC    5
    6  FUNC    6
    7  FUNC    7
    8  FUNC    8
    9  FUNC    9
   10  FUNC    10
   11  FUNC    11
   12  FUNC    12
   13  FUNC    13
   14  FUNC    14
  END REFERENCE SIGNALS
  FUNCTIONS
! 1: Ejection process - firing mechanism
  18
  0.000000  0000
  0.010000  3000
  0.020000  6000
  0.030000  10000
  0.040000  11000
  0.050000  13000
  0.060000  15000
  0.070000  17000
  0.080000  19000
  0.090000  18000
  0.100000  17000
  0.110000  16500
  0.120000  16000
  0.130000  15000
  0.140000  15000
  0.150000  14000
  0.160000  14000
  0.500000  0.000000
! 2: Ejection process - rocket booster
  5
  0.000000   0.000000
  0.160000   0.000000
  0.161000   15000
  0.200000   15000
  10.00000   0.00
!
! The forces below are given using F=1148*M^2*sin^2(alpha) lbf.
! 1148lbf=5106.56N
! Alpha is the angle of attack.  M is the Mach number
! (M=windspeed/735mph).  This equation was derived by Schneck in
! "Studies of Limb-Dislodging Forces Acting on an Ejection Seat
! Occupant" (Aerospace Medical Association c1980)
!
! 3: windblast associated with the head (M=.9   alpha=90 degrees)
  4
  0.000000  0.000
  0.089000  0.000
```

```
  0.090000  -4136.31
  1.000000  -4136.31
! 4: windblast associated with the upper torso (M=.9   alpha=90 degrees)
  4
  0.000000  0.000
  0.124000  0.000
  0.125000  -4136.31
  1.000000  -4136.31
! 5: windblast associated with the lt up arm (M=.9   alpha=90 degrees)
  4
  0.000000  0.000
  0.124000  0.000
  0.125000  -4136.31
  1.000000  -4136.31
! 6: windblast associated with the rt up arm (M=.9   alpha=90 degrees)
  4
  0.000000  0.000
  0.124000  0.000
  0.125000  -4136.31
  1.000000  -4136.31
! 7: windblast associated with the sternum (M=.9   alpha=90 degrees)
  4
  0.000000  0.000
  0.143000  0.000
  0.144000  -4136.31
  1.000000  -4136.31
! 8: windblast associated with the lt low arm (M=.9   alpha=90 degrees)
  4
  0.000000  0.000
  0.155000  0.000
  0.156000  -4136.31
  1.000000  -4136.31
! 9: windblast associated with the rt low arm (M=.9   alpha=90 degrees)
  4
  0.000000  0.000
  0.155000  0.000
  0.156000  -4136.31
  1.000000  -4136.31
! 10: windblast associated with the lower torso (M=.9  alpha=90 degrees)
  4
  0.000000  0.000
  0.159000  0.000
  0.160000  -4136.31
  1.000000  -4136.31
! 11: windblast associated with the femur (M=.9   alpha=90 degrees)
  4
  0.000000  0000
  0.164000  0.000
  0.165000  -4136.31
  1.000000  -4136.31
! 12: windblast associated with the femur (M=.9   alpha=90 degrees)
  4
  0.000000  0000
  0.164000  0.000
```

```
  0.165000  -4136.31
  1.000000  -4136.31
! 13: windblast associated with the tibia (M=.9   alpha=90 degrees)
  4
  0.000000  0000
  0.189000  0.000
  0.190000  -4136.31
  1.000000  -4136.31
! 14: windblast associated with the tibia (M=.9   alpha=90 degrees)
  4
  0.000000  0000
  0.189000  0.000
  0.190000  -4136.31
  1.000000  -4136.31
 END FUNCTIONS
  BODY ACTUATORS
    1  FORCE  REFERENCE SIGNAL  1  LOCAL  0.00000  0.00  1.0000   2  2 +
         0  0.0000  0.0000  0.00000   -1  0  0  0.0       0.0   0.0
    2  FORCE  REFERENCE SIGNAL  2  LOCAL  0.31134  0.00  0.9503   2  2 +
         0  0.0851  0.0000  -0.1189   -1  0  0  0.085100  0.0  -0.1189
    3  FORCE  REFERENCE SIGNAL  3  INERTIAL  1.00  0.00  0.00   1  11  +
         0  0.00  0.00  0.00
    4  FORCE  REFERENCE SIGNAL  4  INERTIAL  1.00  0.00  0.00   1  5  +
         0  0.00  0.00  0.00
    5  FORCE  REFERENCE SIGNAL  5  INERTIAL  1.00  0.00  0.00   1  14  +
         0  0.00  0.00  0.00
    6  FORCE  REFERENCE SIGNAL  6  INERTIAL  1.00  0.00  0.00   1  15  +
         0  0.00  0.00  0.00
    7  FORCE  REFERENCE SIGNAL  7  INERTIAL  1.00  0.00  0.00   1  32  +
         0  0.00  0.00  0.00
    8  FORCE  REFERENCE SIGNAL  8  INERTIAL  1.00  0.00  0.00   1  16  +
         0  0.00  0.00  0.00
    9  FORCE  REFERENCE SIGNAL  9  INERTIAL  1.00  0.00  0.00   1  17  +
         0  0.00  0.00  0.00
   10  FORCE  REFERENCE SIGNAL  10  INERTIAL  1.00  0.00  0.00   1  1  +
         0  0.00  0.00  0.00
   11  FORCE  REFERENCE SIGNAL  11  INERTIAL  1.00  0.00  0.00   1  20 +
         0  0.00  0.00  0.00
   12  FORCE  REFERENCE SIGNAL  12  INERTIAL  1.00  0.00  0.00   1  21 +
         0  0.00  0.00  0.00
   13  FORCE  REFERENCE SIGNAL  13  INERTIAL  1.00  0.00  0.00   1  24 +
         0  0.00  0.00  0.00
   14  FORCE  REFERENCE SIGNAL  14  INERTIAL  1.00  0.00  0.00   1  25 +
         0  0.00  0.00  0.00
  END BODY ACTUATORS
  END CONTROL MODULE
!
```

Some of the OUTPUT PARAMETERS below were already specified in the ejection.opt file developed by MADYMO and are not needed for this specific case study. However, the OUPUT PARAMETERS needed are as follows:

```
!
  RELDIS
   1  5   0.1718 0.0000 0.0628  1  32  0.0000 0.0000 0.0000  0  Sternum
```

```
   2  2   0.0000 0.0000 0.0000 -1   0  -.2850 0.0000 -.0689  0  Seat
  END
  DISVEL
   1  32  0.0000 0.0000 0.0000  1  5   0.1718 0.0000 0.0628  Sternum
  END
  LINACC
!   1:3
!   acceleration corrected for pulse in x direction
   1  1  -0.0538 0.0000 -.0224  1  0  0  1   Lower Torso
   1  5   0.0518 0.0000 0.0648  1  0  0  1   Upper Torso
   1  11  0.0178 0.0000 0.0343  1  0  0  1   Head
    FILTERLIST  CFC1000
   2  2   0.0000 0.0000 0.0000  1  0  1  1   Gun
   1  29  0.0000 0.0000 0.0000  0  0  0  1   Lt. Upper Arm
   1  29  0.0000 0.0000 0.0000  0  0  0  1   Lt. Upper Arm
   1  30  0.0000 0.0000 0.0000  0  0  0  1   Rt. Upper Arm
   1  31  0.0000 0.0000 0.0000  0  0  0  1   Lt. Lower Arm
   1  32  0.0000 0.0000 0.0000  0  0  0  1   Rt. Lower Arm
  END
  ORIENTATIONS
!   1: lower torso accelerometer: x front, y right, z down
    1  0   1   1  3.14159
!   2: upper torso accelerometer: x front, y right, z down
    2  0   1   1  3.14159  2  0.07833
!   3: head accelerometer: x front, y right, z down
    3  0   1   1  3.14159
  END
  FORCES
!  Output belt forces
    4  1  1
    4  2  1
  END FORCES
  TORQU1
!   Pitch of seat
    0  1  1
  END TORQU1
  JOINT LOADS
    1  14  left shoulder
    1  15  right shoulder
    1  16  left elbow
    1  17  right elbow
  END JOINT LOADS
 CONSTRAINT LOADS
!   lower lumbar load cell
   1  3
!   upper lumbar load cell
   1  5
!   lower neck load cell
   1  8
!   upper neck load cell
   1  11
!   left and right femur load cells
   1  22
   1  23
```

```
!   left and right upper tibia load cells
   1  26
   1  27
!   left and right lower tibia load cells
   1  28
   1  29
  END
  JNTPOS
   2   1
   2   2
  END JNTPOS
  JNTVEL
   2   1
   2   2
  END JNTVEL
  INJURY PARAMETERS
    HIC
      3  0.036  head
    END
    GSI
      3
    END
    3MS
!     Upper Torso acceleration
      2
    END
    VC
!     Sternum deflection VC=1.3 m/s then 50% of severe thoracic injury
!    (AIS>4)
      1  0.254
    END
    FNIC
!     Neck Injury Criteria
!     SEQNR  TYPE     FILTER   ID
      3      TENSION  CFC1000  d3hyb395
      3      SHEAR    CFC1000  d3hyb395
      3      BENDING  CFC600   d3hyb395
    END
    NIJ
!     Neck Injury Predictor
!     SEQNR  TYPE  MYC  FZC   ECC     MFILTER  FFILTER  ID
!     Tension-extension
      3      NTE   125  3600  0.0178  CFC600   CFC1000  d3hyb395
!     Tension-flexion
      3      NTF   410  3600  0.0178  CFC600   CFC1000  d3hyb395
!     Compression-extension
      3      NCE   125  3600  0.0178  CFC600   CFC1000  d3hyb395
!     Compression-flexion
      3      NCF   410  3600  0.0178  CFC600   CFC1000  d3hyb395
    END
    LOAD CELL
!     Load cell signals for in the *.injury file
!     Not standard load cell output is swiched off
!     SEQNR  TYPE    DIR       FILTER   ID
```

```
!     Lower neck load cell (forces & torques)
      3       FORCE   JOINT2.R  CFC1000  Fres lwr neck d3hyb395
      3       FORCE   JOINT2.X  CFC1000  Fx shear lwr neck d3hyb395
      3       FORCE   JOINT2.Y  CFC1000  Fy shear lwr neck d3hyb395
      3       FORCE   JOINT2.Z  CFC1000  Fz axial lwr neck d3hyb395
      3       TORQUE  JOINT2.R  CFC600   Mres lwr neck d3hyb395
      3       TORQUE  JOINT2.X  CFC600   Mx lwr neck (roll) d3hyb395
      3       TORQUE  JOINT2.Y  CFC600   My lwr neck (pitch) d3hyb395
      3       TORQUE  JOINT2.Z  CFC600   Mz lwr neck (yaw) d3hyb395
!     Upper neck load cell (forces & torques)
      4       FORCE   JOINT2.R  CFC1000  Fres upp neck d3hyb395
      4       FORCE   JOINT2.X  CFC1000  Fx shear upp neck d3hyb395
      4       FORCE   JOINT2.Y  CFC1000  Fy shear upp neck d3hyb395
      4       FORCE   JOINT2.Z  CFC1000  Fz axial upp neck d3hyb395
      4       TORQUE  JOINT2.R  CFC600   Mres upp neck d3hyb395
      4       TORQUE  JOINT2.X  CFC600   Mx upp neck (roll) d3hyb395
      4       TORQUE  JOINT2.Y  CFC600   My upp neck (pitch) d3hyb395
      4       TORQUE  JOINT2.Z  CFC600   Mz upp neck (yaw) d3hyb395
!     Left femur load cell (forces & torque's)
      5       FORCE   JOINT1.R  CFC600   Fres left femur d3hyb395
      5       FORCE   JOINT1.X  CFC600   Fx shear left femur d3hyb395
      5       FORCE   JOINT1.Y  CFC600   Fy shear left femur d3hyb395
       5       FORCE   JOINT1.Z  CFC600   Fz axial left femur d3hyb395
      5       TORQUE  JOINT1.R  CFC600   Mres left femur d3hyb395
      5       TORQUE  JOINT1.X  CFC600   Mx left femur (roll) d3hyb395
      5       TORQUE  JOINT1.Y  CFC600   My left femur (pitch) d3hyb395
      5       TORQUE  JOINT1.Z  CFC600   Mz left femur (yaw) d3hyb395
!     Right femur load cell (forces & torque's)
      6       FORCE   JOINT1.R  CFC600   Fres right femur d3hyb395
      6       FORCE   JOINT1.X  CFC600   Fx shear right femur d3hyb395
      6       FORCE   JOINT1.Y  CFC600   Fy shear right femur d3hyb395
       6       FORCE   JOINT1.Z  CFC600   Fz axial right femur d3hyb395
      6       TORQUE  JOINT1.R  CFC600   Mres right femur d3hyb395
      6       TORQUE  JOINT1.X  CFC600   Mx right femur (roll) d3hyb395
      6       TORQUE  JOINT1.Y  CFC600   My right femur (pitch) d3hyb395
      6       TORQUE  JOINT1.Z  CFC600   Mz right femur (yaw) d3hyb395
!     Left upper tibia load cell (forces & torque's)
      7       FORCE   JOINT1.R  CFC600   Fres left upp tibia d3hyb395
      7       FORCE   JOINT1.X  CFC600   Fx shear left upp tibia d3hyb395
      7       FORCE   JOINT1.Y  CFC600   Fy shear left upp tibia d3hyb395
      7       FORCE   JOINT1.Z  CFC600   Fz axial left upp tibia d3hyb395
      7       TORQUE  JOINT1.R  CFC600   Mres left upp tibia d3hyb395
       7       TORQUE  JOINT1.X  CFC600   Mx left upp tibia d3hyb395
       7       TORQUE  JOINT1.Y  CFC600   My left upp tibia d3hyb395
      7       TORQUE  JOINT1.Z  CFC600   Mz left upp tibia d3hyb395
!     Right upper tibia load cell (forces & torque's)
      8       FORCE   JOINT1.R  CFC600   Fres right upp tibia d3hyb395
      8       FORCE   JOINT1.X  CFC600   Fx shear right upp tibia d3hyb395
      8       FORCE   JOINT1.Y  CFC600   Fy shear right upp tibia d3hyb395
      8       FORCE   JOINT1.Z  CFC600   Fz axial right upp tibia d3hyb395
      8       TORQUE  JOINT1.R  CFC600   Mres right upp tibia d3hyb395
       8       TORQUE  JOINT1.X  CFC600   Mx right upp tibia d3hyb395
       8       TORQUE  JOINT1.Y  CFC600   My right upp tibia d3hyb395
      8       TORQUE  JOINT1.Z  CFC600   Mz right upp tibia d3hyb395
```

```
!     Left lower tibia load cell (forces & torque's)
     9      FORCE   JOINT1.R  CFC600   Fres left lwr tibia d3hyb395
      9      FORCE   JOINT1.X  CFC600   Fx shear left lwr tibia d3hyb395
      9      FORCE   JOINT1.Y  CFC600   Fy shear left lwr tibia d3hyb395
      9      FORCE   JOINT1.Z  CFC600   Fz axial left lwr tibia d3hyb395
     9      TORQUE  JOINT1.R  CFC600   Mres left lwr tibia d3hyb395
      9      TORQUE  JOINT1.X  CFC600   Mx left lwr tibia d3hyb395
      9      TORQUE  JOINT1.Y  CFC600   My left lwr tibia d3hyb395
     9      TORQUE  JOINT1.Z  CFC600   Mz left lwr tibia d3hyb395
!     Right lower tibia load cell (forces & torque's)
     10     FORCE   JOINT1.R  CFC600   Fres right lwr tibia d3hyb395
     10     FORCE   JOINT1.X  CFC600   Fx shear right lwr tibia d3hyb395
     10     FORCE   JOINT1.Y  CFC600   Fy shear right lwr tibia d3hyb395
     10     FORCE   JOINT1.Z  CFC600   Fz axial right lwr tibia d3hyb395
     10     TORQUE  JOINT1.R  CFC600   Mres right lwr tibia d3hyb395
     10     TORQUE  JOINT1.X  CFC600   Mx right lwr tibia d3hyb395
     10     TORQUE  JOINT1.Y  CFC600   My right lwr tibia d3hyb395
     10     TORQUE  JOINT1.Z  CFC600   Mz right lwr tibia d3hyb395
    END
  END INJURY PARAMETERS
!
```

These were the text lines altered or added to the ejection.dat application file (ejection.opt), developed by TNO-MADYMO N.A., to simulate pilot ejection and windblast. The other ejection simulations were performed similarly.

Plantar Fasciitis Text File Changes and Additions

```
Case Study 2
Plantar Fascitis (human male)
March 1, 2000
!
GENERAL INPUT
T0   0
TE   0.53
INT  RUKU4
TS   1E-4
END GENERAL INPUT
!
INERTIAL SPACE
GROUND
PLANES
0  -1  .25  -.01375  -1  -.25  -.01375  1.25  -.25  -.01375  +
       0  0  0.0    Base
END PLANES
END INERTIAL SPACE
!
NULL SYSTEM
Balast
ELLIPSOIDS
!BODY  A      B       C      Mx    My  Mz     n  LO UNLO  HYS   ID
! to control the flatness of the rocks top surface change "n" (degree)
! in the y-direction row 1 (center row)
! ellipsoids 1:6
  0   .04  .027344  .01375  0.000  0.000  0.000    5  0   0     0
  0   .04  .027344  .01375  0.080  0.000  0.000    5  0   0     0
  0   .04  .027344  .01375  0.160  0.000  0.000    5  0   0     0
  0   .04  .027344  .01375  0.240  0.000  0.000    5  0   0     0
  0   .04  .027344  .01375  0.320  0.000  0.000    5  0   0     0
  0   .04  .027344  .01375  0.400  0.000  0.000    5  0   0     0
! in the +y-direction row #2
! ellipsoids 7:14
  0   .027344  .04  .01375  0.0000  0.0673  0.000    5  0   0     0
  0   .027344  .04  .01375  0.0547  0.0673  0.000    5  0   0     0
  0   .027344  .04  .01375  0.1094  0.0673  0.000    5  0   0     0
  0   .027344  .04  .01375  0.1641  0.0673  0.000    5  0   0     0
  0   .027344  .04  .01375  0.2188  0.0673  0.000    5  0   0     0
  0   .027344  .04  .01375  0.2735  0.0673  0.000    5  0   0     0
  0   .027344  .04  .01375  0.3282  0.0673  0.000    5  0   0     0
  0   .027344  .04  .01375  0.3829  0.0673  0.000    5  0   0     0
! in the +y-direction row #3
! ellipsoids 15:20
  0   .04  .027344  .01375  0.000  0.1347  0.000    5  0   0     0
  0   .04  .027344  .01375  0.080  0.1347  0.000    5  0   0     0
  0   .04  .027344  .01375  0.160  0.1347  0.000    5  0   0     0
  0   .04  .027344  .01375  0.240  0.1347  0.000    5  0   0     0
  0   .04  .027344  .01375  0.320  0.1347  0.000    5  0   0     0
  0   .04  .027344  .01375  0.400  0.1347  0.000    5  0   0     0
! in the -y-direction row #2
```

```
! ellipsoids 21:28
  0   .027344  .04  .01375  0.0000  -0.0673  0.000    5  0   0     0
  0   .027344  .04  .01375  0.0547  -0.0673  0.000    5  0   0     0
  0   .027344  .04  .01375  0.1094  -0.0673  0.000    5  0   0     0
  0   .027344  .04  .01375  0.1641  -0.0673  0.000    5  0   0     0
  0   .027344  .04  .01375  0.2188  -0.0673  0.000    5  0   0     0
  0   .027344  .04  .01375  0.2735  -0.0673  0.000    5  0   0     0
  0   .027344  .04  .01375  0.3282  -0.0673  0.000    5  0   0     0
  0   .027344  .04  .01375  0.3829  -0.0673  0.000    5  0   0     0
! ellipsoids 29:30 (this is for contact with the right foot)
  0   .20  .222000  .01375  -.5500   0.000   0.00    5  0   0     0
  0   .20  .222000  .01375  0.8000   0.000   0.01    5  0   0     0
  END ELLIPSOIDS
MOTION
    POSITION
    0  0.0  0.0  0.00
    5  0.0  0.0  0.00
    END POSITION
END NULL SYSTEM
!
```

The human body model developed by TNO-MADYMO N.A. would be inserted here. Some of the following lines in the system file (human body model) have been modified to produce a gait simulation:

```
!
 JOINT DOF
! NOTE: The following orientations, positions, and velocities are
!       overruled by the MOTION specified below JOINT DOF.
!  The following values would produce the MOTION below
! pelvis orientation:  x-rotation    y-rotation    z-rotation
    1   FREEROTATIONS  1  -0.04000    2  0.215    3  0.0000    +
! pelvis position:     x-disp        y-disp        z-disp
                       -0.2800       0.00000       0.8980   +
! pelvis velocities     wx      wy      wz      vx    vy   vz
                       -0.04    0.0    -0.04     2.0   0    0
! BEC/GHZ (always locked)
    2   LOCKROTATIONS
!---------------------------------------------------------------------
! spine joints         y-rot     -x-rot      z-rot         y-disp     -
x-disp      z-disp
!                      flexion    left bend  torsion       left-disp
rear-disp   elongation
! S1/L5
    3   LOCKROTATIONS  1  0.00  2  0.00  3  0.00   0.00   0.00   0.00
! L5/L4
    4   LOCKROTATIONS  1  0.00  2  0.00  3  0.00   0.00   0.00   0.00
! L4/L3
    5   LOCKROTATIONS  1  0.00  2  0.00  3  0.00   0.00   0.00   0.00
! L3/L2
    6   LOCKROTATIONS  1  0.00  2  0.00  3  0.00   0.00   0.00   0.00
! L2/L1
    7   LOCKROTATIONS  1  0.00  2  0.00  3  0.00   0.00   0.00   0.00
! L1/T12
    8   LOCKROTATIONS  1  0.00  2  0.00  3  0.00   0.00   0.00   0.00
```

```
! T12/T11
    9   FREEROTATIONS  1  0.00  2  0.00  3  0.00   0.00   0.00   0.00
! T11/T10
   10   FREEROTATIONS  1  0.00  2  0.00  3  0.00   0.00   0.00   0.00
! T10/T9
   11   FREEROTATIONS  1  0.00  2  0.00  3  0.00   0.00   0.00   0.00
! T9/T8
   12   FREEROTATIONS  1  0.00  2  0.00  3  0.00   0.00   0.00   0.00
! T8/T7
   13   FREEROTATIONS  1  0.00  2  0.00  3  0.00   0.00   0.00   0.00
! T7/T6
   14   FREEROTATIONS  1  0.00  2  0.00  3  0.00   0.00   0.00   0.00
! T6/T5
   15   FREEROTATIONS  1  0.00  2  0.00  3  0.00   0.00   0.00   0.00
! T5/T4
   16   FREEROTATIONS  1  0.00  2  0.00  3  0.00   0.00   0.00   0.00
! T4/T3
   17   FREEROTATIONS  1  0.00  2  0.00  3  0.00   0.00   0.00   0.00
! T3/T2
   18   FREEROTATIONS  1  0.00  2  0.00  3  0.00   0.00   0.00   0.00
! T2/T1
   19   FREEROTATIONS  1  0.00  2  0.00  3  0.00   0.00   0.00   0.00
!-----------------------------------------------------------------------
! Lower neck load output joint (always locked)
   20   LOCK
! neck joints         x-rot      y-rot     z-rot  x-disp  y-disp  z-disp
   21   LOCKROTATIONS  1  0.0000  2  0.0000  3  0.0   0.0   0.0   0.0
   22   LOCKROTATIONS  1  0.0000  2  0.0000  3  0.0   0.0   0.0   0.0
   23   LOCKROTATIONS  1  0.0000  2  0.0000  3  0.0   0.0   0.0   0.0
   24   LOCKROTATIONS  1  0.0000  2  0.0000  3  0.0   0.0   0.0   0.0
   25   LOCKROTATIONS  1  0.0000  2  0.0000  3  0.0   0.0   0.0   0.0
   26   LOCKROTATIONS  1  0.0000  2  0.0000  3  0.0   0.0   0.0   0.0
   27   LOCKROTATIONS  1  0.0000  2  0.0000  3  0.0   0.0   0.0   0.0
   28   LOCKROTATIONS  1  0.0000  2  0.0000  3  0.0   0.0   0.0   0.0
!-----------------------------------------------------------------------
! Upper Sternum
   29   LOCKROTATIONS
!-----------------------------------------------------------------------
! Right arm joints
  !clavicle (SPHE)
   30   LOCKROTATIONS  3  0.000000  1  0.174533  2  0.000000
  !scapula (SPHE)
   31   LOCKROTATIONS  3  0.000000  1  0.000000  2  0.000000
  ! upper arm/humerus (SPHE)
  ! positioning upper arm preferably done by rotation along the x-axis
  ! followed by rotation along the z-axis
   32   FREEROTATIONS  1  1.396263  3  0.400000  2  0.000000
  !lower arm (SPHE)    X (STIFF)    Z (flexion)  Y (axial)
   33   FREEROTATIONS  1  0.000000  3  0.200000  2  0.000000
  !mid hand
   34   LOCKROTATIONS  3  0.000000  1  0.000000  2  0.000000
  !hand parts (thumbs)
   35   LOCKROTATIONS  2  0.000000  3 -0.785398  1  0.523599
   36   LOCKROTATIONS  2  0.000000  3  0.000000  1  0.000000
```

```
   37   LOCKROTATIONS  2  0.000000  3  0.000000  1  0.000000
  !hand parts (fingers)
   38   LOCKROTATIONS  3 -0.087266  1  0.000000  2  0.000000
   39   LOCKROTATIONS  2  0.000000  3  0.000000  1  0.000000
   40   LOCKROTATIONS  2  0.000000  3  0.000000  1  0.000000
!-------------------------------------------------------------------
! Left arm joints
   !clavicle (SPHE)
   41   LOCKROTATIONS  3  0.000000  1 -0.174533  2  0.000000
  !scapula (SPHE)
   42   LOCKROTATIONS  3  0.000000  1  0.000000  2  0.000000
  ! upper arm/humerus (SPHE)
  ! positioning upper arm preferably done by rotation along the x-axis
  ! followed by rotation along the z-axis
   43   FREEROTATIONS  1 -1.396263  3  0.300000  2  0.000000
  !lower arm (SPHE)    X (STIFF)    Z (extens.)  Y (axial)
   44   FREEROTATIONS  1  0.000000  3  0.000000  2  0.000000
  !mid hand
   45   LOCKROTATIONS  3  0.000000  1  0.000000  2  0.000000
  !hand parts (thumbs)
   46   LOCKROTATIONS  2  0.000000  3  0.785398  1 -0.523599
   47   LOCKROTATIONS  2  0.000000  3  0.000000  1  0.000000
   48   LOCKROTATIONS  2  0.000000  3  0.000000  1  0.000000
  !hand parts (fingers)
   49   LOCKROTATIONS  3  0.087266  1  0.000000  2  0.000000
   50   LOCKROTATIONS  2  0.000000  3  0.000000  1  0.000000
   51   LOCKROTATIONS  2  0.000000  3  0.000000  1  0.000000
!-------------------------------------------------------------------
! Upper neck load output joint
   52   LOCKROTATIONS  2  0.000000  1  0.000000  3  0.000000
!-------------------------------------------------------------------
! Right leg joints
  !hip                 Y (rearward) X (left)     Z (medial)
   53   FREEROTATIONS  2  0.118682  1  0.000000  3  0.000000
  !knee                X (STIFF)    Y (flexion)  Z (medial)
   54   FREEROTATIONS  1  0.000000  2  0.795870  3  0.000000
  !ankle               Y (rearward) X (left)     Z (medial)
   55   FREEROTATIONS  2 -1.570796  1  0.000000  1  0.000000
  !foot ball
   56   LOCKROTATIONS  2  0.000000  1  0.000000  3  0.000000
!-------------------------------------------------------------------
! Left leg joints
  !hip                 Y (rearward) X (left)     Z (medial)
   57   FREEROTATIONS  2 -0.65450   1  0.000000  3  0.000000
  !knee                X (STIFF)    Y (flexion)  Z (lateral)
   58   FREEROTATIONS  1  0.000000  2  0.069290  3  0.000000
  !ankle               Y (rearward) X (left)     Z (lateral)
   59   FREEROTATIONS  2 -1.570796  1  0.000000  1  0.000000
  !foot ball
   60   LOCKROTATIONS  2  0.000000  1  0.000000  3  0.000000
!-------------------------------------------------------------------
! Ribs
   61   LOCKROTATIONS  2  0.000000  3  0.000000  1  0.000000
   62   LOCKROTATIONS  2  0.000000  3  0.000000  1  0.000000
```

```
   63   LOCKROTATIONS  2  0.000000  3  0.000000  1  0.000000
   64   LOCKROTATIONS  2  0.000000  3  0.000000  1  0.000000
   65   LOCKROTATIONS  2  0.000000  3  0.000000  1  0.000000
   66   LOCKROTATIONS  2  0.000000  3  0.000000  1  0.000000
   67   LOCKROTATIONS  2  0.000000  3  0.000000  1  0.000000
   68   LOCKROTATIONS  2  0.000000  3  0.000000  1  0.000000
 END JOINT DOF
!
```

The motion values used below were found using SIMM. It should be noted that the pelvis motion specified was not used. An explanation for this can be found in section 5.3 of this thesis.

```
MOTION
!1   ROTXYZ  1  2  0  3  0  0
57  ROTXYZ  6  5  7  0  0  0
58  ROTXYZ  0  8  0  0  0  0
59  ROTXYZ  0  9  0  0  0  0
53  ROTXYZ  11  10  12  0  0  0
54  ROTXYZ  0  13  0  0  0  0
55  ROTXYZ  0  14  0  0  0  0
43  ROTXYZ  16  0  15  0  0  0
32  ROTXYZ  18  0  17  0  0  0
END MOTION
FUNCTIONS
! pelvis rx
10
0.0   -0.01012
0.1   -0.0604
0.2   -0.0672
0.3   -0.0148
0.4   0.0026
0.5   0.0134
0.6   0.0646
0.7   0.0716
0.8   0.0262
0.9   0.0105
! pelvis ry
10
0.0   0.2250
0.1   0.2471
0.2   0.2332
0.3   0.2332
0.4   0.2838
0.5   0.3314
0.6   0.3222
0.7   0.3315
0.8   0.3222
0.9   0.2925
! pelvis velocity
3
0      0
0.05   0.08
0.10   0.16
! pelvis z-position
```

```
10
0.0   0.0
0.1   0.0
0.2   0.0
0.3   0.0
0.4   0.0
0.5   0.0
0.6   0.0
0.7   0.0
0.8   0.0
0.9   0.0
! left hip flexion
10
0.0   -0.6545
0.1   -0.6074
0.2   -0.4014
0.3   -0.2164
0.4   -0.05236
0.5   0.07854
0.6   -0.07156
0.7   -0.3840
0.8   -0.6109
0.9   -0.6597
! left hip adduction
10
0.0   -0.0209
0.1   -0.0960
0.2   -0.1005
0.3   -0.0803
0.4   -0.0738
0.5   -0.0454
0.6   0.0436
0.7   0.0670
0.8   0.0134
0.9   -0.0100
! left hip rotation
10
0.0   -0.0681
0.1   -0.0291
0.2   -0.0267
0.3   -0.0079
0.4   0.0122
0.5   0.0112
0.6   0.0098
0.7   0.0291
0.8   0.0960
0.9   0.0000
! left knee angle
10
0.0   0.06929
0.1   0.3463
0.2   0.3292
0.3   0.1936
0.4   0.1347
```

```
0.5   0.2419
0.6   0.6761
0.7   1.1191
0.8   0.9297
0.9   0.3014
! left ankle angle (from straight up +z)
10
0.0   -1.6081
0.1   -1.6081
0.2   -1.5027
0.3   -1.4626
0.4   -1.3998
0.5   -1.3963
0.6   -1.7279
0.7   -1.6947
0.8   -1.5324
0.9   -1.5446
! right hip flexion
10
0.0   -0.07156
0.1   -0.3840
0.2   -0.6109
0.3   -0.6597
0.4   -0.6545
0.5   -0.6074
0.6   -0.4014
0.7   -0.2164
0.8   -0.05236
0.9    0.07854
! right hip adduction
10
0.0   0.0436
0.1   0.0670
0.2   0.0134
0.3   -0.0100
0.4   -0.0209
0.5   -0.0960
0.6   -0.1005
0.7   -0.0803
0.8   -0.0738
0.9   -0.0454
! right hip rotation
10
0.0   0.0098
0.1   0.0291
0.2   0.0960
0.3   0.0000
0.4   -0.0681
0.5   -0.0291
0.6   -0.0267
0.7   -0.0079
0.8   0.0122
0.9   0.0112
! right knee angle
```

```
10
0.0   0.6761
0.1   1.1191
0.2   0.9297
0.3   0.3014
0.4   0.06929
0.5   0.3463
0.6   0.3292
0.7   0.1936
0.8   0.1347
0.9   0.2419
! right ankle angle (from straight up +z)
10
0.0   -1.7279
0.1   -1.6947
0.2   -1.5324
0.3   -1.5446
0.4   -1.6081
0.5   -1.6081
0.6   -1.5027
0.7   -1.4626
0.8   -1.3998
0.9   -1.3963
! left arm
2
0.0  0.15
0.9  -1.25
2
0.0  -1.3
0.9  -1.3
! right arm
2
0.0  0.4
0.9  -1.0
2
0.0  1.3
0.9  1.3
END FUNCTIONS
!
```

Gravity was also added to the model as follows:

```
!
FORCE MODELS
ACCELERATION FIELDS
1  0  0  0  1
END ACCELERATION FIELDS
FUNCTIONS
2
0  -9.81
5  -9.81
END FUNCTIONS
!
```

Below are the contact interactions that I defined between the feet and the ballast. It should be noted that each contact interaction is identical except for the ellipsoid

number that is defined for contact. Ellipsoids 1 through 30 were chosen as the ellipsoids that will contact the bottom of the human model's foot. Loading functions ("new foot heel to rigid flat plate" and "new foot front to rigid flat plate") were defined from TNO-MADYMO's experimental results that can be found in the original d3hyb350.dat file developed by MADYMO and found in the share directory as stated in the "In-House" User's Manual (Appendix A). The loading characteristics of the "foot to rigid flat plate contact" given in the d3humb50.dat file, also in the share directory, are outdated, according to MADYMO, and this is why they were not used.

```
!
CONTACT INTERACTIONS
!
! This is for the left leg
!
ELLIPSOID-VERTEX
    NULL SYSTEM        1
    ELLIPSOID          1
    VERTEXSET          leg_left_vert
    CONTACT MODEL      FORCE
    LOADING FUNCTION   1
    UNLOADING FUNCTION 2
    HYSTERESIS MODEL   1
    HYSTERESIS SLOPE  -6.0E6
    FRICTION FUNCTION  3
    FUNCTIONS
! 1: new foot heel to rigid flat plate contact, loading
    8
    0.0             0.0
    2.51908E-003   89.0
    4.21946E-003  356.0
    6.04579E-003  890.0
    7.49426E-003 1510.24
    9.00571E-003 2588.9
    1.05801E-002 4585.0
    1.27843E-002  1.75069E+004
! 2: new foot heel to rigid flat plate contact, unloading
    3
    0.0             0.0
    7.49426E-003    0.0
    1.27843E-002    3.93437E+003
! 3: friction
         3
         0.0     0.8
         1.0     0.8
         2.0     0.8
    END FUNCTIONS
END ELLIPSOID-VERTEX
ELLIPSOID-VERTEX
    NULL SYSTEM        1
    ELLIPSOID          2
    VERTEXSET          leg_left_vert
    CONTACT MODEL      FORCE
```

```
    LOADING FUNCTION   1
    UNLOADING FUNCTION 2
    HYSTERESIS MODEL   1
    HYSTERESIS SLOPE  -6.0E6
    FRICTION FUNCTION  3
    FUNCTIONS
! 1: new foot heel to rigid flat plate contact, loading
    8
    0.0             0.0
    2.51908E-003   89.0
    4.21946E-003  356.0
    6.04579E-003  890.0
    7.49426E-003 1510.24
    9.00571E-003 2588.9
    1.05801E-002 4585.0
    1.27843E-002  1.75069E+004
! 2: new foot heel to rigid flat plate contact, unloading
    3
    0.0             0.0
    7.49426E-003    0.0
    1.27843E-002    3.93437E+003
! 3: friction
         3
         0.0     0.8
         1.0     0.8
         2.0     0.8
    END FUNCTIONS
END ELLIPSOID-VERTEX
ELLIPSOID-VERTEX
    NULL SYSTEM        1
    ELLIPSOID          3
    VERTEXSET          leg_left_vert
    CONTACT MODEL      FORCE
    LOADING FUNCTION   1
    UNLOADING FUNCTION 2
    HYSTERESIS MODEL   1
    HYSTERESIS SLOPE  -6.0E6
    FRICTION FUNCTION  3
    FUNCTIONS
! 1: new foot heel to rigid flat plate contact, loading
    8
    0.0             0.0
    2.51908E-003   89.0
    4.21946E-003  356.0
    6.04579E-003  890.0
    7.49426E-003 1510.24
    9.00571E-003 2588.9
    1.05801E-002 4585.0
    1.27843E-002  1.75069E+004
! 2: new foot heel to rigid flat plate contact, unloading
    3
    0.0             0.0
    7.49426E-003    0.0
    1.27843E-002    3.93437E+003
```

```
! 3: friction
         3
         0.0     0.8
         1.0     0.8
         2.0     0.8
    END FUNCTIONS
END ELLIPSOID-VERTEX
ELLIPSOID-VERTEX
    NULL SYSTEM        1
    ELLIPSOID          4
    VERTEXSET          leg_left_vert
    CONTACT MODEL      FORCE
    LOADING FUNCTION   1
    UNLOADING FUNCTION 2
    HYSTERESIS MODEL   1
    HYSTERESIS SLOPE  -6.0E6
    FRICTION FUNCTION  3
    FUNCTIONS
! 1: new foot heel to rigid flat plate contact, loading
    8
    0.0             0.0
    2.51908E-003   89.0
    4.21946E-003  356.0
    6.04579E-003  890.0
    7.49426E-003 1510.24
    9.00571E-003 2588.9
    1.05801E-002 4585.0
    1.27843E-002  1.75069E+004
! 2: new foot heel to rigid flat plate contact, unloading
    3
    0.0             0.0
    7.49426E-003    0.0
    1.27843E-002    3.93437E+003
! 3: friction
         3
         0.0     0.8
         1.0     0.8
         2.0     0.8
    END FUNCTIONS
END ELLIPSOID-VERTEX
ELLIPSOID-VERTEX
    NULL SYSTEM        1
    ELLIPSOID          5
    VERTEXSET          leg_left_vert
    CONTACT MODEL      FORCE
    LOADING FUNCTION   1
    UNLOADING FUNCTION 2
    HYSTERESIS MODEL   1
    HYSTERESIS SLOPE  -6.0E6
    FRICTION FUNCTION  3
    FUNCTIONS
! 1: new foot heel to rigid flat plate contact, loading
    8
    0.0             0.0
```

```
    2.51908E-003   89.0
    4.21946E-003  356.0
    6.04579E-003  890.0
    7.49426E-003 1510.24
    9.00571E-003 2588.9
    1.05801E-002 4585.0
    1.27843E-002  1.75069E+004
! 2: new foot heel to rigid flat plate contact, unloading
    3
    0.0             0.0
    7.49426E-003    0.0
    1.27843E-002    3.93437E+003
! 3: friction
         3
         0.0     0.8
         1.0     0.8
         2.0     0.8
    END FUNCTIONS
END ELLIPSOID-VERTEX
ELLIPSOID-VERTEX
    NULL SYSTEM        1
    ELLIPSOID          6
    VERTEXSET          leg_left_vert
    CONTACT MODEL      FORCE
    LOADING FUNCTION   1
    UNLOADING FUNCTION 2
    HYSTERESIS MODEL   1
    HYSTERESIS SLOPE  -6.0E6
    FRICTION FUNCTION  3
    FUNCTIONS
! 1: new foot heel to rigid flat plate contact, loading
    8
    0.0             0.0
    2.51908E-003   89.0
    4.21946E-003  356.0
    6.04579E-003  890.0
    7.49426E-003 1510.24
    9.00571E-003 2588.9
    1.05801E-002 4585.0
    1.27843E-002  1.75069E+004
! 2: new foot heel to rigid flat plate contact, unloading
    3
    0.0             0.0
    7.49426E-003    0.0
    1.27843E-002    3.93437E+003
! 3: friction
         3
         0.0     0.8
         1.0     0.8
         2.0     0.8
    END FUNCTIONS
END ELLIPSOID-VERTEX
ELLIPSOID-VERTEX
    NULL SYSTEM        1
```

```
    ELLIPSOID          7
    VERTEXSET          leg_left_vert
    CONTACT MODEL      FORCE
    LOADING FUNCTION   1
    UNLOADING FUNCTION 2
    HYSTERESIS MODEL   1
    HYSTERESIS SLOPE  -6.0E6
    FRICTION FUNCTION  3
    FUNCTIONS
! 1: new foot heel to rigid flat plate contact, loading
    8
    0.0             0.0
    2.51908E-003   89.0
    4.21946E-003  356.0
    6.04579E-003  890.0
    7.49426E-003 1510.24
    9.00571E-003 2588.9
    1.05801E-002 4585.0
    1.27843E-002  1.75069E+004
! 2: new foot heel to rigid flat plate contact, unloading
    3
    0.0             0.0
    7.49426E-003    0.0
    1.27843E-002    3.93437E+003
! 3: friction
         3
         0.0     0.8
         1.0     0.8
         2.0     0.8
    END FUNCTIONS
END ELLIPSOID-VERTEX
ELLIPSOID-VERTEX
    NULL SYSTEM        1
    ELLIPSOID          8
    VERTEXSET          leg_left_vert
    CONTACT MODEL      FORCE
    LOADING FUNCTION   1
    UNLOADING FUNCTION 2
    HYSTERESIS MODEL   1
    HYSTERESIS SLOPE  -6.0E6
    FRICTION FUNCTION  3
    FUNCTIONS
! 1: new foot heel to rigid flat plate contact, loading
    8
    0.0             0.0
    2.51908E-003   89.0
    4.21946E-003  356.0
    6.04579E-003  890.0
    7.49426E-003 1510.24
    9.00571E-003 2588.9
    1.05801E-002 4585.0
    1.27843E-002  1.75069E+004
! 2: new foot heel to rigid flat plate contact, unloading
    3
```

```
    0.0             0.0
    7.49426E-003    0.0
    1.27843E-002    3.93437E+003
! 3: friction
         3
         0.0     0.8
         1.0     0.8
         2.0     0.8
    END FUNCTIONS
END ELLIPSOID-VERTEX
ELLIPSOID-VERTEX
    NULL SYSTEM        1
    ELLIPSOID          9
    VERTEXSET          leg_left_vert
    CONTACT MODEL      FORCE
    LOADING FUNCTION   1
    UNLOADING FUNCTION 0
    HYSTERESIS MODEL   1
    HYSTERESIS SLOPE  -2.5E6
    FRICTION FUNCTION  2
    FUNCTIONS
! 1: new foot front to rigid flat plate contact
    4
    0.0       0.0
    0.0071  2.49319E+003
    0.0128  4.41549E+003
    0.0207  8.57049E+003
! 2: friction
         3
         0.0     0.8
         1.0     0.8
         2.0     0.8
    END FUNCTIONS
END ELLIPSOID-VERTEX
ELLIPSOID-VERTEX
    NULL SYSTEM        1
    ELLIPSOID          10
    VERTEXSET          leg_left_vert
    CONTACT MODEL      FORCE
    LOADING FUNCTION   1
    UNLOADING FUNCTION 0
    HYSTERESIS MODEL   1
    HYSTERESIS SLOPE  -2.5E6
    FRICTION FUNCTION  2
    FUNCTIONS
! 1: new foot front to rigid flat plate contact
    4
    0.0       0.0
    0.0071  2.49319E+003
    0.0128  4.41549E+003
    0.0207  8.57049E+003
! 2: friction
         3
         0.0     0.8
```

```
         1.0     0.8
         2.0     0.8
    END FUNCTIONS
END ELLIPSOID-VERTEX
ELLIPSOID-VERTEX
    NULL SYSTEM        1
    ELLIPSOID          11
    VERTEXSET          leg_left_vert
    CONTACT MODEL      FORCE
    LOADING FUNCTION   1
    UNLOADING FUNCTION 0
    HYSTERESIS MODEL   1
    HYSTERESIS SLOPE  -2.5E6
    FRICTION FUNCTION  2
    FUNCTIONS
! 1: new foot front to rigid flat plate contact
    4
    0.0       0.0
    0.0071  2.49319E+003
    0.0128  4.41549E+003
    0.0207  8.57049E+003
! 2: friction
         3
         0.0     0.8
         1.0     0.8
         2.0     0.8
    END FUNCTIONS
END ELLIPSOID-VERTEX
ELLIPSOID-VERTEX
    NULL SYSTEM        1
    ELLIPSOID          12
    VERTEXSET          leg_left_vert
    CONTACT MODEL      FORCE
    LOADING FUNCTION   1
    UNLOADING FUNCTION 0
    HYSTERESIS MODEL   1
    HYSTERESIS SLOPE  -2.5E6
    FRICTION FUNCTION  2
    FUNCTIONS
! 1: new foot front to rigid flat plate contact
    4
    0.0       0.0
    0.0071  2.49319E+003
    0.0128  4.41549E+003
    0.0207  8.57049E+003
! 2: friction
         3
         0.0     0.8
         1.0     0.8
         2.0     0.8
    END FUNCTIONS
END ELLIPSOID-VERTEX
ELLIPSOID-VERTEX
    NULL SYSTEM        1
```

```
    ELLIPSOID          13
    VERTEXSET          leg_left_vert
    CONTACT MODEL      FORCE
    LOADING FUNCTION   1
    UNLOADING FUNCTION 0
    HYSTERESIS MODEL   1
    HYSTERESIS SLOPE  -2.5E6
    FRICTION FUNCTION  2
    FUNCTIONS
! 1: new foot front to rigid flat plate contact
    4
    0.0       0.0
    0.0071  2.49319E+003
    0.0128  4.41549E+003
    0.0207  8.57049E+003
! 2: friction
         3
         0.0     0.8
         1.0     0.8
         2.0     0.8
    END FUNCTIONS
END ELLIPSOID-VERTEX
ELLIPSOID-VERTEX
    NULL SYSTEM        1
    ELLIPSOID          14
    VERTEXSET          leg_left_vert
    CONTACT MODEL      FORCE
    LOADING FUNCTION   1
    UNLOADING FUNCTION 0
    HYSTERESIS MODEL   1
    HYSTERESIS SLOPE  -2.5E6
    FRICTION FUNCTION  2
    FUNCTIONS
! 1: new foot front to rigid flat plate contact
    4
    0.0       0.0
    0.0071  2.49319E+003
    0.0128  4.41549E+003
    0.0207  8.57049E+003
! 2: friction
         3
         0.0     0.8
         1.0     0.8
         2.0     0.8
    END FUNCTIONS
END ELLIPSOID-VERTEX
ELLIPSOID-VERTEX
    NULL SYSTEM        1
    ELLIPSOID          15
    VERTEXSET          leg_left_vert
    CONTACT MODEL      FORCE
    LOADING FUNCTION   1
    UNLOADING FUNCTION 0
    HYSTERESIS MODEL   1
```

```
    HYSTERESIS SLOPE  -2.5E6
    FRICTION FUNCTION  2
    FUNCTIONS
! 1: new foot front to rigid flat plate contact
    4
    0.0       0.0
    0.0071  2.49319E+003
    0.0128  4.41549E+003
    0.0207  8.57049E+003
! 2: friction
         3
         0.0     0.8
         1.0     0.8
         2.0     0.8
    END FUNCTIONS
END ELLIPSOID-VERTEX
ELLIPSOID-VERTEX
    NULL SYSTEM        1
    ELLIPSOID          16
    VERTEXSET          leg_left_vert
    CONTACT MODEL      FORCE
    LOADING FUNCTION   1
    UNLOADING FUNCTION 0
    HYSTERESIS MODEL   1
    HYSTERESIS SLOPE  -2.5E6
    FRICTION FUNCTION  2
    FUNCTIONS
! 1: new foot front to rigid flat plate contact
    4
    0.0       0.0
    0.0071  2.49319E+003
    0.0128  4.41549E+003
    0.0207  8.57049E+003
! 2: friction
         3
         0.0     0.8
         1.0     0.8
         2.0     0.8
    END FUNCTIONS
END ELLIPSOID-VERTEX
ELLIPSOID-VERTEX
    NULL SYSTEM        1
    ELLIPSOID          17
    VERTEXSET          leg_left_vert
    CONTACT MODEL      FORCE
    LOADING FUNCTION   1
    UNLOADING FUNCTION 0
    HYSTERESIS MODEL   1
    HYSTERESIS SLOPE  -2.5E6
    FRICTION FUNCTION  2
    FUNCTIONS
! 1: new foot front to rigid flat plate contact
    4
    0.0       0.0
```

```
    0.0071  2.49319E+003
    0.0128  4.41549E+003
    0.0207  8.57049E+003
! 2: friction
         3
         0.0     0.8
         1.0     0.8
         2.0     0.8
    END FUNCTIONS
END ELLIPSOID-VERTEX
ELLIPSOID-VERTEX
    NULL SYSTEM        1
    ELLIPSOID          18
    VERTEXSET          leg_left_vert
    CONTACT MODEL      FORCE
    LOADING FUNCTION   1
    UNLOADING FUNCTION 0
    HYSTERESIS MODEL   1
    HYSTERESIS SLOPE  -2.5E6
    FRICTION FUNCTION  2
    FUNCTIONS
! 1: new foot front to rigid flat plate contact
    4
    0.0       0.0
    0.0071  2.49319E+003
    0.0128  4.41549E+003
    0.0207  8.57049E+003
! 2: friction
         3
         0.0     0.8
         1.0     0.8
         2.0     0.8
    END FUNCTIONS
END ELLIPSOID-VERTEX
ELLIPSOID-VERTEX
    NULL SYSTEM        1
    ELLIPSOID          19
    VERTEXSET          leg_left_vert
    CONTACT MODEL      FORCE
    LOADING FUNCTION   1
    UNLOADING FUNCTION 0
    HYSTERESIS MODEL   1
    HYSTERESIS SLOPE  -2.5E6
    FRICTION FUNCTION  2
    FUNCTIONS
! 1: new foot front to rigid flat plate contact
    4
    0.0       0.0
    0.0071  2.49319E+003
    0.0128  4.41549E+003
    0.0207  8.57049E+003
! 2: friction
         3
         0.0     0.8
```

```
         1.0     0.8
         2.0     0.8
    END FUNCTIONS
END ELLIPSOID-VERTEX
ELLIPSOID-VERTEX
    NULL SYSTEM        1
    ELLIPSOID          20
    VERTEXSET          leg_left_vert
    CONTACT MODEL      FORCE
    LOADING FUNCTION   1
    UNLOADING FUNCTION 0
    HYSTERESIS MODEL   1
    HYSTERESIS SLOPE  -2.5E6
    FRICTION FUNCTION  2
    FUNCTIONS
! 1: new foot front to rigid flat plate contact
    4
    0.0       0.0
    0.0071  2.49319E+003
    0.0128  4.41549E+003
    0.0207  8.57049E+003
! 2: friction
         3
         0.0     0.8
         1.0     0.8
         2.0     0.8
    END FUNCTIONS
END ELLIPSOID-VERTEX
ELLIPSOID-VERTEX
    NULL SYSTEM        1
    ELLIPSOID          21
    VERTEXSET          leg_left_vert
    CONTACT MODEL      FORCE
    LOADING FUNCTION   1
    UNLOADING FUNCTION 0
    HYSTERESIS MODEL   1
    HYSTERESIS SLOPE  -2.5E6
    FRICTION FUNCTION  2
    FUNCTIONS
! 1: new foot front to rigid flat plate contact
    4
    0.0       0.0
    0.0071  2.49319E+003
    0.0128  4.41549E+003
    0.0207  8.57049E+003
! 2: friction
         3
         0.0     0.8
         1.0     0.8
         2.0     0.8
    END FUNCTIONS
END ELLIPSOID-VERTEX
ELLIPSOID-VERTEX
    NULL SYSTEM        1
```

```
    ELLIPSOID          22
    VERTEXSET          leg_left_vert
    CONTACT MODEL      FORCE
    LOADING FUNCTION   1
    UNLOADING FUNCTION 0
    HYSTERESIS MODEL   1
    HYSTERESIS SLOPE  -2.5E6
    FRICTION FUNCTION  2
    FUNCTIONS
! 1: new foot front to rigid flat plate contact
    4
    0.0       0.0
    0.0071  2.49319E+003
    0.0128  4.41549E+003
    0.0207  8.57049E+003
! 2: friction
         3
         0.0     0.8
         1.0     0.8
         2.0     0.8
    END FUNCTIONS
END ELLIPSOID-VERTEX
ELLIPSOID-VERTEX
    NULL SYSTEM        1
    ELLIPSOID          23
    VERTEXSET          leg_left_vert
    CONTACT MODEL      FORCE
    LOADING FUNCTION   1
    UNLOADING FUNCTION 0
    HYSTERESIS MODEL   1
    HYSTERESIS SLOPE  -2.5E6
    FRICTION FUNCTION  2
    FUNCTIONS
! 1: new foot front to rigid flat plate contact
    4
    0.0       0.0
    0.0071  2.49319E+003
    0.0128  4.41549E+003
    0.0207  8.57049E+003
! 2: friction
         3
         0.0     0.8
         1.0     0.8
         2.0     0.8
    END FUNCTIONS
END ELLIPSOID-VERTEX
ELLIPSOID-VERTEX
    NULL SYSTEM        1
    ELLIPSOID          24
    VERTEXSET          leg_left_vert
    CONTACT MODEL      FORCE
    LOADING FUNCTION   1
    UNLOADING FUNCTION 0
    HYSTERESIS MODEL   1
```

```
    HYSTERESIS SLOPE  -2.5E6
    FRICTION FUNCTION  2
    FUNCTIONS
! 1: new foot front to rigid flat plate contact
    4
    0.0       0.0
    0.0071  2.49319E+003
    0.0128  4.41549E+003
    0.0207  8.57049E+003
! 2: friction
         3
         0.0     0.8
         1.0     0.8
         2.0     0.8
    END FUNCTIONS
END ELLIPSOID-VERTEX
ELLIPSOID-VERTEX
    NULL SYSTEM        1
    ELLIPSOID          25
    VERTEXSET          leg_left_vert
    CONTACT MODEL      FORCE
    LOADING FUNCTION   1
    UNLOADING FUNCTION 0
    HYSTERESIS MODEL   1
    HYSTERESIS SLOPE  -2.5E6
    FRICTION FUNCTION  2
    FUNCTIONS
! 1: new foot front to rigid flat plate contact
    4
    0.0       0.0
    0.0071  2.49319E+003
    0.0128  4.41549E+003
    0.0207  8.57049E+003
! 2: friction
         3
         0.0     0.8
         1.0     0.8
         2.0     0.8
    END FUNCTIONS
END ELLIPSOID-VERTEX
ELLIPSOID-VERTEX
    NULL SYSTEM        1
    ELLIPSOID          26
    VERTEXSET          leg_left_vert
    CONTACT MODEL      FORCE
    LOADING FUNCTION   1
    UNLOADING FUNCTION 0
    HYSTERESIS MODEL   1
    HYSTERESIS SLOPE  -2.5E6
    FRICTION FUNCTION  2
    FUNCTIONS
! 1: new foot front to rigid flat plate contact
    4
    0.0       0.0
```

```
    0.0071  2.49319E+003
    0.0128  4.41549E+003
    0.0207  8.57049E+003
! 2: friction
         3
         0.0     0.8
         1.0     0.8
         2.0     0.8
    END FUNCTIONS
END ELLIPSOID-VERTEX
ELLIPSOID-VERTEX
    NULL SYSTEM        1
    ELLIPSOID          27
    VERTEXSET          leg_left_vert
    CONTACT MODEL      FORCE
    LOADING FUNCTION   1
    UNLOADING FUNCTION 0
    HYSTERESIS MODEL   1
    HYSTERESIS SLOPE  -2.5E6
    FRICTION FUNCTION  2
    FUNCTIONS
! 1: new foot front to rigid flat plate contact
    4
    0.0       0.0
    0.0071  2.49319E+003
    0.0128  4.41549E+003
    0.0207  8.57049E+003
! 2: friction
         3
         0.0     0.8
         1.0     0.8
         2.0     0.8
    END FUNCTIONS
END ELLIPSOID-VERTEX
ELLIPSOID-VERTEX
    NULL SYSTEM        1
    ELLIPSOID          28
    VERTEXSET          leg_left_vert
    CONTACT MODEL      FORCE
    LOADING FUNCTION   1
    UNLOADING FUNCTION 0
    HYSTERESIS MODEL   1
    HYSTERESIS SLOPE  -2.5E6
    FRICTION FUNCTION  2
    FUNCTIONS
! 1: new foot front to rigid flat plate contact
    4
    0.0       0.0
    0.0071  2.49319E+003
    0.0128  4.41549E+003
    0.0207  8.57049E+003
! 2: friction
         3
         0.0     0.8
```

```
         1.0     0.8
         2.0     0.8
    END FUNCTIONS
END ELLIPSOID-VERTEX
!
! This is for the right leg
!
ELLIPSOID-VERTEX
    NULL SYSTEM        1
    ELLIPSOID          29
    VERTEXSET          leg_right_vert
    CONTACT MODEL      FORCE
    LOADING FUNCTION   1
    UNLOADING FUNCTION 0
    HYSTERESIS MODEL   1
    HYSTERESIS SLOPE  -2.5E6
    FRICTION FUNCTION  2
    FUNCTIONS
! 1: new foot front to rigid flat plate contact
    4
    0.0       0.0
    0.0071  2.49319E+003
    0.0128  4.41549E+003
    0.0207  8.57049E+003
! 2: friction
         3
         0.0     0.8
         1.0     0.8
         2.0     0.8
    END FUNCTIONS
END ELLIPSOID-VERTEX
ELLIPSOID-VERTEX
    NULL SYSTEM        1
    ELLIPSOID          30
    VERTEXSET          leg_right_vert
    CONTACT MODEL      FORCE
    LOADING FUNCTION   1
    UNLOADING FUNCTION 0
    HYSTERESIS MODEL   1
    HYSTERESIS SLOPE  -2.5E6
    FRICTION FUNCTION  2
    FUNCTIONS
! 1: new foot front to rigid flat plate contact
    4
    0.0       0.0
    0.0071  2.49319E+003
    0.0128  4.41549E+003
    0.0207  8.57049E+003
! 2: friction
         3
         0.0     0.8
         1.0     0.8
         2.0     0.8
    END FUNCTIONS
```

```
END ELLIPSOID-VERTEX
END CONTACT INTERACTIONS
!
```

Some examples of the output files used for the human model are already supplied in the human model file created by TNO-MADYMO N.A., but the following output is needed to find the forces on the feet.

```
!
 FORCES
!  For Nr Cho Sysnr ID
! Left foot
    9   1  0  1  left foot1
    9   2  0  1  left foot2
    9   3  0  1  left foot3
    9   4  0  1  left foot4
    9   5  0  1  left foot5
    9   6  0  1  left foot6
    9   7  0  1  left foot7
    9   8  0  1  left foot8
    9   9  0  1  left foot9
    9  10  0  1  left foot10
    9  11  0  1  left foot11
    9  12  0  1  left foot12
    9  13  0  1  left foot13
    9  14  0  1  left foot14
    9  15  0  1  left foot15
    9  16  0  1  left foot16
    9  17  0  1  left foot17
    9  18  0  1  left foot18
    9  19  0  1  left foot19
    9  20  0  1  left foot20
    9  21  0  1  left foot21
    9  22  0  1  left foot22
    9  23  0  1  left foot23
    9  24  0  1  left foot24
    9  25  0  1  left foot25
    9  26  0  1  left foot26
    9  27  0  1  left foot27
    9  28  0  1  left foot28
  END
!
```

These were the text lines added to the human model system file (d3humb50.dat), developed by TNO-MADYMO N.A., to simulate human gait.

Appendix D MADYMO Files for Simple Whiplash Problem

MADYMO Output File for the Angular Acceleration of the Head

```
Result Verification
 Pinned Head Example
   2   4
 Head - Head - INERTIAL - wrt_inertial_cs
 Head - Head - LOCAL - wrt_bodylocal_cs
 Res. ang. acc. (rad/s**2)
 X-comp. ang. acc. (rad/s**2)
 Y-comp. ang. acc. (rad/s**2)
 Z-comp. ang. acc. (rad/s**2)
  0.000000E+000
  1.842666E+002  6.768491E-004 -1.842666E+002  0.000000E+000
  1.842666E+002  6.768491E-004 -1.842666E+002  0.000000E+000
```

MADYMO Output File for the Reaction Forces at the Pin Joint

```
Result Verification
 Pinned Head Example
   2  10
 On Body            from Head           ; pinjoint
 On Head            from Body           ; pinjoint
 Resultant constraint force (N)
 Inertial X-comp. force (N)
 Inertial Y-comp. force (N)
 Inertial Z-comp. force (N)
 Joint x-comp. force (N)
 Joint y-comp. force (N)
 Joint z-comp. force (N)
 Body x-comp. force (N)
 Body y-comp. force (N)
 Body z-comp. force (N)
  0.00000E+000
  1.17435E+002 -1.09214E+002  1.06022E-004 -4.31640E+001
5.07188E-004  1.09214E+002 -4.31640E+001 -1.09214E+002
1.06022E-004 -4.31640E+001
  1.17435E+002  1.09214E+002 -1.06022E-004  4.31640E+001 -
5.07188E-004 -1.09214E+002  4.31640E+001  1.09214E+002 -
1.06022E-004  4.31640E+001
```

MADYMO Input File for the Simplified Whiplash Model

```
Pinned Head Example
Result Verification
October 20, 2000
!
GENERAL INPUT
T0   0.0
TE   0.0
INT  RUKU4
TS   0.001
END GENERAL INPUT
!
SYSTEM
Head
CONFIGURATION
2  1
END CONFIGURATION
GEOMETRY
0.0  0.0  0.0  0.0  0.0  0.25  Body
0.0  0.0  0.5  0.0  0.0  0.0356  Head
END GEOMETRY
INERTIA
! M     Ixx     Iyy     Izz     Ixy  Ixz  Iyz
0.0001  0.00001  0.00001  0.00001  0.0  0.0  0.0
4.4000  0.0204  0.0211  0.0143  0.0  0.0  0.0
END INERTIA
JOINTS
1  FREE
2  REVOLUTE
END JOINTS
ORIENTATIONS
2  1  1  3  1.5708
2  2  1  3  1.5708
END ORIENTATIONS
ELLIPSOIDS
1  0.1  0.2  0.25  0.0  0.0  0.25  2  0  0  0  Body_Ellip
1  0.0356  0.0356  0.0356  0.0  0.0  0.0356  2  0  0  0
Head_Ellip
END ELLIPSOIDS
INITIAL CONDITIONS

JOINT DOF
1  LOCKROTATIONS   1  0.0   2  0.0   3  0.0  0.0  0.0  0.0
```

```
2  FREE   0.0000
END JOINT DOF
END SYSTEM
!
FORCE MODELS
ACCELERATION FIELDS
1  0  1  0  2
END ACCELERATION FIELDS
FUNCTIONS
4
0.000  -31.3813
0.100  -31.3813
0.101    0.0000
5.000    0.0000
2
0  -9.81  5  -9.81
END FUNCTIONS
END FORCE MODELS
!
OUTPUT CONTROL
TSKIN  0.001
KIN3  EXTENDED
TSOUT  0.001
ANGACC
1  2  0  wrt_inertial_cs
1  2  1  wrt_bodylocal_cs
END ANGACC
CONSTRAINT LOADS
1  2  pinjoint
END CONSTRAINT LOADS
END OUTPUT CONTROL
!
END INPUT
```

Vita

Brent Travis Tuohy

1288 Chardonnay #B. • Gardnerville, NV 89410 • Phone: (775) 265-8883 • brent.tuohy@bently.com

Education

Master of Science in Engineering Mechanics
Virginia Tech, December 2000; GPA 3.61/4.0

Bachelor of Science in Mechanical Engineering
University of Nevada at Reno, May 1998; GPA 3.77/4.0
Business Administration (minor)
Registered Engineering Intern in the state of Nevada

Work Experience

Sept.-present — **Engineer**, Bently Rotor Dynamics Research Corporation; Minden, Nevada
- Participate in all levels of design, modeling, testing, and installation of the revolutionary ServoFluid™ Control Bearing

May 2000-Aug. 2000, May 1999-Aug. 1999 — **Fishing Guide**, Riversong Lodge, Alaska;
- Guided clients from around the world for salmon and trout fishing; directly responsible for guests' satisfaction and successful operation of the lodge; operated an 18 ft. boat with a 40 hp jet outboard

Aug. 1999-May 2000, Aug. 1998-May 1999 — **Graduate Teaching Assistant**, Virginia Tech; Blacksburg, Virginia
- Instruct students on how to operate materials testing equipment in Mechanical Behavior of Materials Laboratory (Instron, MTS, LabVIEW, etc.); evaluated laboratory reports

Engineering Research Assistant, University of Nevada, Reno (UNR);

Jan. 1997-Feb. 1998
- *Job#1*: Designed, fabricated, and performed tests on a grooved channel for the purpose of heat transfer enhancement; conducted a statistical analysis of the data; results submitted to ASME Journal of Heat Transfer (funded by the National Science Foundation)

Jan. 1998-May 1998
- *Job#2*: Orthopedic biomechanics; researched the failure mechanics of human bones

Sept. 1997-May 1998 — **Co-Chairman of Human Powered Vehicle Team**, UNR; Reno, Nevada
- Directed a team of 30 students in designing and producing a human powered vehicle for the National ASME HPV Competition (tied for 3rd place); responsible for the design (Pro/E), construction, and testing of the Kevlar/ Carbon fiber aerodynamic fairing; primary male rider

Computer Skills

- Experience in computer analysis and dynamic modeling using MADYMO
- Use of Pro/ENGINEER, AutoCAD, Excel, Mathcad, and MATLAB

Achievements

- Pratt Fellowship for "outstanding academic record" (Virginia Tech)
- 1998 Outstanding Senior of the Year in the Mechanical Engineering Department (UNR)
- American Society of Mechanical Engineers (ASME) Six-year member and the 1997/98 student Chair (UNR)
- Recipient of a four year Presidential Scholarship (UNR)
- 1st place in Doc Harris Technical Speaking Contest (4th at ASME RSC)
- Member of: Society for the Advancement of Materials and Process Engineering (SAMPE), Tau Beta Pi Engineering Honor Society, Golden Key National Honor Society, and National Society of Professional Engineers
- Built an 8½-foot hydroplane; summer 1995
- Member of the Montana State University Baseball Team; 1996